EXACTLY SOLVABLE POTENTIALS WITH DIRAC DELTA POINT INTERACTIONS

by

Hakan Erkol

B.S., Physics, Yıldız Technical University, 2000

M.S., Physics, Boğaziçi University, 2003

Submitted to the Institute for Graduate Studies in
Science and Engineering in partial fulfillment of
the requirements for the degree of
Doctor of Philosophy

Graduate Program in Physics

Boğaziçi University

2009

EXACTLY SOLVABLE POTENTIALS WITH DIRAC DELTA POINT INTERACTIONS

APPROVED BY:

Prof. Ersan Demiralp (Thesis Supervisor)	.....
Prof. Metin Arık	.....
Prof. Ömer Faruk Dayı	.....
Assoc. Prof. Nihat Sadık Değer	.....
Prof. Osman Teoman Turgut	.....

DATE OF APPROVAL: 1.June.2009

ACKNOWLEDGEMENTS

In the first place, I would like to thank my thesis supervisor Prof. Ersan Demiralp for all his encouragement, foresight and relieving guidance throughout my Ph.D. thesis study, creating a productive and cooperative atmosphere for research.

I would like to express my gratitude to Prof. Haluk Beker for his support and help to me as I was learning the subject. I furthermore would like to thank the Faculty members for exciting and instructive courses.

My deepest appreciation to my father, mother and brother for their support.

Special thank to my friends Azmi Ali Altıntaş, Haydar Uncu, Fatih Erman, Mehmet Deliömeroğlu for the endless, inspiring and interesting conversations on Physics and Mathematics. In addition, I gratefully acknowledge Ahmet Baykal, Kaan Atak and Peker Milas for helpful discussions and for their assistance when I was writing my thesis.

ABSTRACT

EXACTLY SOLVABLE POTENTIALS WITH DIRAC DELTA POINT INTERACTIONS

A general method to obtain s-wave bound states of the Schrödinger equation for analytically solvable potentials together with a finite number of the Dirac delta functions is presented for three-dimensional systems. The eigenvalue equations for the finite number of the Dirac delta decorated Woods-Saxon potential and Morse potential are obtained and the eigenvalue equations are calculated numerically for one Dirac delta function. The eigenvalue equation is solved numerically for two delta function case for the Woods-Saxon potential. The change of the ground state energies as a function of strength and locations of the Dirac delta functions are investigated for these potentials. For a hydrogen molecule, which is described by the Morse potential, transition probabilities between the initial state of the Hamiltonian and the final state of the perturbed Hamiltonian for a sudden, very local perturbation are calculated. The conditions for the number of bound states for given parameters of the Woods-Saxon and the Morse potentials are analyzed. Our results for the Woods-Saxon potential can be used to model very short range interactions for atomic and nuclear systems. Our method is applied to hydrogen molecule, which is described by the Morse potential, in C_{60} fullerene cage and the stabilization energy is calculated by representing the interaction potential between H_2 and C_{60} by the Dirac delta interaction. Interatomic interactions that are described by the Morse potential together with local deformations can be investigated by using our model.

ÖZET

DİRAC DELTA NOKTASAL ETKİLEŞMELER İÇEREN KESİN OLARAK ÇÖZÜLEBİLEN POTANSİYELLER

Sonlu sayıda Dirac delta fonksiyonu içeren analitik olarak çözülebilen üç boyutlu sistemlerin potansiyellerinin s (l=0 açısal kuantum sayısı) dalga hali bağlı durumlarının enerjilerini elde etmek için genel bir metod tanıtıldı. Sonlu sayıda Dirac delta fonksiyonu içeren Woods-Saxon ve Morse potansiyelleri için enerji denklemleri elde edildi ve enerji denklemleri bir Dirac delta fonksiyonu için nümerik olarak hesaplandı. Ayrıca iki Dirac delta fonksiyonuna sahip Woods-Saxon potansiyeli için enerji denklemi nümerik olarak çözüldü. Bu potansiyeller için temel durum enerjilerinin Dirac delta fonksiyonunun gücüne ve konumuna bağlı olarak değişimi araştırıldı. Hidrojen molekülü ile çok hızlı ve kısa erimli perturbe edilmiş hidrojen molekülü arasındaki kuantum durumu geçiş olasılıkları Morse potansiyeli ile incelenen hidrojen molekülü için hesaplandı. Woods-Saxon ve Morse potansiyellerinin bağlı durum enerjilerinin sayısı üzerine koşullar incelendi. Woods-Saxon potansiyeli için elde ettiğimiz sonuçlar atomik fizik ve nükleer fizikte oldukça kısa erimli etkileşmeleri modellemek için kullanılabilir. Metodumuz fullerene C_{60} kafesi içerisindeki Morse potansiyeli ile incelenen hidrojen molekülüne uygulandı ve C_{60} ile hidrojenin arasındaki etkileşme Dirac delta etkileşmesi ile ifade edilerek dengeleme enerjisi hesaplandı. Morse potansiyelinin açıkladığı atomlar arası etkileşmeler yerel deformasyonlara sahip ise bu tür sistemler öne sürdüğümüz model kullanılarak incelenebilir.

TABLE OF CONTENTS

ACKNOWLEDGEMENTS iii
ABSTRACT iv
ÖZET v
LIST OF FIGURES vii
LIST OF TABLES xiii
LIST OF SYMBOLS/ABBREVIATIONS xiv
1. INTRODUCTION 1
1.1. Main Results of This Thesis 5
2. BOUND STATE SOLUTIONS OF THE SCHRÖDINGER EQUATION FOR SOLVABLE POTENTIALS WITH DIRAC DELTA FUNCTIONS 7
2.1. Decoration of a Solvable Potential with Dirac Delta Functions for Three-Dimensional Systems 7
3. BOUND STATE ENERGIES FOR THE DIRAC DELTA POTENTIAL . . . 13
4. CONDITION ON THE NUMBER OF BOUND STATES FOR AN ATTRACTIVE POTENTIAL 16
4.1. Condition on the Number of Bound States of Square Well 17
4.2. Condition on the Number of Bound States of the Dirac Delta Potential 18
4.3. Condition on the Number of Bound States of the Woods-Saxon Potential 18
4.4. Condition on the Number of Bound States of the Morse Potential . . . 19
5. THE WOODS-SAXON POTENTIAL WITH POINT INTERACTIONS . . 21
6. THE MORSE POTENTIAL WITH POINT INTERACTIONS 40
6.1. Sudden Perturbations 60
6.2. Encapsulation of H_2 in C_{60} Fullerene Cage 61
7. THE ONE DIMENSIONAL MORSE POTENTIAL WITH POINT INTERACTIONS 67
8. CONCLUSIONS 81
APPENDIX A: SOME PROPERTIES OF THE DIRAC DELTA FUNCTION 85
REFERENCES 89

LIST OF FIGURES

Figure 2.1. Division of Space 9

Figure 4.1. $\frac{V_M}{D}$ vs. $\frac{r}{r_0}$ for the Morse potential $V_M(r) = D(e^{-2\alpha\frac{r-r_0}{r_0}} - 2e^{-\alpha\frac{r-r_0}{r_0}})$ for $r \geq r_0(1 - \frac{ln2}{\alpha})$ where $\alpha = 1.445$ and α is calculated from the reference [64]. 20

Figure 5.1. $\frac{V_{WS}}{V_0}$ vs. $\frac{r}{a}$ for the Woods-Saxon Potential $V_{WS}(r) = -\frac{V_0}{1+e^{\frac{r-R}{a}}}$ where $\frac{R}{a} = 25$. 21

Figure 5.2. Ground state energy E_0 (in units of $\frac{\hbar^2}{2ma^2}$) vs. $\zeta = \sigma a$ for $\gamma = 0.5$. ($\Diamond$, $+$, $\Box$, $\times$ represent $r_1 = 2a, 4a, 10a, 30a$ cases respectively.) . . 31

Figure 5.3. The ground state energy E_0 (in units of $\frac{\hbar^2}{2ma^2}$) vs. the position of the Dirac delta function r_1 for $\zeta = \sigma a = 0.1$ (attractive interaction), $\gamma = 0.5$. Here, r_1 is in units of a 35

Figure 5.4. $\frac{\Delta E_0}{|E_0|} = \frac{E_0^{W,\delta} - E_0}{|E_0|}$ vs. the position of the Dirac delta function r_1 for $\zeta = \sigma a$ (attractive interaction) where $E_0^{W,\delta}$, E_0 stand for the ground state energies for the Woods-Saxon potential with delta function and the Woods-Saxon potential, respectively for $\gamma = 0.5$. Here, r_1 is in units of a. ($\Box$, $+$, $\Diamond$ represent $\zeta = 0.01, 0.05, 0.1$ cases respectively.) 35

Figure 5.5. The ground state energy E_0 (in units of $\frac{\hbar^2}{2ma^2}$) vs. the position of the Dirac delta function r_1 for $\zeta = \sigma a = -0.1$ (repulsive interaction), $\gamma = 0.5$. Here, r_1 is in units of a 36

Figure 5.6. $\frac{\Delta E_0}{|E_0|} = \frac{E_0^{W,\delta} - E_0}{|E_0|}$ vs. the position of the Dirac delta function r_1 for $\zeta = \sigma a$ (repulsive interaction) where $E_0^{W,\delta}$, E_0 stand for the ground state energies for the Woods-Saxon potential with delta function and the Woods-Saxon potential, respectively for $\gamma = 0.5$. Here, r_1 is in units of a. (+, □, ◊ represent $\zeta = -0.01, -0.05, -0.1$ cases respectively.) 36

Figure 5.7. The ground state energy E_0 (in units of $\frac{\hbar^2}{2ma^2}$) vs. configuration of different arrangements of the Dirac delta functions at $r_1 = 5a$ and $r_2 = 10a$ for $\zeta = \sigma a = 0.1$ and $\gamma = 0.5$. (◊, +, □ represent $P = 0, 1, 2$ cases respectively.) 38

Figure 5.8. The ground state energy E_0 (in units of $\frac{\hbar^2}{2ma^2}$) vs. configuration of different arrangements of the Dirac delta functions at $r_1 = 5a$ and $r_2 = 20a$ for $\zeta = \sigma a = 0.1$ and $\gamma = 0.5$. (◊, +, □ represent $P = 0, 1, 2$ cases respectively.) 38

Figure 5.9. The ground state energy E_0 (in units of $\frac{\hbar^2}{2ma^2}$) vs. configuration of different arrangements of the Dirac delta functions at $r_1 = 5a$ and $r_2 = 10a$ for $\zeta = \sigma a = 0.5$ and $\gamma = 0.5$. (◊, +, □ represent $P = 0, 1, 2$ cases respectively.) 39

Figure 5.10. The ground state energy E_0 (in units of $\frac{\hbar^2}{2ma^2}$) vs. configuration of different arrangements of the Dirac delta functions at $r_1 = 5a$ and $r_2 = 20a$ for $\zeta = \sigma a = 0.5$ and $\gamma = 0.5$. (◊, +, □ represent $P = 0, 1, 2$ cases respectively.) 39

Figure 6.1. $\frac{V_M}{D}$ vs. $\frac{r}{r_0}$ for the Morse potential $V_M(r) = D(e^{-2\alpha\frac{r-r_0}{r_0}} - 2e^{-\alpha\frac{r-r_0}{r_0}})$ where $\alpha = 1.445$. 40

Figure 6.2. The ground state energy E_0 (in units of $\frac{\hbar^2}{2mr_0{}^2}$) vs. $\tau = \sigma r_0$ for $\gamma = 25.04$. ($\Diamond$, $+$, $\Box$ represent $r_1 = 0.8r_0, r_0, 1.2r_0$ cases respectively.) 50

Figure 6.3. The ground state energy E_0 (in units of $\frac{\hbar^2}{2mr_0{}^2}$) vs. the position of the Dirac delta function r_1 for $\tau = \sigma r_0 = 5$ (attractive interaction), $\gamma = 25.04$, and r_1 is in units of r_0 52

Figure 6.4. The ground state energy E_0 (in units of $\frac{\hbar^2}{2mr_0{}^2}$) vs. the position of the Dirac delta function r_1 for $\tau = \sigma r_0 = -5$ (repulsive interaction), $\gamma = 25.04$, and r_1 is in units of r_0 52

Figure 6.5. $\frac{\Delta E_0}{|E_0|} = \frac{E_0^{M,\delta} - E_0}{|E_0|}$ vs. the position of the Dirac delta function r_1 for $\tau = \sigma r_0$ (attractive interaction) where $E_0^{M,\delta}$, E_0 stand for the ground state energies for the Morse potential with delta function and the Morse potential, respectively for $\gamma = 25.04$. Here, r_1 is in units of r_0. ($\Box$, $+$, $\Diamond$ represent $\tau = 1, 2, 5$ cases respectively.) . . . 53

Figure 6.6. $\frac{\Delta E_0}{|E_0|} = \frac{E_0^{M,\delta} - E_0}{|E_0|}$ vs. the position of the Dirac delta function r_1 for $\tau = \sigma r_0$ (repulsive interaction) where $E_0^{M,\delta}$, E_0 stand for the ground state energies for the Morse potential with delta function and the Morse potential, respectively for $\gamma = 25.04$. ($+$, $\Box$, $\Diamond$ represent $\tau = -1, -2, -5$ cases respectively.) 54

Figure 6.7. The change of the frequency for the transition between the first excited and the ground states, $w_0 = \frac{E_1 - E_0}{\hbar}$ (in units of $\frac{\hbar}{2mr_0{}^2}$) vs. $\tau = \sigma r_0$ for one Dirac delta function located at $r_1 = 1.3r_0$ for $\gamma = 25.04$. 54

Figure 6.8. The normalized square of the ground state wave function $|\Psi_0|^2$ vs. r where $\gamma = 25.04$ and r is in units of r_0 for (a) $\sigma_1 = 0$ and (b) the Dirac delta function located at $r_1 = 1.3r_0$ for $\sigma_1 r_0 = 15$. 55

Figure 6.9. The normalized square of the first excited state wave function $|\Psi_1|^2$ vs. r where $\gamma = 25.04$ and r is in units of r_0 for (a) $\sigma_1 = 0$ and (b) the Dirac delta function located at $r_1 = 1.3r_0$ for $\sigma_1 r_0 = 15$. 56

Figure 6.10. The change of the frequency for the transition between the second excited and the first excited states, $w_1 = \frac{E_2 - E_1}{\hbar}$ (in units of $\frac{\hbar}{2mr_0{}^2}$) vs. $\tau = \sigma r_0$ for one Dirac delta function located at $r_1 = 1.3r_0$ for $\gamma = 25.04$. 57

Figure 6.11. The normalized square of the second excited state wave function $|\Psi_2|^2$ vs. r where $\gamma = 25.04$ and r is in units of r_0 for (a) $\sigma_1 = 0$ and (b) the Dirac delta function located at $r_1 = 1.3r_0$ for $\sigma_1 r_0 = 15$. 58

Figure 6.12. Expectation value of r is in units of r_0, $< r >= \int_0^\infty \Psi_0^* r \Psi_0 dr$ vs. $\tau = \sigma r_0$ for one Dirac delta function located at $r_1 = r_0$ for $\gamma = 25.04$. 59

Figure 6.13. Expectation value of r is in units of r_0, $< r >= \int_0^\infty \Psi_0^* r \Psi_0 dr$ vs. r_1 for $\tau = 5$ and $\gamma = 25.04$. ($\Diamond$ and + represent one delta and no delta function cases, respectively.) 59

Figure 6.14. Encapsulation of hydrogen molecule in C_{60} fullerene cage [82]. . . 62

Figure 6.15. Van der Waals contact model for H_2 in C_{60} fullerene cage. R_H, R_C and R_{60} represent the radius of hydrogen, carbon and C_{60} cage, respectively. 63

Figure 7.1. The ground state energy E_0 (in units of $\frac{\hbar^2}{2mx_0{}^2}$) vs. $\tau = \sigma x_0$ for $\gamma = 25.04$. ($\Diamond$, +, $\Box$ represent $x_1 = 0.8x_0, x_0, 1.2x_0$ cases respectively.) 73

Figure 7.2. The change of the frequency for the transition between the first excited and the ground states, $w_0 = \frac{E_1 - E_0}{\hbar}$ (in units of $\frac{\hbar}{2mx_0{}^2}$) vs. $\tau = \sigma x_0$ for one Dirac delta function located at $x_1 = 0.8x_0$ for $\gamma = 25.04$. 74

Figure 7.3. The normalized square of the ground state wave function $|\Psi_0|^2$ vs. x where $\gamma = 25.04$ and x is in units of x_0 for (a) $\sigma_1 = 0$ and (b) the Dirac delta function located at $x_1 = 0.8x_0$ for $\sigma_1 x_0 = 15$. 75

Figure 7.4. The normalized square of the first excited state wave function $|\Psi_1|^2$ vs. x where $\gamma = 25.04$ and x is in units of x_0 for (a) $\sigma_1 = 0$ and (b) the Dirac delta function located at $x_1 = 0.8x_0$ for $\sigma_1 x_0 = 15$. . . . 76

Figure 7.5. The change of the frequency for the transition between the second excited and the first excited states, $w_1 = \frac{E_2 - E_1}{\hbar}$ (in units of $\frac{\hbar}{2mx_0{}^2}$) vs. $\tau = \sigma x_0$ for one Dirac delta function located at $x_1 = 0.8x_0$ for $\gamma = 25.04$. 77

Figure 7.6. The normalized square of the second excited state wave function $|\Psi_2|^2$ vs. x where $\gamma = 25.04$ and x is in units of x_0 for (a) $\sigma_1 = 0$ and (b) the Dirac delta function located at $x_1 = 0.8x_0$ for $\sigma_1 x_0 = 15$. 78

Figure 7.7. The change of the oscillator strength for the transition between the first excited and the ground states, $f_{10} = \frac{2m}{\hbar^2}(E_1 - E_0)\left|\int_{-\infty}^{\infty} \Psi_1^* x \Psi_0 dx\right|^2$ vs. $\tau = \sigma x_0$ for one Dirac delta function located at $x_1 = 0.8x_0$ for $\gamma = 25.04$. 79

Figure 7.8. The change of the oscillator strength for the transition between the second and the first excited states, $f_{21} = \frac{2m}{\hbar^2}(E_2 - E_1)\left|\int_{-\infty}^{\infty} \Psi_2^* x \Psi_1 dx\right|^2$ vs. $\tau = \sigma x_0$ for one Dirac delta function located at $x_1 = 0.8x_0$ for $\gamma = 25.04$. 79

Figure A.1. $\delta_\epsilon(x)=\frac{1}{\epsilon\sqrt{\pi}}e^{-\frac{x^2}{\epsilon^2}}$ vs. x for $\epsilon = 5, 0.5, 0.1$ values. 87

LIST OF TABLES

Table 5.1. Configuration Numbers (N_{conf}) for the ordered (P=1, 2) Dirac delta functions. A and R denote the attractive and repulsive Dirac delta functions respectively. 37

Table 6.1. Transition probabilities between the initial eigenstate ($i \equiv \Phi_M$) and the final eigenstate ($f \equiv \Phi_{M\delta}$) for the low-lying states ($i, f = 0, 1, 2$). 61

Table 6.2. Vibrational frequency ν and stabilization energy ΔE are in units of cm^{-1} and kcal/mol, respectively. For DFT calculations, basis set superposition error corrections are included. 66

LIST OF SYMBOLS/ABBREVIATIONS

$\mathbb{M}$	Transfer Matrix
$\mathbb{X}$	Total Transfer Matrix
${}_2F_1(\alpha, \beta, \gamma; y)$	Hypergeometric function
${}_1F_1(\alpha, \beta; y)$	Confluent hypergeometric function
$I_{\frac{1}{2}}(x)$, $K_{\frac{1}{2}}(x)$	Modified Bessel functions of order $\frac{1}{2}$
σ	Strength of the Dirac delta function

1. INTRODUCTION

Contact interactions of some particles with molecules are some of the physical systems which may be modeled by using the Dirac delta potentials. For the electrons in a crystal, periodic Dirac delta-function potential model is used and is called as the Kronig-Penney model [1]. This is an approximate potential for an electron in a crystal. This model explains successfully energy band of electrons in a metal [1, 2]. Mendez et al. studied particles in periodic potentials by introducing Kronig-Penney model with several Dirac delta potentials [3]. Maksymowcz et al. described a disordered system by the Dirac delta functions in which the atoms are strongly localized scattering centers [4].

Arrighini et al. evaluated one and two-photon ionization cross sections for the negative hydrogen ion H^- by representing the effective intra-atomic potential energy with the Dirac delta functions [5]. In this paper, for a single (nonrelativistic) electron, the Hamiltonian operator of H of the model system is $V(r) = -\frac{1}{2}\nabla^2 - V\delta(r - rR)$ where V and R are two (positive) parameters which characterize the (intra-atomic) interaction potential energy of the spherical shell. Mur et al. solved Coulomb problem with short range interaction by introducing the Dirac delta function [6]. In this work, Mur et al. studied systems with a potential $V(r) = -\frac{A}{r} - \frac{g}{2r_o}\delta(r - r_o)$. Blinder studied hyperfine interactions with delta function potential by representing the nuclear moment by a uniformly magnetized spherical shell where the potential has the form $V(r) = -\frac{A}{r} + \frac{8\pi}{3} g g_I \mu_B \mu_n \overrightarrow{s} \cdot \overrightarrow{I} \frac{\delta(r-r_o)}{4\pi r_o^2}$ [7].

Uncu et al. studied Dirac delta decorated linear potential where the potential $U(x) = f\,x - \frac{\hbar^2}{2m} \sum_{i=1}^{P} \sigma_i\, \delta\,(x - x_i)$ [8]. The linear potential is useful to describe the motion of a charged particle in a constant electric field. For GaAs/GaAlAs semiconductor there is a electric field at the junction of GaAs and GaAlAs due to charge transfers. This electric field is approximately constant [9]. If there are impurities in the medium of motion, this impurities can be added to linear potential. Thus, these impurities can be represented by using the Dirac delta functions. Linear potential with

one Dirac delta function can be applied to the charmonium. Uncu et al. investigated charmonium system by using the Dirac delta function in order to describe very short range interaction in addition to linear potential [8].

Uncu et al. also studied bound state solutions of the Schrödinger equation for $\mathcal{PT}$ symmetric Dirac delta potentials [10].

The dimple type of potentials which are used to increase the phase space density of a Bose-Einstein condensate can be modeled by using the Dirac delta function [11], [12]. Demiralp gave a methodology for the solutions of the potentials with a finite number of Dirac delta shells and applied this method to harmonic potential in $\mathbb{R}^n$. Meanwhile, Altunkaynak et al. studied point interactions on Riemanian manifolds $\mathcal{S}^2$, $\mathcal{H}^2$ and $\mathcal{H}^3$. In this study, a lower bound estimate for the ground state energy is found by renormalization utilizing the heat kernel method [13, 14].

Any solvable potential such as linear potential, the Woods-Saxon potential or the Morse potential together with a finite number (P) of the Dirac delta functions can be utilized to model systems that may have very short range interactions in addition to these potentials. Since these point interactions modify the energy levels for these potentials, it can be used to describe some realistic potentials which has roughly the potential shape, but exhibits some local deviations from the potential.

The Woods and Saxon potential was introduced to study elastic scattering of 20-MeV protons by a heavy nuclei [15]. The Woods-Saxon potential is a reasonable potential for nuclear shell models and hence attracts lots of attention in nuclear physics and it is used to represent the distribution of nuclear densities [16]-[28]. Behavior of valence electrons are very important to understand the abundance of metallic clusters [21]. Thus, a good description of the motions of these valence electrons is very useful to study metallic systems. The Woods-Saxon potential is utilized to represent the mean field which is felt by valence electrons in jellium model [29]. It is also used in a nonlinear theory of scalar mesons [29, 30]. In addition to these, the three-dimensional Woods-Saxon potential is studied within the context of Supersymmetric Quantum Mechanics

[31]. This potential can be utilized to model systems that may have very short range interactions in addition to the Woods-Saxon potential.

The Morse potential is a realistic anharmonic potential for diatomic molecules since it gives a good description of the vibrational levels and includes bond breaking effects [32]. Mahlanen et al. used the Morse potentials to describe C-C, C-X, X-X (X=F, Cl, Br) interatomic potentials [33]. It is also utilized to represent many interatomic interactions in molecular calculations [34]-[41]. The potential energy curve for the $^1\sum_g^+$ state of the hydrogen molecule which has double minimum is an example of a deformation [42] so it can be modeled by introducing the Dirac delta potentials to the Morse potential. Fullerene system, which is the encapsulation of a H_2 molecule in a hollow, spherical C_{60} cage, can be also investigated by using our approximation [43].

Uncu et al. studied Bose-Einstein condensation of noninteracting gases in a harmonic trap with an offcenter, tight and deep dimple potential , which is modeled by a point interaction [44].

Damski et al. [45] showed that slow driving of a focused laser beam through a cloud of trapped cold fermions creates a collective excitation in the system. This collective excitation is very local (Gaussian) so that it can be represented by the Dirac delta potential for the limit case of cross section of the laser beam. A focused laser beam through hydrogen molecule may lead to a very local deformation on the potential energy curve for hydrogen. Thus, such a deformed system can be investigated by using our approach.

The adjoint $H^\dagger$ of an operator H is given by

$$< \varphi_2 \mid H\varphi_1 >=< H^\dagger\varphi_2 \mid \varphi_1 > \tag{1.1}$$

where φ_1 and φ_2 are in the domains of H and $H^\dagger$, respectively. The operator H is

Hermitian if the domain of the adjoint of the operator includes the domain of the operator and if the actions of the operator H and its adjoint $H^\dagger$ are the same [46].

An operator H is called as self adjoint operator if the action of H and the action of $H^\dagger$ are the same and the domains of the operator and its adjoint are equal to each other. In one dimension, a self adjoint operator satisfies the relation [46]-[48]:

$$\int_{-\infty}^{\infty} \varphi_2^*(x) H \varphi_1(x) dx = \int_{-\infty}^{\infty} [H\varphi_2(x)]^* \varphi_1(x) dx \tag{1.2}$$

where $H = H^\dagger$.

Consider the kinetic energy operator $H_0 = -\frac{\hbar^2}{2m}\frac{d^2}{dx^2}$ and its continuous eigenfunctions $\Phi(x)$. The operator $H_g = -\frac{\hbar^2}{2m}\frac{d^2}{dx^2} + \frac{\hbar^2}{2m} g\delta(x)$ with Dirac delta point interaction (g ϵ R) is a self-adjoint extension of H_0 with boundary conditions

$$\Phi'(0^+) - \Phi'(0^-) = g\Phi(0) \tag{1.3}$$

and

$$\Phi(0^+) = \Phi(0^-) = \Phi(0) \tag{1.4}$$

where $'$ denotes the derivative with respect to x [46]-[49]. An operator of the type $H = H_0 + V + \frac{\hbar^2}{2m} g\delta(x_i)$ with the potential V can be analyzed by utilizing similar boundary conditions for the eigenfunctions of the operator $H_0 + V$. Detailed investigation of a self adjoint extension of an operator is given in reference [50].

Some properties of the Dirac delta function are given in the Appendix A.

1.1. Main Results of This Thesis

A methodology is presented to obtain bound state solutions of the three-dimensional Schrödinger equation for a solvable potential together with a finite number of Dirac delta function for s-wave states (zero angular momentum quantum number). This methodology can be also generalized to higher dimensions for solvable potentials. Some potentials together with a finite number of the Dirac delta functions are studied in three-dimension for s-wave case.

The condition on the number of bound states for some specific potentials, namely; the Woods-Saxon potential, and the Morse potential, are obtained.

The Woods-Saxon potential together with a finite number of P Dirac delta functions is studied. Transfer matrix for this potential is obtained and eigenvalue equation is solved for the cases $P = 1, 2$. The change of the ground state energy as a function of the strength and position of the Dirac delta function is investigated. The ground state energy of the Woods-Saxon potential is calculated for different locations of the Dirac delta potentials for two delta functions case ($P = 2$). For some limit cases of the strength of the Dirac delta potential and Woods-Saxon potential parameters, the results for delta decorated Woods-Saxon potential are investigated. The condition for the number of bound states of the Woods-Saxon potential is presented.

The Morse potential including finite number of the Dirac delta potentials P is examined. First of all, transfer matrix is presented. After obtaining an eigenvalue equation for bound state energies, the ground state energy and the frequencies for the transitions between the low-lying energy levels are calculated for one delta function case. The behavior of the ground state energy as a function of the strength and position of the Dirac delta function is investigated. The normalized square of the wave functions for the ground, the first and the second excited states are plotted for both no delta and one Dirac delta function cases. For some limit cases of the strength of the Dirac delta potential and the Morse potential parameters, the results for the Morse potential together with a finite number of delta functions are examined. Average

value of interatomic bond distance is investigated for different location and strength values of delta function. Transition probabilities between the initial eigenstates for the Morse potential and the final eigenstates for the potential perturbed by the Dirac delta interaction are calculated. The condition on the number of bound states for the Morse potential is obtained. Our method is applied to hydrogen molecule which is encapsulated in C_{60} cage. The location of the Dirac delta interaction is obtained by using the van der Waals contact distance. Vibrational motion of H_2 molecule is assumed to be along the diameter of the cage and the center of mass of the hydrogen molecule is taken at the center of the C_{60} cage. The strength of the Dirac delta interaction is calculated by using the experimental shift.

For a focused laser beam through trapped cold fermions, the effective potential for the atomic motion in one dimension is given by $V(x) = \frac{x^2}{2} + U_0(x_0)e^{-\frac{(x-x_0)^2}{2\sigma^2}}$ where $U_0(x_0) < 0$ for a laser detuning and σ is related to the cross section of the Gaussian laser beam [45]. Laser fields are described by Gaussian potentials. For limit case $\sigma \to 0$, function $\frac{e^{-\frac{(x-x_0)^2}{2\sigma^2}}}{\sqrt{2\pi\sigma^2}}$ is equal to $\delta(x - x_0)$. Hence, since laser beam results in the Gaussian collective excitation, it can be represented by the Dirac delta potential. By considering that laser beam through hydrogen molecule may create Gaussian like deformation on the energy curve of hydrogen molecule as a physical motivation, the one dimensional Morse potential with a finite number of delta potentials is studied. An eigenvalue equation is obtained and solved numerically for some strengths of the Dirac delta function. The change of the ground state energy as a function of location of delta potential is investigated for some different strengths of delta potential. Frequencies between the first excited and the ground states are calculated for one delta case. Frequencies between the second and the first excited states are also calculated for one delta case. Ground state, the first excited state and the second excited state wave functions are plotted for both delta and one delta function cases. The change of the oscillator strength for the transition between the first excited and the ground states is investigated as a function of strength of delta function. The change of the oscillator strength corresponding to the transition between the second and the first excited states is also investigated with increasing strength values of delta function.

2. BOUND STATE SOLUTIONS OF THE SCHRÖDINGER EQUATION FOR SOLVABLE POTENTIALS WITH DIRAC DELTA FUNCTIONS

In this chapter, we present a method in order to obtain bound state energies of the Schrödinger equation for a solvable potential including a finite number of the Dirac delta functions in three-dimensions for s-wave states [51, 52]. This process is called as the decoration of the potential with the Dirac delta functions [8, 10, 51, 52, 53]. Here, we consider the bound state solutions of the time independent Schrödinger equation for solvable potentials. A potential $V(\mathbf{r})$ is a solvable potential if it can be solved for the Schrödinger equation

$$-\frac{\hbar^2}{2m}\nabla^2\Phi + V\Phi = E\Phi \; . \tag{2.1}$$

.

2.1. Decoration of a Solvable Potential with Dirac Delta Functions for Three-Dimensional Systems

The time-independent Schrödinger equation reduces to

$$-\frac{\hbar^2}{2m}\,\frac{d^2}{dr^2}\Psi(r) + V(r)\Psi(r) = E\,\Psi(r) \tag{2.2}$$

for $l = 0$ (l is the angular momentum quantum number) case by taking $\Phi = \frac{\Psi(r)}{r}$ for spherically symmetric case. For bound states, we take $E = -\frac{\hbar^2 k^2}{2m}$. Equation (2.2) can be written as

$$\frac{d^2\Psi(r)}{dr^2} - \left(\frac{2m}{\hbar^2}V(r) + k^2\right)\Psi(r) = 0 \; . \tag{2.3}$$

This second order differential equation has two linearly independent solutions $\psi_1(r)$ and $\psi_2(r)$.

A potential together with a finite number of the Dirac delta functions can be written as

$$U(r) = V(r) - \frac{\hbar^2}{2m}\sum_{i=1}^{P}\sigma_i\delta(r - r_i)\ , \tag{2.4}$$

where r_i's are the positions of the Dirac delta functions and σ_i 's are arbitrary real numbers (Positive σ_i represents an attractive potential while negative σ_i represents a repulsive one). The strength of the Dirac delta function is taken as $\left(-\frac{\hbar^2}{2m}\sigma_i\right)$ for calculational convenience.

The time independent Schrödinger equation for this decorated potential can be written as

$$-\frac{\hbar^2}{2m}\frac{d^2\Psi(r)}{dr^2} + \left(V(r) - \frac{\hbar^2}{2m}\sum_{i=1}^{P}\sigma_i\delta(r - r_i)\right)\Psi(r) = E\Psi(r)\ . \tag{2.5}$$

By writing E in terms of k, equation (2.5) can be written as

$$\frac{d^2\Psi(r)}{dr^2} + \left(-\frac{2m}{\hbar^2}V(r) + \sum_{i=1}^{P}\sigma_i\delta(r - r_i) - k^2\right)\Psi(r) = 0\ . \tag{2.6}$$

For $r \neq r_i$, equation (2.6) reduces to the following equation

$$\frac{d^2\Psi(r)}{dr^2} - \left(\frac{2m}{\hbar^2}V(r) + k^2\right)\Psi(r) = 0\ . \tag{2.7}$$

Figure 2.1 [54] shows division of the space by the P number of the Dirac delta functions. Hence, we have $P+1$ intervals.

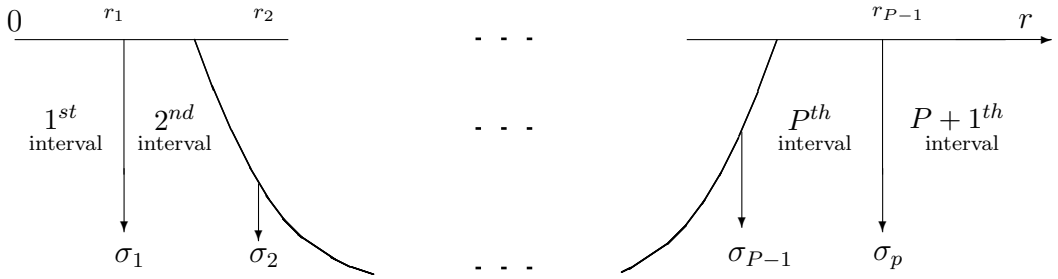


Figure 2.1. Division of Space

By using the solutions of equation (2.7), we define another two linearly independent solutions Ψ_A and Ψ_B satisfying boundary conditions $\Psi_A(0) = 0$ and $\Psi_B(\infty) = 0$.

Thus, for the bound state solutions of equation (2.6), we take wavefunctions Ψ_1 and Ψ_{p+1} as

$$\Psi_1(r) = b_1\Psi_B(r) \tag{2.8}$$

for the first (leftmost) region and

$$\Psi_{p+1}(r) = a_{p+1}\Psi_A(r) \tag{2.9}$$

for the $(p+1)^{th}$ (rightmost) interval, respectively.

For the intermediate regions, we take the wavefunctions in terms of linear combinations of Ψ_A and Ψ_B,

$$\Psi_i(r) = a_i\ \Psi_A(r) + b_i\ \Psi_B(r)\ \ . \tag{2.10}$$

We can find constants a_i and b_i by applying the boundary conditions at the interfaces of the intervals and normalizing the wavefunction. If we integrate equation (2.6) between the interval $r_i - \epsilon$ and $r_i + \epsilon$, and take the limit $\epsilon \to 0^+$, we find that the derivative of Ψ will have a finite jump at $r = r_i$. By using the continuity of the wave function and the discontinuity of its derivative, we obtain the following equations at the interfaces of the intervals (at r_i's)

$$b_i\Psi_B(r_i) + a_i\Psi_A(r_i) = b_{i+1}\Psi_B(r_i) + a_{i+1}\Psi_A(r_i) \tag{2.11}$$

and

$$\begin{aligned} &b_{i+1}\frac{d\Psi_B(r_i)}{dr} + a_{i+1}\frac{d\Psi_A(r_i)}{dr} - \left(b_i\frac{d\Psi_B(r_i)}{dr} + a_i\frac{d\Psi_A(r_i)}{dr}\right) \\ &= -\sigma_i\left(b_i\Psi_B(r_i) + a_i\Psi_A(r_i)\right)\ , \end{aligned} \tag{2.12}$$

where $\frac{d\Psi_B(r_i)}{dr}$ and $\frac{d\Psi_A(r_i)}{dr}$ denote the values of the derivatives of $\Psi_B(r)$ and $\Psi_A(r)$ with respect to r at point r_i. By using the continuity of wavefunction and the jump of its derivative, we can obtain the matrix equation

$$\begin{bmatrix} \Psi_A & \Psi_B \\ \Psi_A^{'} & \Psi_B^{'} \end{bmatrix} \begin{bmatrix} a_{i+1} \\ b_{i+1} \end{bmatrix} = \begin{bmatrix} \Psi_A & \Psi_B \\ \Psi_A^{'} - \sigma_i\Psi_A & \Psi_B^{'} - \sigma_i\Psi_B \end{bmatrix} \begin{bmatrix} a_i \\ b_i \end{bmatrix} \tag{2.13}$$

where primes stand for differentiation with respect to r.

If we multiply this equation by the matrix $\begin{bmatrix} \Psi_A & \Psi_B \\ \Psi_A^{'} & \Psi_B^{'} \end{bmatrix}^{-1} = \frac{1}{\mathcal{W}_i}\begin{bmatrix} \Psi_B^{'} & -\Psi_B \\ -\Psi_A^{'} & \Psi_A \end{bmatrix}$

[55] , we obtain the recursion relation

$$\begin{bmatrix} a_{i+1} \\ b_{i+1} \end{bmatrix} = \begin{bmatrix} 1+\frac{\sigma_i}{\mathcal{W}_i}\Psi_A\Psi_B & \frac{\sigma_i\Psi_B^2}{\mathcal{W}_i} \\ -\frac{\sigma_i\Psi_A^2}{\mathcal{W}_i} & 1-\frac{\sigma_i}{\mathcal{W}_i}\Psi_A\Psi_B \end{bmatrix} \begin{bmatrix} a_i \\ b_i \end{bmatrix} \tag{2.14}$$

where we have used the Wronskian $\mathcal{W}_i[\Psi_A(r), \Psi_B(r)]$ which is calculated at $r = r_i$. The transfer matrix which gives the relation between the coefficients of the wave functions for two successive intervals is denoted as $\mathbb{M}_i(k)$, that is,

$$\mathbb{M}_i(k) = \begin{bmatrix} 1+\frac{\sigma_i}{\mathcal{W}_i}\Psi_A\Psi_B & \frac{\sigma_i\Psi_B^2}{\mathcal{W}_i} \\ -\frac{\sigma_i\Psi_A^2}{\mathcal{W}_i} & 1-\frac{\sigma_i}{\mathcal{W}_i}\Psi_A\Psi_B \end{bmatrix} . \tag{2.15}$$

By using these transfer matrices for a finite number of the Dirac delta functions, we connect the coefficients of the rightmost region to the coefficients of the leftmost region as

$$\begin{bmatrix} a_{P+1} \\ b_{P+1} \end{bmatrix} = \mathbb{M}_P \ldots \mathbb{M}_2\mathbb{M}_1 \begin{bmatrix} a_1 \\ b_1 \end{bmatrix} . \tag{2.16}$$

Since we satisfy the boundary conditions at $r = 0$ and $r \to \infty$ by using Ψ_B and Ψ_A, respectively, we take a_1 and b_{p+1} zero. Thus, by defining the total transfer matrix $\mathbb{X}$ as

$$\mathbb{X} = \mathbb{M}_P \ldots \mathbb{M}_2\mathbb{M}_1 , \tag{2.17}$$

we get

$$\begin{bmatrix} a_{P+1} \\ 0 \end{bmatrix} = \mathbb{X} \begin{bmatrix} 0 \\ b_1 \end{bmatrix} = \begin{bmatrix} x_{11} & x_{12} \\ x_{21} & x_{22} \end{bmatrix} \begin{bmatrix} 0 \\ b_1 \end{bmatrix} \tag{2.18}$$

for bound state solutions since Ψ_B becomes infinite as $r \to \infty$ [or $y \to 0$]. This equation

holds if and only if

$$x_{22}(k^2) = 0 \tag{2.19}$$

which gives the bound state energy spectrum of the potential V(r) by using the roots k^2 of x_{22}.

3. BOUND STATE ENERGIES FOR THE DIRAC DELTA POTENTIAL

We consider a Dirac delta potential located at $x = a$, described by the potential

$$V(x) = -\frac{\hbar^2 \sigma}{2m}\,\delta(x-a) \tag{3.1}$$

where $\sigma > 0$ [2, 56]. The particle is free everywhere except for the isolated singular point at $x = a$. The wave functions in the left and right regions are

$$\Psi_L = A\frac{e^{ik_0 x}}{\sqrt{2\pi}} + B\frac{e^{-ik_0 x}}{\sqrt{2\pi}} \tag{3.2}$$

$$\Psi_R = C\frac{e^{ik_0 x}}{\sqrt{2\pi}} + D\frac{e^{-ik_0 x}}{\sqrt{2\pi}}\ . \tag{3.3}$$

By using the continuity of the wave function and the discontinuity of its derivative at the location of delta function, we get

$$\Psi_R(a) = \Psi_L(a) \qquad ; \qquad \Psi_R^{'}(a) - \Psi_L^{'}(a) = -\sigma\Psi(a) \tag{3.4}$$

lead to equations:

$$e^{ik_0 a}A + e^{-ik_0 a}B = e^{ik_0 a}C + e^{-ik_0 a}D \tag{3.5}$$

$$\begin{aligned}\left[ik_0\, e^{ik_0 a}C - ik_0\, e^{-ik_0 a}D\right] \;&-\; \left[ik_0\, e^{ik_0 a}A - ik_0\, e^{-ik_0 a}B\right] = \\ -\sigma\left[e^{ik_0 a}A + e^{-ik_0 a}B\right] \qquad &.\end{aligned} \tag{3.6}$$

We write these equations in matrix form as:

$$\begin{bmatrix} e^{ik_0a} & e^{-ik_0a} \\ \left(1+\frac{i\sigma}{k_0}\right)e^{ik_0a} & \left(-1+\frac{i\sigma}{k_0}\right)e^{-ik_0a} \end{bmatrix} \begin{bmatrix} A \\ B \end{bmatrix} = \begin{bmatrix} e^{ik_0a} & e^{-ik_0a} \\ e^{ik_0a} & -e^{-ik_0a} \end{bmatrix} \begin{bmatrix} C \\ D \end{bmatrix}, \quad (3.7)$$

so

$$\begin{bmatrix} e^{ik_0a} & e^{-ik_0a} \\ e^{ik_0a} & -e^{-ik_0a} \end{bmatrix}^{-1} \begin{bmatrix} e^{ik_0a} & e^{-ik_0a} \\ \left(1+\frac{i\sigma}{k_0}\right)e^{ik_0a} & \left(-1+\frac{i\sigma}{k_0}\right)e^{-ik_0a} \end{bmatrix} \begin{bmatrix} A \\ B \end{bmatrix} = \begin{bmatrix} C \\ D \end{bmatrix}. \quad (3.8)$$

Here, the transfer matrix $\mathbb{M}$ is defined as:

$$\begin{bmatrix} \mathbb{M} \end{bmatrix} \begin{bmatrix} A \\ B \end{bmatrix} = \begin{bmatrix} C \\ D \end{bmatrix} \ . \quad (3.9)$$

Comparing the above equations we easily see that the transfer matrix $\mathbb{M}$ is given by

$$\mathbb{M} = \begin{bmatrix} 1+\frac{i\sigma}{2k_0} & \frac{i\sigma}{2k_0}e^{-2ik_0a} \\ -\frac{i\sigma}{2k_0}e^{2ik_0a} & 1-\frac{i\sigma}{2k_0} \end{bmatrix} \ . \quad (3.10)$$

In order to obtain bound states, the m_{22} element of the transfer matrix has to be zero. Thus, we obtain

$$m_{22} = 1 - \frac{i\sigma}{2k_0} = 0 \ \Rightarrow \ k_0 = \frac{i\sigma}{2} \ . \quad (3.11)$$

For $k_0 = \frac{i\sigma}{2}$, by setting coefficients A and D to zero, the wave functions in the left and the right regions becomes

$$\Psi_L = B\frac{e^{\frac{\sigma x}{2}}}{\sqrt{2\pi}}, \quad \Psi_R = C\frac{e^{-\frac{\sigma x}{2}}}{\sqrt{2\pi}} \ . \quad (3.12)$$

We calculate the bound state energy eigenvalue from equation (3.11):

$$E = \frac{\hbar^2 k_0^2}{2m} = -\frac{\hbar^2 \sigma^2}{8m} \ . \tag{3.13}$$

Note that the energy is proportional to σ^2 , so it is as if we would have a bound state even for a Dirac delta barrier: $\sigma \to -\sigma$. This unphysical bound state solution is referred to as a Virtual State. Bound and Virtual states are distinguished by their k_0 values; only $Re\,(k_0) = 0$, $Im\,(k_0) > 0$ cases are true bound states, $Re\,(k_0) = 0$ $Im\,(k_0) < 0$ cases are virtual.

Another example is the double Dirac delta well described by the potential:

$$V\,(x) = -\frac{\hbar^2 \sigma}{2m}\left[\delta\left(x + \frac{a}{2}\right) + \delta\left(x - \frac{a}{2}\right)\right]. \tag{3.14}$$

In this case the total transfer matrix is given by

$$\begin{aligned} M_T &= M\left(x + \frac{a}{2}\right) M\left(x - \frac{a}{2}\right) \\ &= \begin{bmatrix} 1 + \frac{i\sigma}{2k_0} & \frac{i\sigma}{2k_0} e^{-ik_0 a} \\ -\frac{i\sigma}{2k_0} e^{ik_0 a} & 1 - \frac{i\sigma}{2k_0} \end{bmatrix} \begin{bmatrix} 1 + \frac{i\sigma}{2k_0} & \frac{i\sigma}{2k_0} e^{ik_0 a} \\ -\frac{i\sigma}{2k_0} e^{-ik_0 a} & 1 - \frac{i\sigma}{2k_0} \end{bmatrix} . \end{aligned}$$

Defining $k_0 \equiv i\kappa_0$; $y \equiv \kappa_0 a$, $\alpha \equiv \dfrac{\sigma a}{2}$ we get

$$M_T = \begin{bmatrix} 1 + \frac{\alpha}{y} & \frac{\alpha}{y} e^{y} \\ -\frac{\alpha}{y} e^{-y} & 1 - \frac{\alpha}{y} \end{bmatrix} \begin{bmatrix} 1 + \frac{\alpha}{y} & \frac{\alpha}{y} e^{-y} \\ -\frac{\alpha}{y} e^{y} & 1 - \frac{\alpha}{y} \end{bmatrix} \tag{3.15}$$

and then setting m_{22} equal to zero, we obtain

$$e^{-2y} = \left(1 - \frac{y}{\alpha}\right)^2, \tag{3.16}$$

a transcendental equation, which has one or two solutions according to the value of the parameter α . Hence, the solutions of this transcendental equation give us the bound states.

4. CONDITION ON THE NUMBER OF BOUND STATES FOR AN ATTRACTIVE POTENTIAL

In this chapter, we summarize some conditions on the number of bound states of an attractive potential for s-wave ($l = 0$, angular momentum quantum number) states for some specific potentials. The number of bound states of a potential can be determined by evaluating numerical integral of the potential. Jost and Pais [57] showed that the necessary condition for the number of bound states is:

$$\frac{2m}{\hbar^2}\int_0^\infty r \mid V(r) \mid dr \geq 1. \tag{4.1}$$

Bargmann [58] presents an extended condition such that maximum number of the bound states

$$n_l \leq \frac{1}{(2l+1)}\frac{2m}{\hbar^2}\int_0^\infty r \mid V(r) \mid dr. \tag{4.2}$$

Calogero [59]-[62] has derived both upper and lower limits for the number of bound states in a central potential for s-wave states.

$$n_l \leq n_0 \leq \frac{2}{\pi}\sqrt{\frac{2m}{\hbar^2}}\int_0^\infty \mid V(r) \mid^{1/2} dr \tag{4.3}$$

with the condition $V(r)' \geq 0$.

Equation (4.3) gives a better result than equation (4.2).

4.1. Condition on the Number of Bound States of Square Well

We consider square well of depth V_0 and range R which is given by

$$V(r) \leq \begin{cases} 0 & for\ r > R, \\ -V_0 & for\ r \leq R. \end{cases} \tag{4.4}$$

By using Bargmann's integral formula, we get

$$n_0 \leq \frac{2m}{\hbar^2} \int_0^\infty r \mid V(r) \mid dr = \frac{2m}{\hbar^2} \int_0^R r V_0 dr = \frac{1}{2} \frac{2mV_0R^2}{\hbar^2}, \tag{4.5}$$

$$2n_0 \leq \frac{2mV_0R^2}{\hbar^2}. \tag{4.6}$$

By using Calogero's integral formula, we have

$$n_0 \leq \frac{2}{\pi} \sqrt{\frac{2m}{\hbar^2}} \int_0^\infty \mid V(r) \mid^{1/2} dr = \frac{2}{\pi} \sqrt{\frac{2m}{\hbar^2}} \int_0^R V_0^{1/2} dr = \frac{2}{\pi} \sqrt{\frac{2mV_0R^2}{\hbar^2}}, \tag{4.7}$$

$$\frac{\pi^2}{4} n_0^2 \leq \frac{2m}{\hbar^2} V_0 R^2. \tag{4.8}$$

The exact solutions of the number of bound states for square well is

$$\frac{\pi^2}{4}(2n_0 - 1)^2 \leq \frac{2m}{\hbar^2}V_0R^2. \tag{4.9}$$

Hence, Calogero's result is very close to exact result.

4.2. Condition on the Number of Bound States of the Dirac Delta Potential

We can calculate the maximum number of bound states of the Dirac delta potential $V(r) = -\frac{\hbar^2}{2m}\sigma\delta(r - r_i)$.

In this example, we cannot use Calogero's formula because the condition $V(r)' \geq 0$ is violated. We use Bargmann's formula so that

$$n_0 \leq \frac{2m}{\hbar^2}\int_0^\infty r \mid V(r) \mid dr = \sigma r_i \tag{4.10}$$

for s states. Demiralp and Beker [51] showed that there are at most P number of bound states for P finite number of the Dirac delta function. For one delta function, at most we have one bound state and this bound depends on the condition $\sigma r_1 > 1$.

4.3. Condition on the Number of Bound States of the Woods-Saxon Potential

The Woods-Saxon potential is given by

$$V_{WS}(r) = -\frac{V_0}{1 + e^{\frac{r-R}{a}}}. \tag{4.11}$$

For nuclear physics applications, the parameter R is the average radius of the nucleus, and the parameter a is taken as the thickness of the surface layer of nucleus. We can

obtain a condition on the number of bound states of the Woods-Saxon potential by applying Calogero's integral formula. By using Calogero's formula, we have a condition on the number of the bound states:

$$n_0 \leq \frac{2}{\pi}\sqrt{\frac{2m}{\hbar^2}}\int_0^\infty \mid V(r) \mid^{1/2} dr = \frac{2}{\pi}\sqrt{\frac{2m}{\hbar^2}}\int_0^\infty (\frac{V_0}{1+e^{\frac{r-R}{a}}})^{1/2} dr, \tag{4.12}$$

$$n_0 \leq \frac{4}{\pi}\sqrt{\frac{2mV_0}{\hbar^2}a^2}\ \text{arcsinh}[e^{\frac{R}{2a}}]. \tag{4.13}$$

Hence, the Woods-Saxon potential can have a finite number of bound states and it has no bound state if $\frac{4}{\pi}\sqrt{\frac{2mV_0}{\hbar^2}a^2}\ \text{arcsinh}[e^{\frac{R}{2a}}] < 1$.

4.4. Condition on the Number of Bound States of the Morse Potential

The Morse potential is given by

$$V_M(r) = D(e^{-2\alpha\frac{r-r_0}{r_0}} - 2e^{-\alpha\frac{r-r_0}{r_0}}). \tag{4.14}$$

Here, r_0 is the equilibrium interatomic distance, D is the well depth and α is a dimensionless parameter which modifies the shape of the potential. By using Bargmann's formula, we only take the attractive part of the potential by setting the positive part of the potential to zero [63]. By equating equation (4.14) to zero, we find such an $r_l = r_0(1 - \frac{ln2}{\alpha})$ value that intersects x-axes (Figure 4.4).

For the negative part of the potential $r \geq r_l = r_0(1 - \frac{ln2}{\alpha})$ and $\alpha \geq \ln 2$, we can apply Bargmann's integral formula to the Morse potential. Here r_l is the lower limit of the integral. For $0 < \alpha \leq \ln 2$, $r_l = 0$. Hence, we get the condition for the number

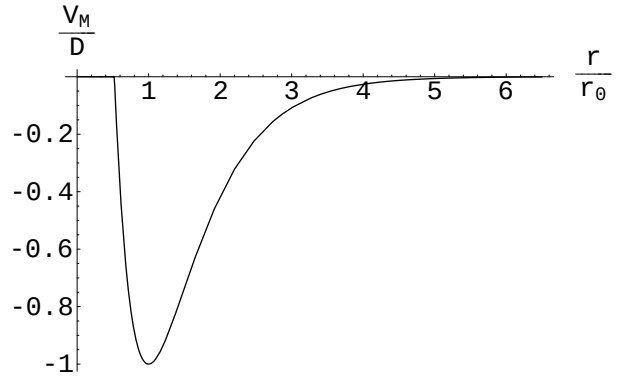


Figure 4.1. $\frac{V_M}{D}$ vs. $\frac{r}{r_0}$ for the Morse potential $V_M(r) = D(e^{-2\alpha\frac{r-r_0}{r_0}} - 2e^{-\alpha\frac{r-r_0}{r_0}})$ for $r \geq r_0(1 - \frac{ln2}{\alpha})$ where $\alpha = 1.445$ and α is calculated from the reference [64].

of bound states n_0:

$$n_0 \leq \frac{2m}{\hbar^2}\int_{r_l}^{\infty} r \mid V(r) \mid dr. \tag{4.15}$$

By evaluating the integral, we get

$$n_0 \leq \begin{cases} \frac{2mD}{\hbar^2}{r_0}^2(\frac{2\alpha+3-2\ln 2}{\alpha^2}) & for\ \alpha \geq \ln 2, \\ \frac{2mD}{\hbar^2}{r_0}^2(\frac{8e^{\alpha}-e^{2\alpha}}{4\alpha^2}) & for\ 0 < \alpha \leq \ln 2. \end{cases} \tag{4.16}$$

For realistic systems, $\alpha > \ln 2$ since we have the very repulsive part of the potential due to the Pauli exclusion effects for very small r values. Hence, for $\alpha > \ln 2$, there is no bound state for the Morse potential if $\frac{2mD}{\hbar^2}{r_0}^2(\frac{2\alpha+3-2\ln 2}{\alpha^2}) < 1$.

Here, we cannot use Calogero's formula because monotonically decreasing condition is violated for the Morse potential.

5. THE WOODS-SAXON POTENTIAL WITH POINT INTERACTIONS

The Woods-Saxon potential, which is a shell model for the nucleus, makes a good description to explain the interaction between the nucleon and the nucleus. The Woods-Saxon potential is given by

$$V_{WS}(r) = -\frac{V_0}{1 + e^{\frac{r-R}{a}}}. \tag{5.1}$$

For nuclear physics applications, the parameter R is the average radius of the nucleus, and the parameter a is taken as the thickness of the surface layer of nucleus [65]. For $a << R$, the potential approaches to $-V_0$ inside the nucleus and 0 outside the nucleus for $(r - R) >> a$ [15] (Figure 5.1).

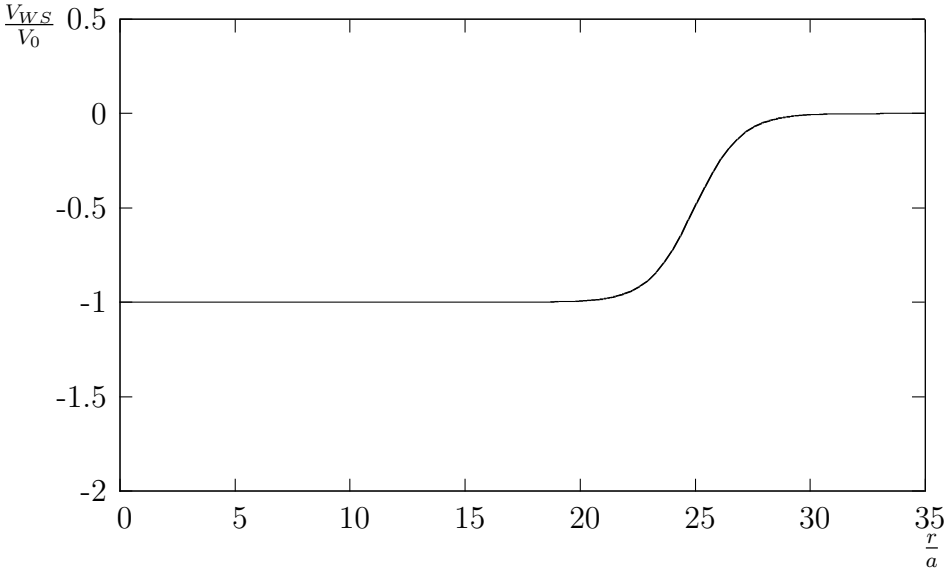


Figure 5.1. $\frac{V_{WS}}{V_0}$ vs. $\frac{r}{a}$ for the Woods-Saxon Potential $V_{WS}(r) = -\frac{V_0}{1+e^{\frac{r-R}{a}}}$ where $\frac{R}{a} = 25$.

For describing very short range (localized) interactions together with the Woods-Saxon potential, we decorate the Woods-Saxon potential with a finite number (P) of

the Dirac delta functions. The potential is given as

$$V(r) = -\frac{V_0}{1+e^{\frac{r-R}{a}}} - \frac{\hbar^2}{2m}\sum_{i=1}^{P}\sigma_i\delta(r-r_i). \tag{5.2}$$

Here, r_i's are the positions of P Dirac delta functions and the strengths σ_i's are arbitrary real numbers (Positive σ_i represents an attractive potential while negative σ_i represents a repulsive one.). We treat (-$\frac{\hbar^2}{2m}\sigma_i$) as the strengths of the Dirac delta functions for calculational convenience. For $l = 0$ (l is the angular momentum quantum number), we search for the solutions of the time-independent Schrödinger equation

$$-\frac{\hbar^2}{2m}\nabla^2\Phi + V\Phi = E\,\Phi \ . \tag{5.3}$$

For bound states, we take

$$E = -\frac{\hbar^2 k^2}{2m} \tag{5.4}$$

and

$$\Phi = \frac{\Psi(r)}{r}. \tag{5.5}$$

We obtain from equation (5.3)

$$\frac{d^2\Psi(r)}{dr^2} + \left(\frac{2m}{\hbar^2}\frac{V_0}{1+e^{\frac{r-R}{a}}} + \sum_{i=1}^{P}\sigma_i\delta(r-r_i) - k^2\right)\Psi(r) = 0. \tag{5.6}$$

We denote $(0, r_1)$ as the 1^{st}, (r_i, r_{i+1}) as the $(i+1)^{th}$, and (r_P, ∞) as the $(P+1)^{th}$ intervals for $i = 1, ..., P-1$. For $r \neq r_i$ equation (5.6) reduces to

$$\frac{d^2\Psi(r)}{dr^2} + \left[\left(\frac{2m}{\hbar^2}\frac{V_0}{1+e^{\frac{r-R}{a}}}\right) - k^2\right]\Psi(r) = 0. \tag{5.7}$$

By defining

$$y = \frac{1}{1 + e^{\frac{r-R}{a}}}, \tag{5.8}$$

$$-\beta^2 = \frac{2mE}{\hbar^2}a^2 = -k^2a^2 \tag{5.9}$$

and

$$\gamma^2 = \frac{2mV_0}{\hbar^2}a^2, \tag{5.10}$$

equation (5.7) takes the following form:

$$y(1-y)\frac{d^2\Psi(y)}{dy^2} + (1-2y)\frac{d\Psi(y)}{dy} + \frac{\gamma^2 y - \beta^2}{y(1-y)}\Psi(y) = 0. \tag{5.11}$$

By introducing

$$\Psi(y) = y^{\nu}(1-y)^{\mu} f(y), \tag{5.12}$$

this differential equation reduces to hypergeometric differential equation:

$$y(1-y)\frac{d^2 f(y)}{dy^2} + [2\nu + 1 - y(2\nu + 2\mu + 2)]\frac{df(y)}{dy} - (\mu+\nu)(\mu+\nu+1)f(y) = 0 \tag{5.13}$$

(where $\nu = \beta$, and $\mu^2 = \beta^2 - \gamma^2$). This equation has two linearly independent solutions

$$f_1(y) = {}_2F_1(\mu + \nu,\ \mu + \nu + 1,\ 2\nu + 1; y) \tag{5.14}$$

and

$$f_2(y) = y^{-2\nu}\ {}_2F_1(\mu - \nu,\ \mu - \nu + 1, 1 - 2\nu; y) \tag{5.15}$$

where ${}_2F_1(\alpha,\ \beta,\ \gamma; y)$ is the hypergeometric function. The general solution of equation (5.13) is

$$f\,(y) = c_1\ {}_2F_1(\mu{+}\nu,\ \mu{+}\nu{+}1,\ 2\nu{+}1;\ y){+}c_2 y^{-2\nu}\ {}_2F_1(\mu{-}\nu,\ \mu{-}\nu{+}1, 1{-}2\nu; y). \quad (5.16)$$

For bound states, we note that $\gamma^2 > \beta^2$, and $\mu = i\epsilon$ where $\epsilon = \sqrt{\gamma^2 - \beta^2}$. From now on, for a short-hand notation, we will use notations

$$F(y) \equiv\ {}_2F_1(\mu + \nu,\ \mu + \nu + 1,\ 2\nu + 1;\ y) \quad (5.17)$$

and

$$G(y) \equiv y^{-2\nu}\ {}_2F_1(\mu - \nu,\ \mu - \nu + 1, 1 - 2\nu;\ y). \quad (5.18)$$

Since $r = 0$ and $r = \infty$ correspond to $y_0 \cong 1 (R \gg a)$ and $y = 0$, we have $\psi(y_0) = 0$ and $\psi(0) = 0$ as the boundary conditions. Let us define

$$\Psi_A = y^\nu (1 - y)^\mu F \quad (5.19)$$

and

$$\Psi_B = y^\nu (1 - y)^\mu [F - \lambda G] \quad (5.20)$$

where

$$\lambda = \frac{F(y_0)}{G(y_0)} \quad (5.21)$$

and

$$y_0 = \frac{1}{1 + e^{-\frac{R}{a}}}. \quad (5.22)$$

For $\nu > 0$, the boundary conditions at $y = 0$ and $y = y_0$ are satisfied since $\psi_A(0) = 0$ and $\psi_B(y_0) = 0$, respectively. Thus, for the bound state solutions of equation (5.6), we take wavefunction

$$\Psi_1 = b_1 \Psi_B(y) \tag{5.23}$$

for the first (leftmost) region and

$$\Psi_{p+1} = a_{p+1} \Psi_A(y) \tag{5.24}$$

for the wavefunction of the $(p+1)^{th}$ (rightmost) interval. For the intermediate regions, we take the wavefunctions in terms of linear combinations of Ψ_A and Ψ_B,

$$\Psi_i = a_i \ \Psi_A + b_i \ \Psi_B. \tag{5.25}$$

We can find constants a_i and b_i by applying the boundary conditions at the interfaces of the intervals and normalizing the wavefunction. If we integrate equation (5.6) between the interval $r_i - \epsilon$ and $r_i + \epsilon$, and take the limit $\epsilon \to 0^+$, we find that the derivative of Ψ will have a finite jump at $r = r_i$. By using the continuity of wavefunction and the jump of its derivative, we can obtain the matrix equation

$$\begin{bmatrix} \Psi_A & \Psi_B \\ \Psi_A^{'} & \Psi_B^{'} \end{bmatrix} \begin{bmatrix} a_{i+1} \\ b_{i+1} \end{bmatrix} = \begin{bmatrix} \Psi_A & \Psi_B \\ \Psi_A^{'} - \sigma_i \Psi_A & \Psi_B^{'} - \sigma_i \Psi_B \end{bmatrix} \begin{bmatrix} a_i \\ b_i \end{bmatrix} \tag{5.26}$$

where primes stand for differentiations with respect to r. If we solve this equation for the column vector $\begin{bmatrix} a_{i+1} \\ b_{i+1} \end{bmatrix}$, we obtain the recursion relation

$$\begin{bmatrix} a_{i+1} \\ b_{i+1} \end{bmatrix} = \begin{bmatrix} 1 + \frac{\sigma_i}{\mathcal{W}_i} \Psi_A \Psi_B & \frac{\sigma_i \Psi_B^2}{\mathcal{W}_i} \\ -\frac{\sigma_i \Psi_A^2}{\mathcal{W}_i} & 1 - \frac{\sigma_i}{\mathcal{W}_i} \Psi_A \Psi_B \end{bmatrix} \begin{bmatrix} a_i \\ b_i \end{bmatrix} \tag{5.27}$$

where we have used the Wronskian

$$\mathcal{W}_i\left[\Psi_A\left(r\right),\Psi_B\left(r\right)\right]=W_i\left[F_i,G_i\right]\frac{\lambda}{a}y_i^{2\nu+1}(1-y_i)^{2\mu+1} \tag{5.28}$$

(Here, we denote the Wronskian of F and G as W. W_i is the Wronskian calculated at $y=y_i$.)

By substituting Ψ_A and Ψ_B into equation (5.27), we get

$$\begin{bmatrix} a_{i+1} \\ b_{i+1} \end{bmatrix} = \mathbb{M}_i \begin{bmatrix} a_i \\ b_i \end{bmatrix} \tag{5.29}$$

where the transfer matrix, $\mathbb{M}_i$ is given as

$$\mathbb{M}_i = \begin{bmatrix} 1+\frac{\sigma_i a}{\lambda}\frac{1}{W_i y_i(1-y_i)}F_i(F_i-\lambda G_i) & \frac{\sigma_i a}{\lambda}\frac{1}{W_i y_i(1-y_i)}(F_i-\lambda G_i)^2 \\ -\frac{\sigma_i a}{\lambda}\frac{1}{W_i y_i(1-y_i)}F_i^2 & 1-\frac{\sigma_i a}{\lambda}\frac{1}{W_i y_i(1-y_i)}F_i(F_i-\lambda G_i) \end{bmatrix} \tag{5.30}$$

in terms of F_i and G_i.

Here, F_i and G_i denote $F(y_i)$ and $G(y_i)$ respectively. By using transfer matrix method which was given in Chapter 2, we get the following equation

$$x_{22}(\beta)=0 \tag{5.31}$$

which gives the bound state energy spectrum of the system by using the roots β ($-\beta^2=-k^2a^2$) of x_{22}. It is instructive to obtain the equation for the energy spectrum for P=1 case in order to observe how the energy eigenvalues change as a function of ζ (We define a dimensionless quantity $\zeta=\sigma a$.). For $P=1$, the total transfer matrix reduces to $\mathbb{M}_1$. By equating x_{22} element of this matrix to zero, and inserting $W\left[\Psi_A\left(r\right),\Psi_B\left(r\right)\right]$,

we get the following eigenvalue equation

$$\sigma a = \frac{\lambda(F(y_1)G(y_1)' - F(y_1)'G(y_1))y_1(1-y_1)}{F(y_1)(F(y_1) - \lambda G(y_1))} \tag{5.32}$$

where $y_1 = \frac{1}{1+e^{\frac{(r_1-R)}{a}}}$ for the Dirac delta function located at r_1 and $'$ denotes derivative with respect to r. Since F, G are functions of β, we solve this equation for the eigenvalues. Note that equation (5.32) reduces to the well known energy eigenvalue equation of the Woods-Saxon potential as $\sigma \to 0$,

$$\lambda = \frac{F(y_0)}{G(y_0)} \to 0 \qquad \text{or} \qquad F(y_0) \to 0 \quad . \tag{5.33}$$

For $V_0 = 0$, our results reduce to the results in reference [51] with the Dirac delta functions. For demonstrating this limit case, we take the following scaled wavefunctions

$$\Psi_{A,new} = -\sqrt{\pi}\Psi_A \tag{5.34}$$

and

$$\Psi_{B,new} = \frac{\Psi_B}{\sqrt{\pi}} \tag{5.35}$$

with the corresponding Wronskian $\mathcal{W}_{i,new}$. For $V_0 = 0$, $\gamma = 0$ so that $\mu = \nu = \beta$ and $\beta = ka$.

Here, we use the series expansion of the hypergeometric function

$${}_2F_1(a,b,c;y) = \frac{\Gamma(c)}{\Gamma(a)\Gamma(b)} \sum_{n=1}^{\infty} \frac{\Gamma(a+n)\Gamma(b+n)}{\Gamma(c+n)} \frac{y^n}{n!}. \tag{5.36}$$

For the special case $b = c$, we have

$$ {}_2F_1(a,b,b;y) = 1 + ay + a(a+1)\frac{y^2}{2!} + a(a+1)(a+2)\frac{y^3}{3!} + ... = (1-y)^{-a}. \quad (5.37) $$

For our limit case,

$$ F(y) =_2 F_1(\mu+\nu,\ \mu+\nu+1,\ 2\nu+1;\ y) =_2 F_1(2\beta,\ 1+2\beta,\ 1+2\beta;\ y) = (1-y)^{-2\beta} \quad (5.38) $$

and

$$ G(y) = y^{-2\beta}\ {}_2F_1(\mu-\nu,\ \mu-\nu+1, 1-2\nu;\ y) = y^{-2\beta}\ {}_2F_1(0,\ 1, 1-2\beta;\ y) = y^{-2\beta} \quad (5.39) $$

where we have used the relation of hypergeometric functions

$$ {}_2F_1(0,b,b;y) = 1. \quad (5.40) $$

The Wronskian of F and G at $y = y_1$ is

$$ W_1 = \frac{-2\beta(1-y_1)^{-2\beta} y_1^{-2\beta}}{y_1(1-y_1)} \quad (5.41) $$

and

$$ \lambda = \frac{F(y_0)}{G(y_0)} = (\frac{1}{y_0} - 1)^{-2\beta}. \quad (5.42) $$

If we insert these relations into the matrix element m_{11} of the transfer matrix $\mathbb{M}_i$, which is given in equation (5.30), we get

$$m_{11} = 1 + \frac{\sigma_i a}{\lambda} \frac{1}{W_i y_i (1 - y_i)} F_i (F_i - \lambda G_i) = 1 + \frac{\sigma_i a}{-2\beta} [(\frac{(1 - y_i)}{(1 - y_0)\frac{y_i}{y_0}})^{-2\beta} - 1]. \quad (5.43)$$

By writing y_0, y_1 in terms of exponentials, we get

$$m_{11} = 1 + \frac{-\sigma_i a}{2\beta} [e^{\frac{-2\beta r_i}{a}} - 1], \quad (5.44)$$

$$m_{11} = 1 + \frac{-\sigma_i a}{2\beta} e^{\frac{-\beta r_i}{a}} [e^{\frac{-\beta r_i}{a}} - e^{\frac{\beta r_i}{a}}]. \quad (5.45)$$

Then, for $\gamma \to 0$, $\nu = \beta$ and $\beta = ka$, we get

$$m_{11} = 1 + \frac{\sigma_i}{2k} e^{-kr_i} [e^{kr_i} - e^{-kr_i}] = 1 + \frac{\sigma_i}{k} e^{-kr_i} \sinh(kr_i). \quad (5.46)$$

Finally, we have

$$m_{11} = 1 - \sigma_i r_i \sqrt{\frac{\pi}{2}} \frac{e^{-kr_i}}{\sqrt{kr_i}} \sqrt{\frac{2}{\pi}} \frac{\sinh(kr_i)}{\sqrt{kr_i}} = 1 - \sigma_i r_i I_{\frac{1}{2}}(kr_i) K_{\frac{1}{2}}(kr_i) \quad (5.47)$$

where

$$I_{\frac{1}{2}}(x) = \frac{\sqrt{\frac{2}{\pi}}\sinh(x)}{\sqrt{x}} \tag{5.48}$$

and

$$K_{\frac{1}{2}}(x) = \frac{\sqrt{\frac{\pi}{2}}e^{-x}}{\sqrt{x}} \tag{5.49}$$

are the modified Bessel functions of order $\frac{1}{2}$.

By performing the same steps for the other matrix elements in equation (5.30) we obtain:

$$\mathbb{M}_i = \begin{bmatrix} 1+\sigma_i r_i I_{\frac{1}{2}}(kr_i)K_{\frac{1}{2}}(kr_i) & \sigma_i r_i (I_{\frac{1}{2}}(kr_i))^2 \\ -\sigma_i r_i (K_{\frac{1}{2}}(kr_i))^2 & 1-\sigma_i r_i I_{\frac{1}{2}}(kr_i)K_{\frac{1}{2}}(kr_i) \end{bmatrix}. \tag{5.50}$$

These matrices are exactly same matrices which are given in reference [51] when we have only P Dirac delta functions for three-dimensional delta shells. For only one Dirac delta function case, we get the following eigenvalue equation by using $m_{22} = 0$

$$1-\sigma_1 r_1 I_{\frac{1}{2}}(kr_1)K_{\frac{1}{2}}(kr_1) = 0. \tag{5.51}$$

This is the result of Antoine et al. [66].

For atomic physics applications, we take m as the mass of electron, $V_0 = 4.6$ eV and the parameter $a = 0.3$Å which lead to $\gamma = 0.33$ [29]. For nuclear physics applications, we take m as the mass of proton, $V_0 = 38$ MeV and $a = 0.49$ fm, which lead to $\gamma = 0.66$ [15]. In addition to these, by using reference [67] for lambda Λ^0

nucleon, the mass of $\Lambda^0 = 1116\ MeV/c^2$, $V_0 = 27.7$ MeV, and $a = 0.5$ fm, we find $\gamma = 0.62$. Since these realistic values give $\gamma = 0.33 - 0.66$, we take $\gamma = 0.5$ for numerical calculations of ground state energies for $P = 1$. We also take $\frac{R}{a} = 25$.

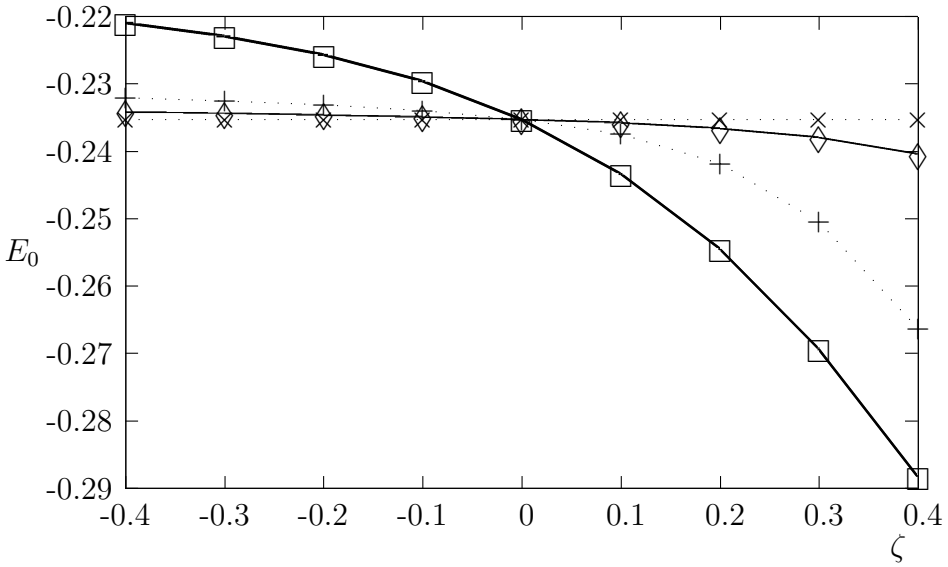


Figure 5.2. Ground state energy E_0 (in units of $\frac{\hbar^2}{2ma^2}$) vs. $\zeta = \sigma a$ for $\gamma = 0.5$. ($\Diamond$, $+$, $\Box$, $\times$ represent $r_1 = 2a, 4a, 10a, 30a$ cases respectively.)

For different r_1 values ($r_1 = 2a, 4a, 10a, 30a$), we calculated numerically the ground state energy, E_0, in units of $\frac{\hbar^2}{2ma^2}$. Figure 5.2 shows how E_0 changes as a function of ζ. We note that the change in E_0 as a function of ζ shows an interesting behavior which can be explained by using equation (5.51). For $\sigma_1 \to \infty$, $I_{\frac{1}{2}}(kr_1)K_{\frac{1}{2}}(kr_1)$ goes to zero to satisfy equation (5.51). $I_{\frac{1}{2}}(x)K_{\frac{1}{2}}(x)$ is a monotonically decreasing function of x and $I_{\frac{1}{2}}(x)K_{\frac{1}{2}}(x) \to \frac{1}{2x}$ as $x \to \infty$ [51]. Then, we can obtain the asymptotic behavior of the ground state energy. For $\sigma_1 \to \infty$,

$$1 - \sigma_1 r_1 \frac{1}{2k_1 r_1} \approx 0. \tag{5.52}$$

Hence,

$$k_1 \approx \frac{\sigma_1}{2}. \tag{5.53}$$

Thus,

$$E_{0,\delta} \approx -\frac{\hbar^2}{2m}(\frac{\sigma_1}{2})^2 = -\frac{\hbar^2}{8ma^2}\zeta_1^2 \tag{5.54}$$

as

$$\zeta_1 = \sigma_1 a \rightarrow \infty. \tag{5.55}$$

Since the Woods-Saxon potential is purely attractive, then the ground state energy for V(r) is lower than the corresponding ground state energy $E_{0,\delta}$ for only one delta function interaction ($V_0 = 0$). Thus, for attractive case, the ground state energy decreases without any limit as ζ increases.

Cohn [59] and Calogero [60, 61, 62] have shown that for an attractive, monotonically non-decreasing ($\frac{dV(r)}{dr} \geq 0$) potential V(r), the number of bound states N has an upper limit :

$$N \leq \frac{2}{\pi}\sqrt{\frac{2m}{\hbar^2}}\int_0^\infty (\mid V(r) \mid)^{\frac{1}{2}} dr. \tag{5.56}$$

For the Woods-Saxon potential V_{WS}, the integral in equation (5.56) can be obtained exactly. Thus, we get

$$N_{WS} \leq \frac{4}{\pi}\,\gamma\,\text{arcsinh}[e^{\frac{R}{2a}}] \tag{5.57}$$

where $\gamma = \sqrt{\frac{2mV_0}{\hbar^2}a^2}$ and N_{WS} is the number of bound states for V_{WS}. Hence, the Woods-Saxon potential can have a finite number of bound states and it has no bound state if $\frac{4}{\pi}\,\gamma\,\text{arcsinh}[e^{\frac{R}{2a}}] < 1$. Unfortunately, the Calogero-Cohn bound (equation (5.56)) can not be applied to V(r) since equation (5.56) leads to square root of a function plus a delta function and the monotonically non-decreasing condition for the potential is

violated at the location of delta function. It is shown that there will be at most P bound states for a potential which contains only P delta functions [51, 68]. However, for all attractive P delta functions, for sufficiently large σ_i values, delta interactions can induce P bound states [51, 68]. Thus, for this case, by including the Woods-Saxon potential part, V(r) can have at least $\max\{N_{WS}, P\}$.

For a repulsive delta function at $r = r_1$, by using the Hellmann-Feynman theorem, we find

$$\frac{\partial E_n}{\partial |\sigma_1|} = \frac{\hbar^2}{2m} |\Psi_n(r_1)|^2 . \tag{5.58}$$

$\Psi_n(r_1)$ depends also on $|\sigma_1|$ and, for repulsive case, $\Psi_n(r_1)$ should go to zero as $|\sigma_1| \to \infty$ for a bound state. (If $\Psi_n(r_1) \neq 0$ as $|\sigma_1| \to \infty$, by integrating equation (5.58) with respect to $|\sigma_1|$, one can show that E_n becomes larger than zero and Ψ_n will not be a bound state anymore since it can not decay to zero as $r \to \infty$.) Thus, for one delta function case, $\Psi(r_1) = 0$ leads to $F(y_1) = 0$ for $y_1 \neq 0$. (For $y_1 = 0$ ($r \to \infty$), $\Psi(r_1) = 0$ is already satisfied by the boundary condition at infinity.) Hence, for $y_1 \neq 0$, the roots of $F(y_1) = 0$ give β values for bound states. Since $\Psi(r)$ should decay to zero for $y \to 0$ ($r \to \infty$), we take $\beta > 0$.

We consider the Woods-Saxon Hamiltonian $H_{WS} = -\frac{\hbar^2}{2m}\nabla^2 + V_{WS}$ for a given V_{WS}. Since it has only a finite number of bound states, we assume that there are only N bound states for a given V_{WS} ($N > 0$). Thus, we have the ordering of bound state energies:

$$E_0{}^{WS} < E_1{}^{WS} < ... < E_i{}^{WS} < ... < E_N{}^{WS} < 0 \tag{5.59}$$

where subscript i represents the number of nodes of the corresponding wavefunction. For a repulsive delta interaction located at $r = r_1$ (here we assume r_1 is not a position of a node of the wavefunctions for V_{WS}), we get the bound state energies $E_{i,|\sigma|}$ for $V(r)$.

Thus, for a repulsive delta interaction, we have

$$E_i{}^{WS} < E_{i,|\sigma|} \tag{5.60}$$

for $i = 0, ..., N$. For any function ϕ_{N+1} which satisfies boundary conditions and has $(N+1)$ nodes, we have $\langle \phi_{N+1} | H_{WS} | \phi_{N+1} \rangle \geq 0$. Thus, ϕ_{N+1} is not a bound state. The limit $|\sigma_1| \to \infty$ leads to $\Psi_i(r_1) \to 0$ and an increase in the number of nodes of wavefunctions by one. Since $\Psi_i(r)$ is an eigenfunction for the Hamiltonian with $V(r)$, but not for H_{WS} and $\Psi_i(r)$ depends on σ_1 and it has $(i+1)$ nodes as $|\sigma_1| \to \infty$. Then, we have

$$E_{i+1}^{WS} < \lim_{|\sigma_1|\to\infty} \langle \Psi_i \left| H^{WS} \right| \Psi_i \rangle < \lim_{|\sigma_1|\to\infty} \langle \Psi_i \mid H \mid \Psi_i \rangle = E_{i,\infty}. \tag{5.61}$$

Hence, $E_{i+1}^{WS} < E_{i,\infty}$ for $i = 0, 1, ..., N-1$. Since there is no eigenfunction of H_{WS} with $N+1$ nodes, we have $0 \leq E_{N,\infty}$ and the number of bound states is lowered at least by one as $|\sigma_1| \to \infty$. (Here we assume that delta function is not located at the positions of the nodes of bound state eigenfunctions of H_{WS}. If it is located at the position of a node of $\Psi_{N,WS}$, then $\Psi_{N,WS}$ and E_N^{WS} will not change and $\Psi_{N,WS} = \Psi_N$. However, as $|\sigma_1| \to \infty$, Ψ_{N-1} and Ψ_N will have the same number of nodes since $\Psi_{N-1}(r_1) \to 0$ and the same node position at $r = r_1$. Thus, as $|\sigma_1| \to \infty$, Ψ_{N-1} will become identical with Ψ_N to lower the energy since $E_N^{WS} < E_{N-1,\infty}$. Thus, the number of bound states is again lowered by one as $|\sigma_1| \to \infty$.) Equation (5.58) shows that E_N is a continuous function of $|\sigma_1|$. Hence, for a sufficiently large repulsive $|\sigma_i|$ values, the number of bound states for $V(r)$ is reduced at least by one.

In Figure 5.3, we investigate the ground state energy with respect to r_1 values and take $\zeta = 0.1$ (attractive case). We see that the ground state energy has a minimum around $r_1 = 13a$ value and then increases with increasing r_1. We also obtain similar results for different strength values of delta function, $\zeta = 0.05, 0.01$ and present our results in Figure 5.4.

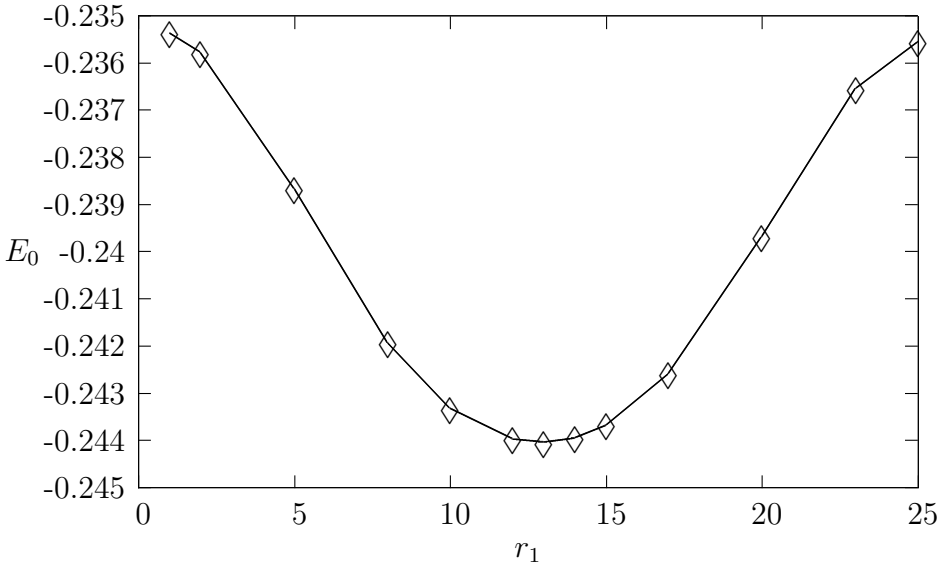


Figure 5.3. The ground state energy E_0 (in units of $\frac{\hbar^2}{2ma^2}$) vs. the position of the Dirac delta function r_1 for $\zeta = \sigma a = 0.1$ (attractive interaction), $\gamma = 0.5$. Here, r_1 is in units of a .

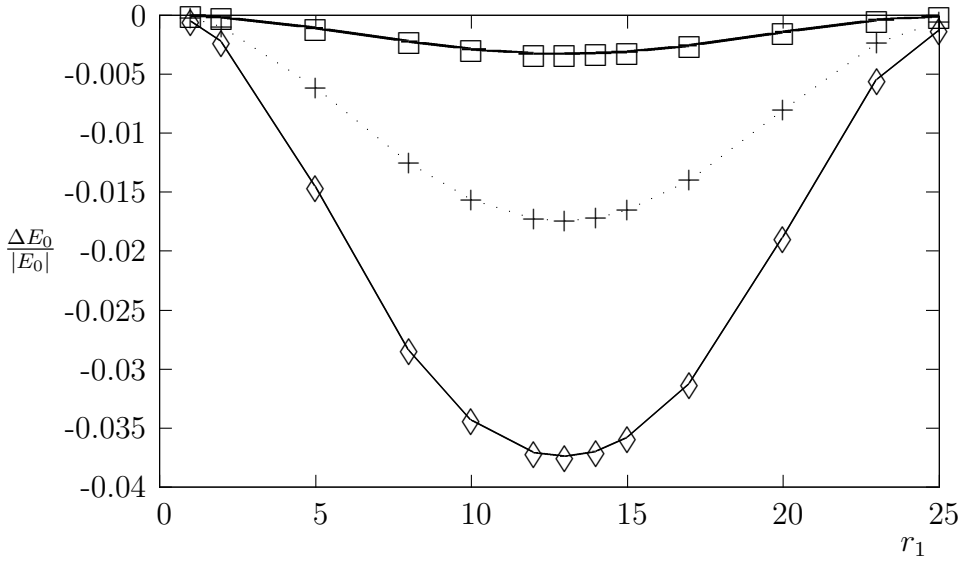


Figure 5.4. $\frac{\Delta E_0}{|E_0|} = \frac{E_0^{W,\delta} - E_0}{|E_0|}$ vs. the position of the Dirac delta function r_1 for $\zeta = \sigma a$ (attractive interaction) where $E_0^{W,\delta}$, E_0 stand for the ground state energies for the Woods-Saxon potential with delta function and the Woods-Saxon potential, respectively for $\gamma = 0.5$. Here, r_1 is in units of a. ($\square$, $+$, $\Diamond$ represent $\zeta = 0.01, 0.05, 0.1$ cases respectively.)

In Figure 5.5, we take $\zeta = -0.1$ (repulsive case) and observe that the ground state energy has also a maximum around $r_1 = 13a$ value and then decreases with

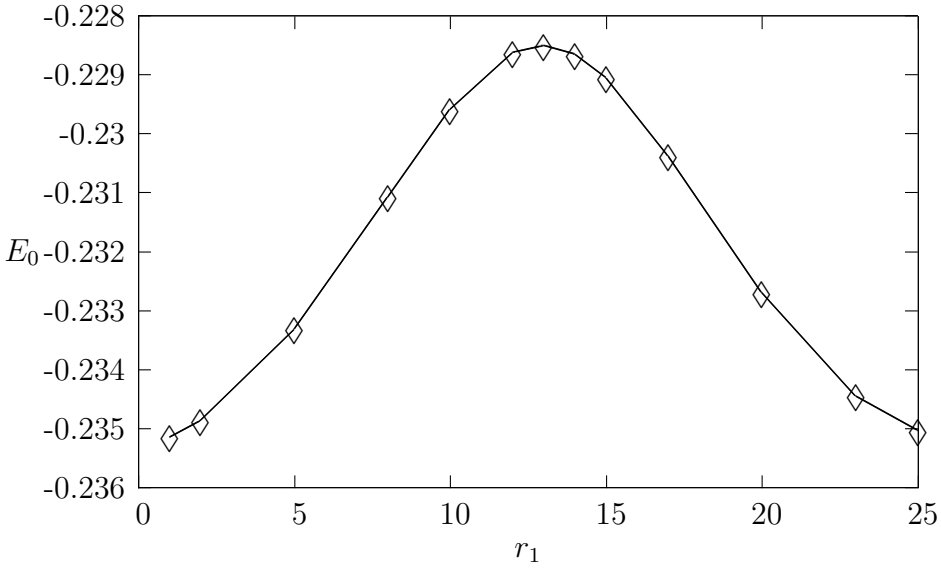


Figure 5.5. The ground state energy E_0 (in units of $\frac{\hbar^2}{2ma^2}$) vs. the position of the Dirac delta function r_1 for $\zeta = \sigma a = -0.1$ (repulsive interaction), $\gamma = 0.5$. Here, r_1 is in units of a .

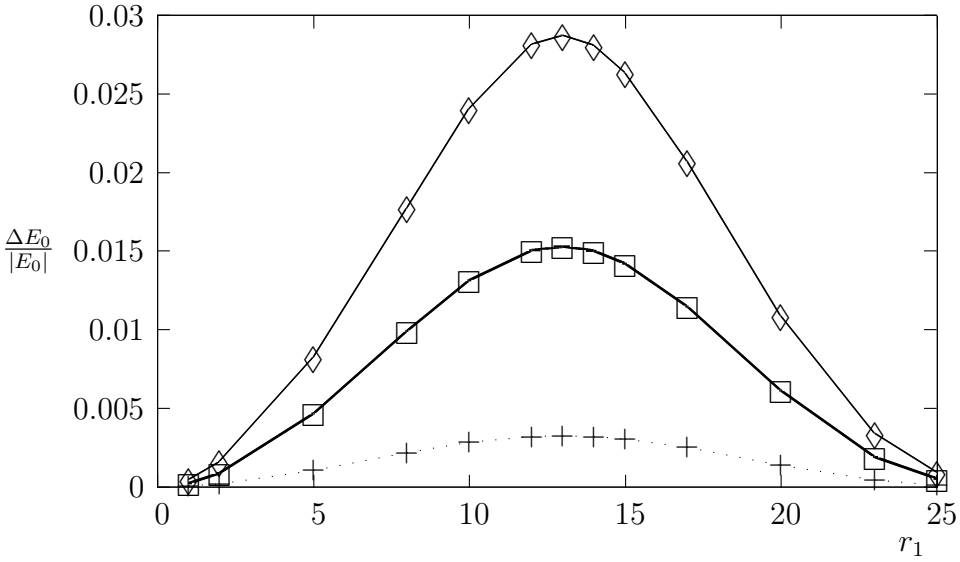


Figure 5.6. $\frac{\Delta E_0}{|E_0|} = \frac{E_0^{W,\delta} - E_0}{|E_0|}$ vs. the position of the Dirac delta function r_1 for $\zeta = \sigma a$ (repulsive interaction) where $E_0^{W,\delta}$, E_0 stand for the ground state energies for the Woods-Saxon potential with delta function and the Woods-Saxon potential, respectively for $\gamma = 0.5$. Here, r_1 is in units of a. ($+$, $\square$, $\Diamond$ represent $\zeta = -0.01, -0.05, -0.1$ cases respectively.)

increasing r_1 values. The Dirac delta part of the potential begins to lose its effect for $r_1 > R = 25a$. We also obtain similar results for different strength values of delta

function, $\zeta = -0.05, -0.01$ and present our results in Figure 5.6. The effect of the Dirac delta function is diminished for very small and very large values because the wave function goes to zero due to the boundary conditions.

Table 5.1. Configuration Numbers (N_{conf}) for the ordered (P=1, 2) Dirac delta functions. A and R denote the attractive and repulsive Dirac delta functions respectively.

N_{conf}	P=1	P=2
1	A	A^2
2	R	AR
3	-	RA
4	-	R^2

For $P > 1$, we can find energy spectrum by using the total transfer matrices and equation $x_{22}(\beta) = 0$.

We calculate the roots of equation (5.31) for the $P = 1, 2$ cases for the attractive and repulsive Dirac delta functions at different locations. For demonstrating all these results together in a figure, we define configuration numbers for different ordered configurations which are presented in Table 5.1. For example, for P=2, two attractive delta functions is shown as AA which has the configuration number 1, attractive and repulsive (AR), delta functions has configuration number 2, etc. Two delta functions are located at different locations. When we calculate the eigenvalue equation numerically for two delta functions case ($P = 2$), we take $\gamma = 0.5$ to get eigenvalues.

In Figures (5.7)-(5.10), we illustrate the ground state energy with respect to configuration numbers for $|\zeta| = 0.1, 0.5$. We also note that the attractive delta function case is more effective than the repulsive delta function case by comparing the AA($N_{conf} = 1$) and RR($N_{conf} = 4$) cases. This effect can also be seen in Figure 5.2 for one delta function case. We can explain this effect by considering the change of the wave function. The wave function has a kink and its derivative has a finite jump at $r = r_i$. Hence, the wave function forms an outward kink and increases the value of $|\Psi|^2$

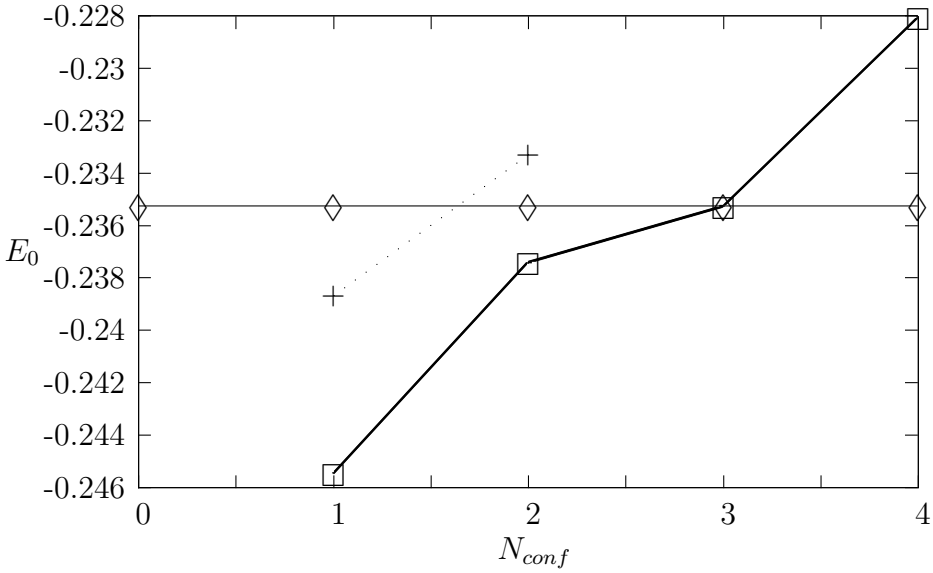


Figure 5.7. The ground state energy E_0 (in units of $\frac{\hbar^2}{2ma^2}$) vs. configuration of different arrangements of the Dirac delta functions at $r_1 = 5a$ and $r_2 = 10a$ for $\zeta = \sigma a = 0.1$ and $\gamma = 0.5$. ($\Diamond$, $+$, $\Box$ represent $P = 0, 1, 2$ cases respectively.)

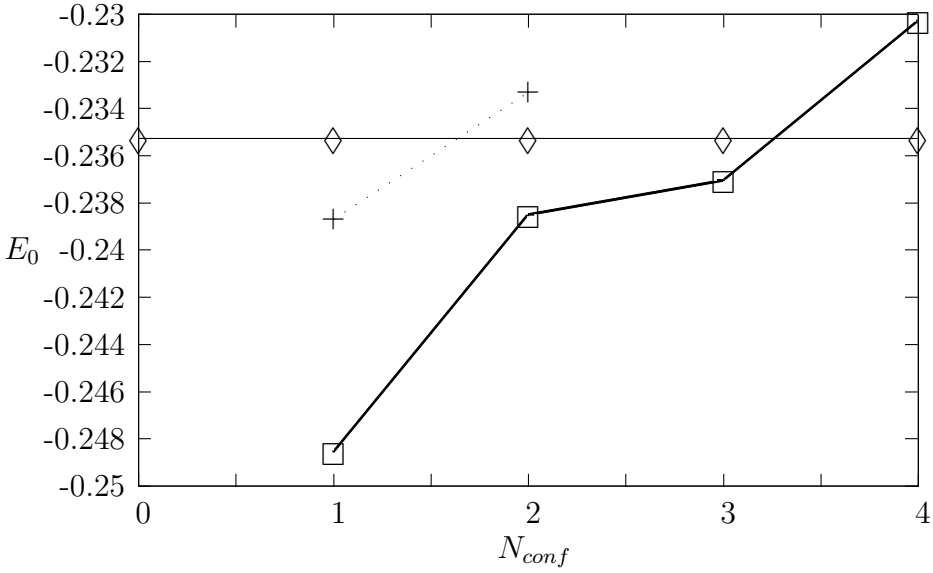


Figure 5.8. The ground state energy E_0 (in units of $\frac{\hbar^2}{2ma^2}$) vs. configuration of different arrangements of the Dirac delta functions at $r_1 = 5a$ and $r_2 = 20a$ for $\zeta = \sigma a = 0.1$ and $\gamma = 0.5$. ($\Diamond$, $+$, $\Box$ represent $P = 0, 1, 2$ cases respectively.)

for the attractive delta function and forms an inward kink and decreases the value of $|\Psi|^2$ for the repulsive delta function. Thus, the attractive Dirac delta functions result in bigger changes in the ground state energy since the energy change due to the Dirac delta functions is proportional to $|\Psi|^2$.

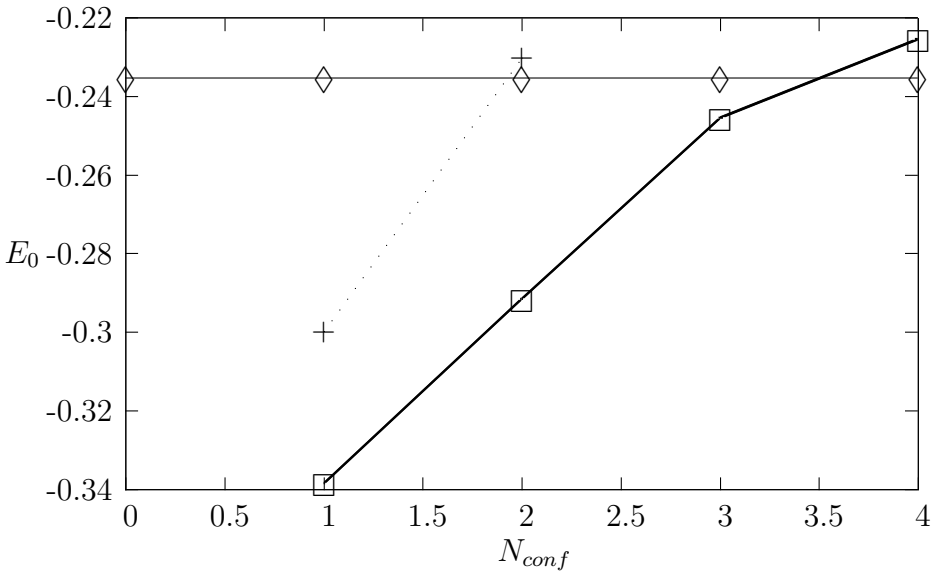


Figure 5.9. The ground state energy E_0 (in units of $\frac{\hbar^2}{2ma^2}$) vs. configuration of different arrangements of the Dirac delta functions at $r_1 = 5a$ and $r_2 = 10a$ for $\zeta = \sigma a = 0.5$ and $\gamma = 0.5$. ($\Diamond$, $+$, $\Box$ represent $P = 0, 1, 2$ cases respectively.)

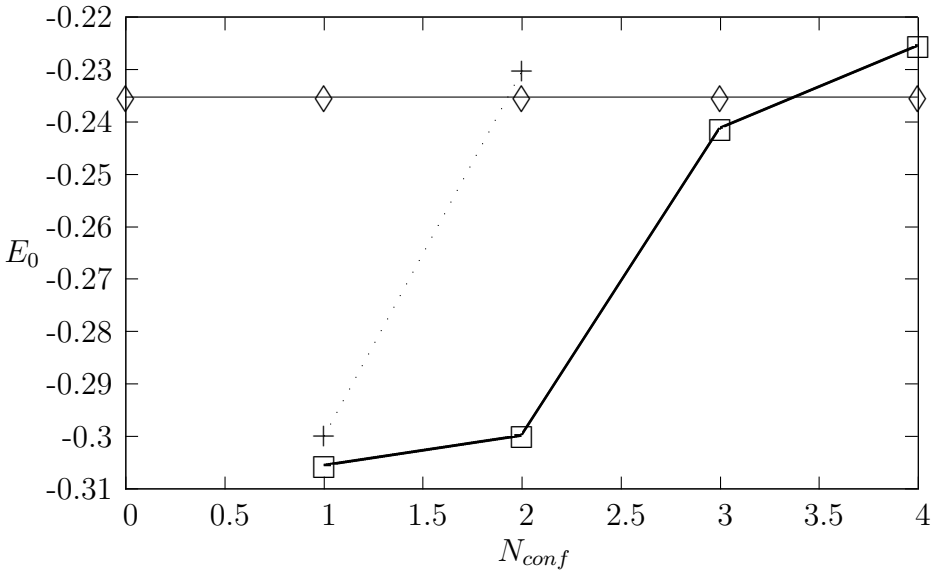


Figure 5.10. The ground state energy E_0 (in units of $\frac{\hbar^2}{2ma^2}$) vs. configuration of different arrangements of the Dirac delta functions at $r_1 = 5a$ and $r_2 = 20a$ for $\zeta = \sigma a = 0.5$ and $\gamma = 0.5$. ($\Diamond$, $+$, $\Box$ represent $P = 0, 1, 2$ cases respectively.)

6. THE MORSE POTENTIAL WITH POINT INTERACTIONS

The Morse potential is very successful to explain the potential energy of a diatomic molecule. The Morse potential includes the bond breaking effects. For this reason compared to the harmonic oscillator, it gives a better approximation.

The Morse potential is given by

$$V_M(r) = D(e^{-2\alpha\frac{r-r_0}{r_0}} - 2e^{-\alpha\frac{r-r_0}{r_0}}). \tag{6.1}$$

Here, r_0 is the equilibrium interatomic distance, D is the well depth and α is a dimensionless parameter which modifies the shape of the potential [65] (Figure 6.1).

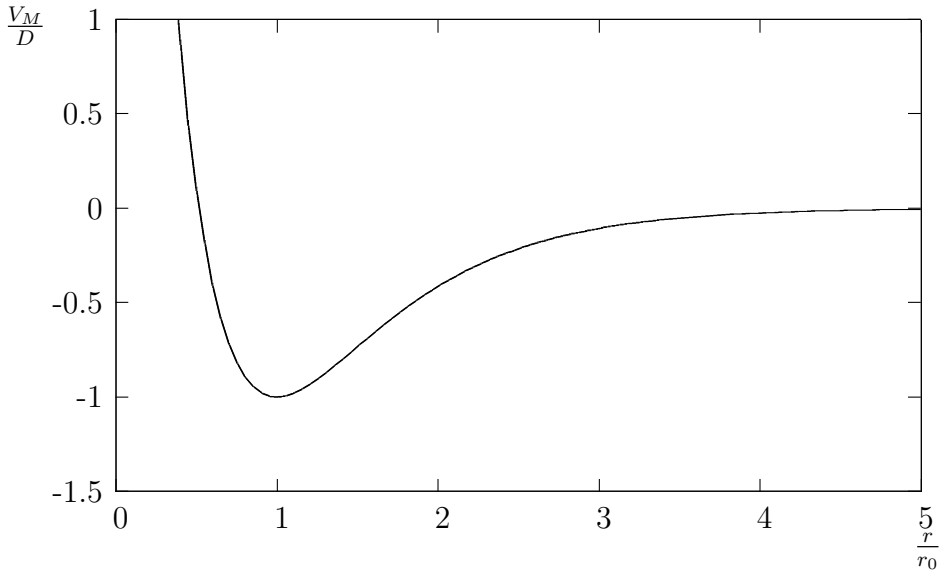


Figure 6.1. $\frac{V_M}{D}$ vs. $\frac{r}{r_0}$ for the Morse potential $V_M(r) = D(e^{-2\alpha\frac{r-r_0}{r_0}} - 2e^{-\alpha\frac{r-r_0}{r_0}})$ where $\alpha = 1.445$.

The Schrödinger equation for the Morse potential is exactly solvable for angular momentum $l = 0$ case [65].

Our motivation in this chapter is to investigate changes in the eigenstate solutions for the Morse potential when there are some very local deviations from the Morse

potential. By modeling very local interactions with the Dirac delta functions, we study the Schrödinger equation for the Morse potential together with a finite number (P) of the Dirac delta functions. This potential can be utilized to model systems that may have very short range interactions in addition to the Morse potential. Since these point interactions modify the energy levels for the Morse potential, it can be used to describe some realistic potentials which has roughly the Morse potential shape, but exhibits some local deviations from the Morse potential. As an example of a deviation from the Morse potential form, we mention the double-minimum potential energy curve for the first excited $^1\sum_g^+$ state of H_2 molecule [42]. We note that the Morse parameters we used are for the ground state of H_2 and our approach is for very local deformations of the Morse potential and not for the double-minimum interaction potential of the excited state of H_2 with a broad peak. As a simple model of the potential of the hydrogen molecule in a hollow, spherical C_{60} cage, our model can be used to describe the interatomic H-H interaction as the Morse potential and the interaction between H_2 and spherical C_{60} cage as a contact interaction which can be represented by the Dirac delta interaction $A\delta(r - r_0)$ where the constant A is the strength of the interaction.

For describing very short range (localized) interactions together with the Morse potential, we decorate the Morse potential with a finite number (P) of the Dirac delta functions. The potential is given as

$$V(r) = D(e^{-2\alpha\frac{r-r_0}{r_0}} - 2e^{-\alpha\frac{r-r_0}{r_0}}) - \frac{\hbar^2}{2m}\sum_{i=1}^{P}\sigma_i\delta(r - r_i). \tag{6.2}$$

Here, r_i's are the positions of P Dirac delta functions and the strengths σ_i's are arbitrary real numbers (Positive σ_i represents an attractive potential while negative σ_i represents a repulsive one.). We treat ($-\frac{\hbar^2}{2m}\sigma_i$) as the strengths of the Dirac delta functions for calculational convenience. For $l = 0$ (l is the angular momentum quantum number), we search for the solutions of the time-independent Schrödinger equation

$$-\frac{\hbar^2}{2m}\nabla^2\Phi + V\Phi = E\,\Phi \ . \tag{6.3}$$

For s-wave bound states, we take

$$E = -\frac{\hbar^2 k^2}{2m} \tag{6.4}$$

and

$$\Phi(r, \theta, \varphi) = \frac{\Psi(r)}{r} Y_{00}(\theta, \varphi). \tag{6.5}$$

By using equation (6.3), we obtain:

$$\frac{d^2\Psi(r)}{dr^2} + \left(\frac{-2m}{\hbar^2} D(e^{-2\alpha\frac{r-r_0}{r_0}} - 2e^{-\alpha\frac{r-r_0}{r_0}}) + \sum_{i=1}^{P} \sigma_i \delta(r - r_i) - k^2 \right) \Psi(r) = 0. \tag{6.6}$$

Since P number of the Dirac delta functions divide space into $P+1$ intervals, we denote $(0, r_1)$ as the 1^{st}, (r_i, r_{i+1}) as the $(i+1)^{th}$, and (r_P, ∞) as the $(P+1)^{th}$ intervals for $i = 1, ..., P-1$. For $r \neq r_i$, equation (6.6) reduces to

$$\frac{d^2\Psi(r)}{dr^2} + \left[\left(\frac{-2m}{\hbar^2} D(e^{-2\alpha\frac{r-r_0}{r_0}} - 2e^{-\alpha\frac{r-r_0}{r_0}}) \right) - k^2 \right] \Psi(r) = 0. \tag{6.7}$$

By defining

$$x = \frac{r - r_0}{r_0}\ , -\beta^2 = \frac{2mE}{\hbar^2} {r_0}^2 = -k^2 {r_0}^2 \quad \text{and } \gamma^2 = \frac{2mD}{\hbar^2} {r_0}^2, \tag{6.8}$$

equation (6.7) takes the following form:

$$\frac{d^2\Psi(x)}{dx^2} + (-\beta^2 + 2\gamma^2 e^{-\alpha x} - \gamma^2 e^{-2\alpha x})\Psi(x) = 0. \tag{6.9}$$

By using a new variable $y = \frac{2\gamma}{\alpha} e^{-\alpha x}$, equation (6.9) becomes

$$y^2 \frac{d^2\Psi(y)}{dy^2} + y\frac{d\Psi(y)}{dy} + (-\frac{\beta^2}{\alpha^2} + \frac{\gamma}{\alpha} y - \frac{1}{4}y^2)\Psi(y) = 0. \tag{6.10}$$

By introducing $\Psi(y) = y^{\frac{\beta}{\alpha}} e^{\frac{-y}{2}} f(y)$, this differential equation reduces to confluent hypergeometric differential equation with the parameters $c = \frac{2\beta}{\alpha} + 1$ and $a = \frac{\beta}{\alpha} - \frac{\gamma}{\alpha} + \frac{1}{2}$:

$$\frac{d^2 f(y)}{dy^2} + (c - y)\frac{df(y)}{dy} - af(y) = 0\ . \tag{6.11}$$

This equation has two linearly independent solutions ${}_1F_1(a, c; y)$ and $y^{1-c}\ {}_1F_1(a - c + 1,\ 2 - c; y)$ where ${}_1F_1(\alpha, \beta; y)$ is the confluent hypergeometric function. The general solution of equation (6.11) is

$$f(y) = c_1\ {}_1F_1(a, c; y) + c_2\ y^{1-c}\ {}_1F_1(a - c + 1, 2 - c; y). \tag{6.12}$$

For the Morse potential, we note that $\gamma^2 > \beta^2$ for bound states.

Hence, the solutions of equation (6.7) are

$$\Psi_1 = y^{\frac{\beta}{\alpha}} e^{\frac{-y}{2}}\ {}_1F_1(\frac{\beta}{\alpha} - \frac{\gamma}{\alpha} + \frac{1}{2}, \frac{2\beta}{\alpha} + 1; y) \tag{6.13}$$

and

$$\Psi_2 = y^{\frac{\beta}{\alpha}} e^{\frac{-y}{2}} y^{-\frac{2\beta}{\alpha}}\ {}_1F_1(-\frac{\beta}{\alpha} - \frac{\gamma}{\alpha} + \frac{1}{2}, -\frac{2\beta}{\alpha} + 1; y). \tag{6.14}$$

From now on, for a short-hand notation, we will use notations

$$F(y) \equiv \ {}_1F_1(\frac{\beta}{\alpha} - \frac{\gamma}{\alpha} + \frac{1}{2}, \frac{2\beta}{\alpha} + 1; y) \tag{6.15}$$

and

$$G(y) \equiv y^{-\frac{2\beta}{\alpha}} \ {}_1F_1(-\frac{\beta}{\alpha} - \frac{\gamma}{\alpha} + \frac{1}{2}, -\frac{2\beta}{\alpha} + 1; y). \tag{6.16}$$

Since $r = 0$ and $r = \infty$ correspond to $y_0 = \frac{2\gamma}{\alpha}e^{\alpha}$ and $y = 0$, we have $\psi(y_0) = 0$ and $\psi(0) = 0$ as the boundary conditions. For $r = \infty$ $(y = 0)$, the first solution of equation (6.7)

$$\Psi_1 = y^{\frac{\beta}{\alpha}} e^{\frac{-y}{2}} F(y) = 0 \tag{6.17}$$

satisfies the boundary condition. However, for $r = 0$ $(y = y_0)$, the second solution of equation (6.7)

$$\Psi_2 = y_0^{\frac{\beta}{\alpha}} e^{\frac{-y_0}{2}} G(y_0) \neq 0 \tag{6.18}$$

does not satisfy the boundary condition.

In order to satisfy boundary conditions and have two independent solutions, we choose a coefficient

$$\lambda = \frac{F(y_0)}{G(y_0)} \tag{6.19}$$

and define

$$\Psi_A = y^{\frac{\beta}{\alpha}} e^{\frac{-y}{2}} F \tag{6.20}$$

and

$$\Psi_B = y^{\frac{\beta}{\alpha}} e^{\frac{-y}{2}} [F - \lambda G]. \tag{6.21}$$

With these choices, for $\beta > 0$, by performing the same steps which are given in the previous chapter, we obtain the eigenvalue equation for one Dirac delta function case:

$$\sigma r_0 = \frac{\lambda \alpha y_1 (F(y_1)G(y_1)' - F(y_1)'G(y_1))}{F(y_1)(F(y_1) - \lambda G(y_1))} \tag{6.22}$$

where $y_1 = \frac{2\gamma}{\alpha} e^{-\alpha \frac{r_1 - r_0}{r_0}}$ for the Dirac delta function located at r_1 and $'$ denotes derivative with respect to r. Since F and G are functions of β, we solve this equation for the eigenvalues. Note that equation (6.22) reduces to the well known energy eigenvalue equation for the three dimensional Morse potential as $\sigma \to 0$,

$$\lambda = \frac{F(y_0)}{G(y_0)} \to 0 \qquad \text{or} \qquad F(y_0) \to 0 \quad . \tag{6.23}$$

By using asymptotic expansions of $F(y_0)$ and $G(y_0)$, it can be shown that for $y_0 \to \infty$ ($\gamma \to \infty$), $\lambda \to 0$ and the wavefunction is finite *only if* $\frac{\beta}{\alpha} - \frac{\gamma}{\alpha} + \frac{1}{2} = -n$ for $n = 0, 1, 2, ...$ This result leads to the energies

$$E(n) = -D + \hbar\omega_0 \{(n + \frac{1}{2}) - \frac{\hbar\omega_0}{4D}(n + \frac{1}{2})^2\} \tag{6.24}$$

where $\hbar\omega_0 = \frac{\hbar^2}{2mr_0^2} 2\alpha\gamma$ and $n = 0, 1, 2, ...$ The same result is obtained for the one-dimensional Morse potential since for $y_0 \to \infty$, the three-dimensional and the one-

dimensional problems have the same boundary conditions. We note that this boundary condition is exactly the third condition stated by Morse [32]: "V(r) should become infinity at $r = 0$ (this need not be exactly true, however, the results are practically the same if V(r) becomes very large at $r = 0$)."

For $D \to 0$ ($\gamma \to 0$), we recover the results in reference [51] for the potential that is described only with the Dirac delta functions. For demonstrating this limit case, we take the following scaled wavefunctions $\Psi_{A,new} = -\sqrt{\pi}\Psi_A$ and $\Psi_{B,new} = \frac{\Psi_B}{\sqrt{\pi}}$ with the corresponding Wronskian $\mathcal{W}_{i,new}$. For $\gamma \to 0$, $\alpha \to 0$ and $\frac{\gamma}{\alpha} \equiv$finite, we obtain the following asymptotic value of the confluent hypergeometric function with finite values of y.

We use series expansion of confluent hypergeometric function $F(a, c; y)$:

$$F(a,c;y) = \frac{\Gamma(c)}{\Gamma(a)} \sum_{n=0}^{\infty} \frac{\Gamma(a+n)}{\Gamma(c+n)} \frac{y^n}{n!} = 1 + \frac{a}{c}\frac{y}{1!} + \frac{a(a+1)}{c(c+1)}\frac{y^2}{2!} + \frac{a(a+1)(a+2)}{c(c+1)(c+2)}\frac{y^3}{3!} + ... \tag{6.25}$$

For $\gamma \to 0$ and $\alpha \to 0$, $a = \frac{\beta}{\alpha} - \frac{\gamma}{\alpha} + \frac{1}{2} \to \frac{\beta}{\alpha}$, $c = \frac{2\beta}{\alpha} + 1 \to \frac{2\beta}{\alpha}$ and thus

$$F(a,c,y) = F(\frac{\beta}{\alpha}, \frac{2\beta}{\alpha}, y) = 1 + \frac{1}{2}\frac{y}{1!} + \frac{1}{2^2}\frac{y^2}{2!} + \frac{1}{2^3}\frac{y^3}{3!} + ... = e^{\frac{y}{2}}. \tag{6.26}$$

Therefore, we have the following asymptotics of F(y), G(y), W and λ with finite values of y:

$$F(y) =_1 F_1(\frac{\beta}{\alpha} - \frac{\gamma}{\alpha} + \frac{1}{2}, \frac{2\beta}{\alpha} + 1; y) \sim e^{\frac{y}{2}}, \tag{6.27}$$

$$G(y) = y^{-\frac{2\beta}{\alpha}}\ {}_1F_1(-\frac{\beta}{\alpha} - \frac{\gamma}{\alpha} + \frac{1}{2}, -\frac{2\beta}{\alpha} + 1; y) \sim y^{-\frac{2\beta}{\alpha}} e^{\frac{y}{2}}, \tag{6.28}$$

$$W_i \sim (-\frac{2\beta}{\alpha}) e^{y_i} {y_i}^{-\frac{2\beta}{\alpha}-1}, \tag{6.29}$$

and

$$\lambda = \frac{F(y_0)}{G(y_0)} \sim \frac{1}{{y_0}^{-\frac{2\beta}{\alpha}}}. \tag{6.30}$$

If we insert these quantities into the transfer matrix

$$\mathbb{M}_i = \begin{bmatrix} 1 + \frac{\sigma_i r_0}{\lambda\alpha} \frac{1}{y_i W_i} F_i(F_i - \lambda G_i) & \frac{\sigma_i r_0}{\lambda\alpha} \frac{1}{y_i W_i} (F_i - \lambda G_i)^2 \\ -\frac{\sigma_i r_0}{\lambda\alpha} \frac{1}{y_i W_i} F_i^2 & 1 - \frac{\sigma_i r_0}{\lambda\alpha} \frac{1}{y_i W_i} F_i(F_i - \lambda G_i) \end{bmatrix} \tag{6.31}$$

and write y_0, y_1 in terms of exponentials, the m_{11} element of the transfer matrix $\mathbb{M}_i$ becomes:

$$m_{11} = 1 + \frac{\sigma_i r_0}{-2\beta}[(\frac{y_i}{y_0})^{\frac{2\beta}{\alpha}} - 1]. \tag{6.32}$$

By writing $\frac{y_i}{y_0} = \frac{2\frac{\gamma}{\alpha} e^{-\alpha(\frac{r_i - r_0}{r_0})}}{2\frac{\gamma}{\alpha} e^{\alpha}} = e^{-\alpha\frac{r_i}{r_0}}$ into m_{11}, we get

$$m_{11} = 1 + \frac{-\sigma_i r_0}{2\beta}[e^{\frac{-2\beta r_i}{r_0}} - 1] \tag{6.33}$$

or

$$m_{11} = 1 + \frac{-\sigma_i r_0}{2\beta} e^{\frac{-\beta r_i}{r_0}} [e^{\frac{-\beta r_i}{r_0}} - e^{\frac{\beta r_i}{r_0}}]. \tag{6.34}$$

Then, for $\gamma \to 0$, $\alpha \to 0$, $\frac{\gamma}{\alpha} \equiv$ finite limits and $\beta = kr_0$, we get,

$$m_{11} = 1 + \frac{\sigma_i}{2k} e^{-kr_i} [e^{kr_i} - e^{-kr_i}] = 1 + \frac{\sigma_i}{k} e^{-kr_i} \sinh(kr_i). \tag{6.35}$$

Finally, we have

$$m_{11} = 1 - \sigma_i r_i \sqrt{\frac{\pi}{2}} \frac{e^{-kr_i}}{\sqrt{kr_i}} \sqrt{\frac{2}{\pi}} \frac{\sinh(kr_i)}{\sqrt{kr_i}} = 1 - \sigma_i r_i I_{\frac{1}{2}}(kr_i) K_{\frac{1}{2}}(kr_i) \tag{6.36}$$

where

$$I_{\frac{1}{2}}(x) = \frac{\sqrt{\frac{2}{\pi}} \sinh(x)}{\sqrt{x}} \tag{6.37}$$

and

$$K_{\frac{1}{2}}(x) = \frac{\sqrt{\frac{\pi}{2}} e^{-x}}{\sqrt{x}} \tag{6.38}$$

are the modified Bessel functions of order $\frac{1}{2}$.

By performing the same steps for the other matrix elements, we obtain:

$$\mathbb{M}_i = \begin{bmatrix} 1+\sigma_i r_i I_{\frac{1}{2}}(kr_i)K_{\frac{1}{2}}(kr_i) & \sigma_i r_i (I_{\frac{1}{2}}(kr_i))^2 \\ -\sigma_i r_i (K_{\frac{1}{2}}(kr_i))^2 & 1-\sigma_i r_i I_{\frac{1}{2}}(kr_i)K_{\frac{1}{2}}(kr_i) \end{bmatrix}. \tag{6.39}$$

Same matrices are obtained in reference [51] when we have only P Dirac delta functions for three dimensional delta shells. Then, for one Dirac delta function case, we reproduce the result of Antoine et al. [66] by equating m_{22} to zero:

$$1-\sigma_1 r_1 I_{\frac{1}{2}}(kr_1)K_{\frac{1}{2}}(kr_1) = 0. \tag{6.40}$$

For molecular physics applications, we take the Morse parameters for H_2 molecule from references [64, 69], $D = 4.748$eV, $r_0 = 0.741$Å and $\hbar w_0 = 0.548$eV. These values lead to $\gamma = 25.04$ and $\alpha = 1.445$.

For different r_1 values ($r_1 = 0.8r_0, r_0, 1.2r_0$), we calculated numerically the ground state energy, E_0, in units of $\frac{\hbar^2}{2mr_0^2}$. We define a dimensionless quantity $\tau = \sigma r_0$. Figure 6.2 shows how E_0 changes as a function of a dimensionless parameter of $\tau = \sigma r_0$. By using equation (6.40) for $D \to 0$, the asymptotic behaviors of $I_\rho(x)$ and $K_\rho(x)$, for $\sigma_1 \to \infty$, we get

$$1-\sigma_1 r_1 \frac{1}{2k_1 r_1} \approx 0. \tag{6.41}$$

From equation (6.41), we obtain $k_1 \approx \frac{\sigma_1}{2}$ and , $E_\delta \approx -\frac{\hbar^2}{2m}(\frac{\sigma_1}{2})^2 = -\frac{\hbar^2}{8mr_0^2}\tau_1^2$ as $\tau_1 = \sigma r_1 \to \infty$. Then, by using the first order perturbation calculations with the ground state for $D = 0$ and considering the extremum values of $V_M(r)$, for a very large σ_1 and $D \neq 0$, we find $E_0 \approx -\frac{\hbar^2}{2m}(\frac{\sigma_1}{2})^2 + cD$ where $\mid c \mid < max\{1, \mid e^{2\alpha} - 2e^{\alpha} \mid\}$. Thus, the ground state energy decreases monotonically as a function of σ_1, for very large σ_1

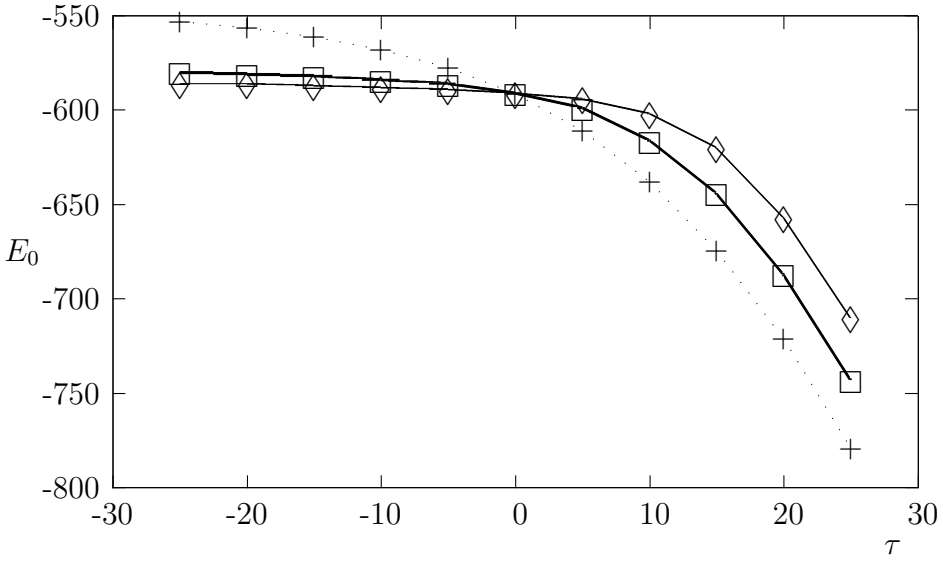


Figure 6.2. The ground state energy E_0 (in units of $\frac{\hbar^2}{2mr_0{}^2}$) vs. $\tau = \sigma r_0$ for $\gamma = 25.04$. ($\Diamond$, +, $\Box$ represent $r_1 = 0.8r_0, r_0, 1.2r_0$ cases respectively.)

values as seen in Figure 6.2.

We also note that attractive Dirac delta case is more effective than repulsive Dirac delta case. This effect can also be seen in Figure 6.2 for one Dirac delta case. We can explain this effect by considering the change of the wave function. The wave function has a kink and its derivative has a finite jump at the location of delta function, $r = r_i$. Hence, the wave function forms an outward kink and increases the value of $|\Psi|^2$ for attractive Dirac delta potential and forms an inward kink and decreases the value of $|\Psi|^2$ for repulsive Dirac delta potential. Thus, attractive Dirac delta functions result in bigger changes in the ground state energy since the energy change due to the Dirac delta functions is proportional to $|\Psi|^2$ from the first order perturbation theory calculations.

Bargmann [58] has shown that the number of bound states N has an upper bound for s-states when the value of the following integral is finite:

$$N \leq \frac{2m}{\hbar^2} \int_0^\infty r \mid V(r) \mid dr. \tag{6.42}$$

Thus, for *an upper bound* for the number of bound states of the Morse potential, we *only* take the attractive part of the potential by setting the positive part of the potential to zero [63] for $r \leq r_l = r_0(1 - \frac{ln2}{\alpha})$ and $\alpha \geq \ln 2$. Here r_l is the lower limit of the integral. For $0 < \alpha \leq \ln 2$, $r_l = 0$. Hence, we get the condition for the number of bound states N_M:

$$N_M \leq \frac{2m}{\hbar^2} \int_{r_l}^{\infty} r \mid V(r) \mid dr. \tag{6.43}$$

By evaluating the integral, we get

$$N_M \leq \begin{cases} \gamma^2(\frac{2\alpha+3-2\ln 2}{\alpha^2}) & for\ \alpha \geq \ln 2, \\ \gamma^2(\frac{8e^{\alpha}-e^{2\alpha}}{4\alpha^2}) & for\ 0 < \alpha \leq \ln 2. \end{cases} \tag{6.44}$$

For realistic systems, $\alpha > \ln 2$ since we have the very repulsive part of the potential due to the Pauli exclusion effects for very small r values. Hence, for $\alpha > \ln 2$, equation (A.1) leads to no bound state for the Morse potential if $\gamma^2(\frac{2\alpha+3-2\ln 2}{\alpha^2}) < 1$. For the case of H_2, N_M can be at most 1352 by using above numerical values of γ, and α.

We note that the number of bound states N_M goes to zero as $\gamma \to 0$ ($D \to 0$). This limit corresponds to free particle case so that $N = 0$. For $\alpha \to 0$, $D \to \infty$ ($\gamma \to \infty$) and $\frac{2D\alpha^2}{r_0^2} = m\omega_0^2 \equiv$ finite, $V(r) \approx -D + \frac{1}{2}(\frac{2D\alpha^2}{r_0^2})(r - r_0)^2 = -D + \frac{1}{2}m\omega_0^2(r - r_0)^2$. Then, V(r) is a harmonic oscillator potential shifted by a constant $-D$ ("infinite well") and the number of bound states of the potential is infinite. The result from equation (6.44) is consistent with this fact since the upper bound for N_M is proportional to $\frac{\gamma^2}{\alpha^2}$ for very small α values.

If we have only P attractive Dirac delta interactions ($D = 0$), there will be at most P bound states [51]. Thus, for $D > 0$, we can deduce that equation (6.6) can have at least max $\{N_M, P\}$ bound state solutions for sufficiently large σ_i values.

Figures (6.3)-(6.4) show the ground state energy versus r_1 for $\tau = \pm 5$ (+ attractive case, - repulsive case) where $\tau = \sigma r_0$. We see that the ground state energy

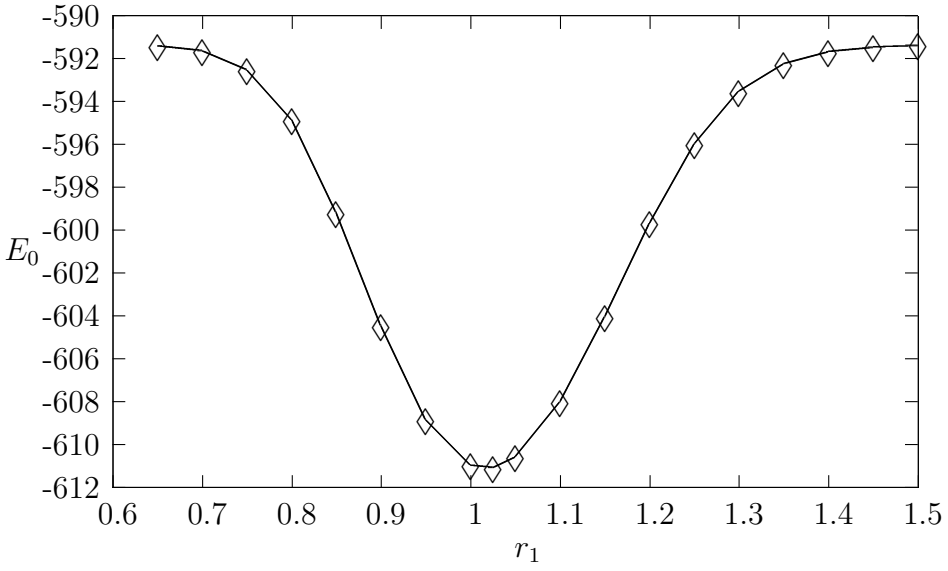


Figure 6.3. The ground state energy E_0 (in units of $\frac{\hbar^2}{2mr_0{}^2}$) vs. the position of the Dirac delta function r_1 for $\tau = \sigma r_0 = 5$ (attractive interaction), $\gamma = 25.04$, and r_1 is in units of r_0 .

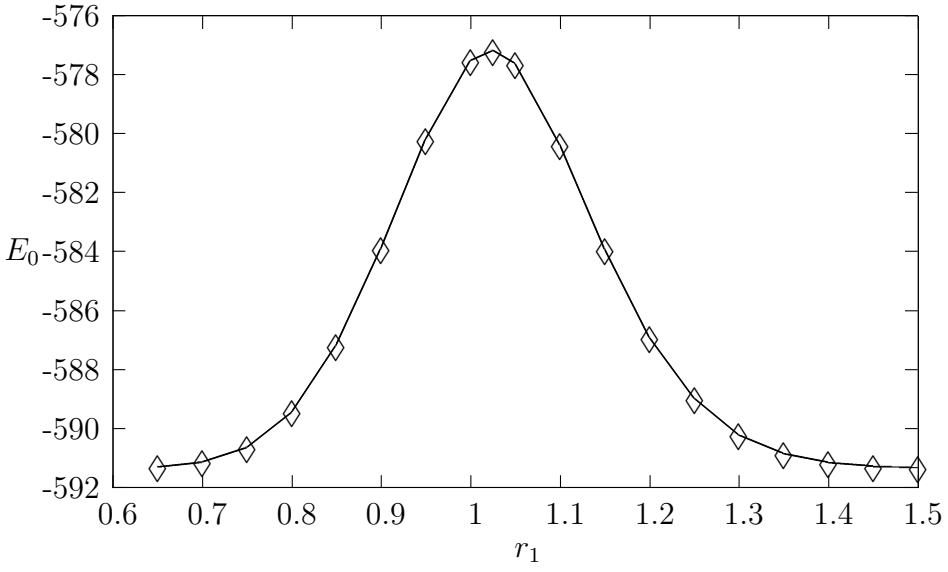


Figure 6.4. The ground state energy E_0 (in units of $\frac{\hbar^2}{2mr_0{}^2}$) vs. the position of the Dirac delta function r_1 for $\tau = \sigma r_0 = -5$ (repulsive interaction), $\gamma = 25.04$, and r_1 is in units of r_0 .

has a minimum and a maximum around $r_1 = r_0$ value for attractive and repulsive cases, respectively. The Dirac delta part of the potential begins to lose its effect for the locations of the Dirac delta potential with very small or very large r_1 values since the wave function goes to zero due to the boundary conditions. We also obtain similar results for different strength values of delta function $\tau = \sigma r_0$, and present our results in Figures (6.5)-(6.6).

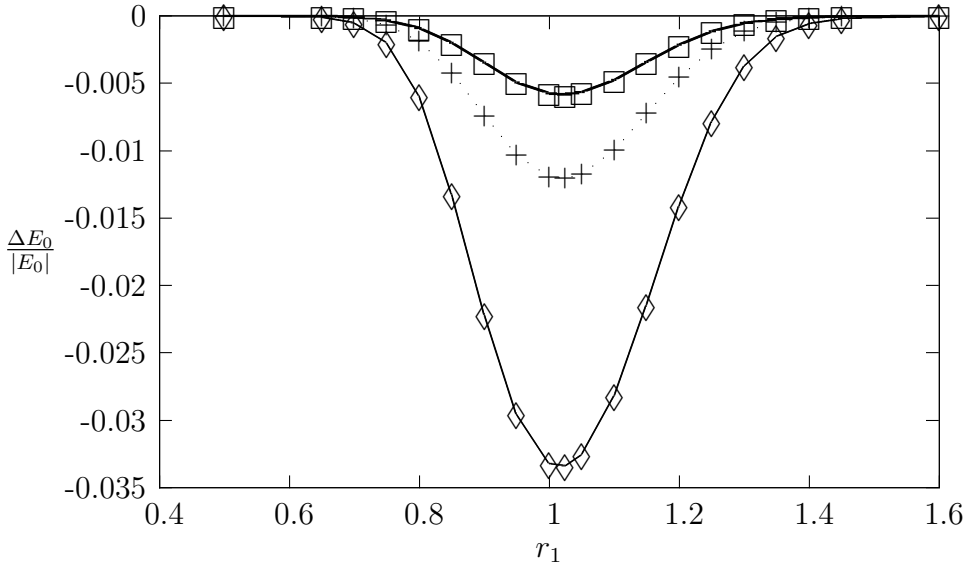


Figure 6.5. $\frac{\Delta E_0}{|E_0|} = \frac{E_0^{M,\delta} - E_0}{|E_0|}$ vs. the position of the Dirac delta function r_1 for $\tau = \sigma r_0$ (attractive interaction) where $E_0^{M,\delta}$, E_0 stand for the ground state energies for the Morse potential with delta function and the Morse potential, respectively for $\gamma = 25.04$. Here, r_1 is in units of r_0. ($\square$, $+$, $\Diamond$ represent $\tau = 1, 2, 5$ cases respectively.)

Figure 6.7 exhibits the frequency $w_0 = \frac{E_1 - E_0}{\hbar}$ for the transition between the first excited and the ground states as a function of τ. This frequency decreases first for small τ values and then makes a minimum and increases for large τ values. This behavior of w_0 can be explained by examining the change of the normalized $|\psi|^2$ since $\frac{\partial E_i}{\partial \sigma} = -\frac{\hbar^2}{2m} |\psi_i(r_1)|^2$ and for small σ_i, $\Delta E_i = (-\frac{\hbar^2}{2m}) |\psi_i(r_1)|^2 \Delta\sigma_i$.

For the ground state, Figure 6 shows $|\psi_0|^2$ versus r for $\sigma_1 = 0 (\tau = 0)$ and $\tau = \sigma_1 r_0 = 15$, respectively. $|\psi_0|^2$ at the location $r_1 = 1.3 r_0$ of delta function increases as τ increases. Thus, the change in E_0 gets larger as τ increases.

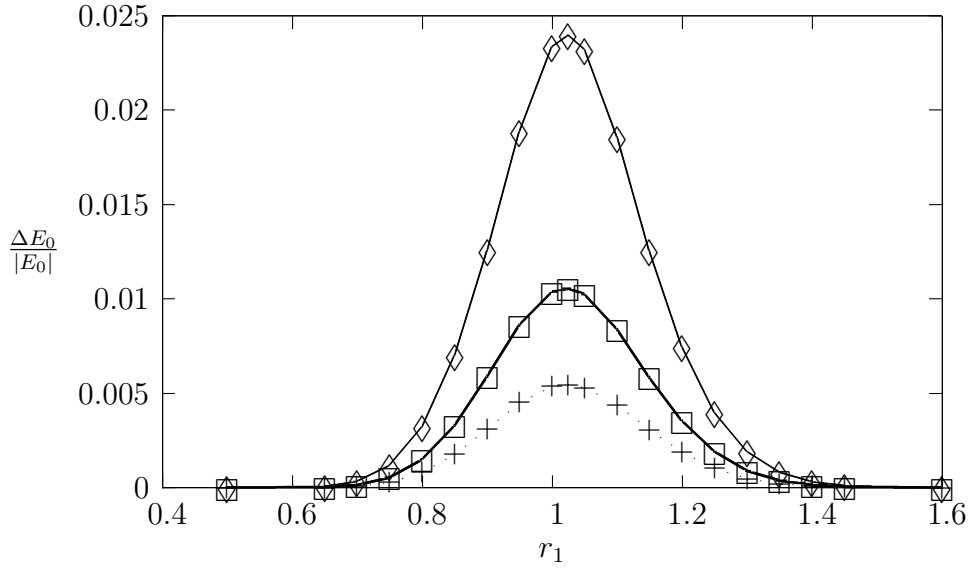


Figure 6.6. $\frac{\Delta E_0}{|E_0|} = \frac{E_0^{M,\delta} - E_0}{|E_0|}$ vs. the position of the Dirac delta function r_1 for $\tau = \sigma r_0$ (repulsive interaction) where $E_0^{M,\delta}$, E_0 stand for the ground state energies for the Morse potential with delta function and the Morse potential, respectively for $\gamma = 25.04$. ($+$, $\square$, $\Diamond$ represent $\tau = -1, -2, -5$ cases respectively.)

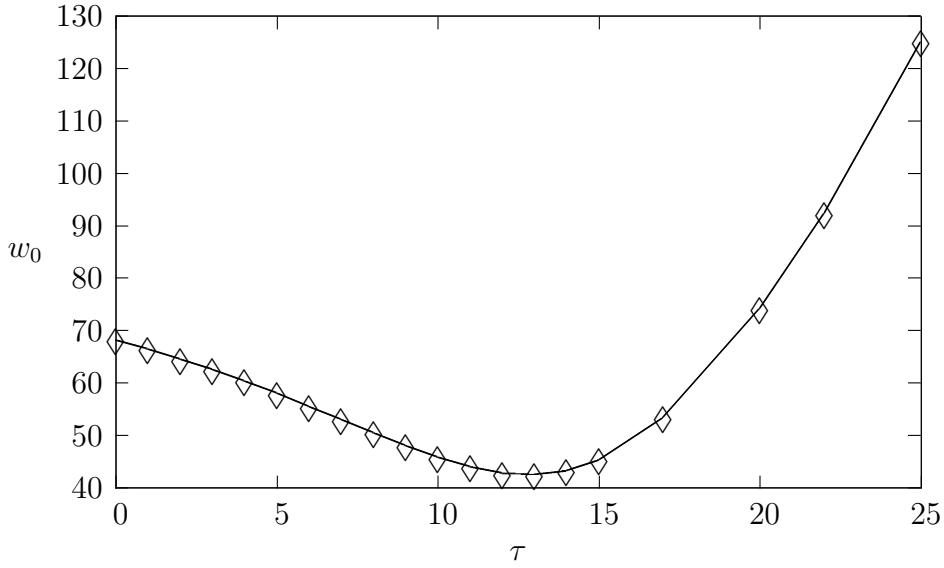


Figure 6.7. The change of the frequency for the transition between the first excited and the ground states, $w_0 = \frac{E_1 - E_0}{\hbar}$ (in units of $\frac{\hbar}{2mr_0{}^2}$) vs. $\tau = \sigma r_0$ for one Dirac delta function located at $r_1 = 1.3r_0$ for $\gamma = 25.04$.

Figure 6 shows $|\psi_1|^2$ versus r for the first excited state. The wave functions change such that they also satisfy orthonormality relations. If $|\psi_0|^2$ gets very large values at $r = r_1$ for very large τ values, then $|\psi_1|^2$ will have very small values. Hence,

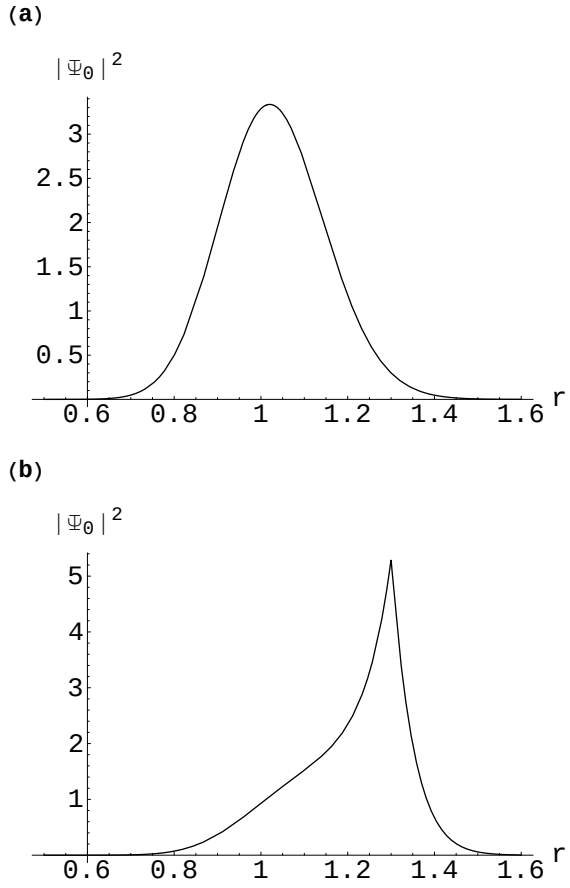


Figure 6.8. The normalized square of the ground state wave function $|\Psi_0|^2$ vs. r where $\gamma = 25.04$ and r is in units of r_0 for (a) $\sigma_1 = 0$ and (b) the Dirac delta function located at $r_1 = 1.3r_0$ for $\sigma_1 r_0 = 15$.

$\Delta w_0 = \Delta(\frac{E_1 - E_0}{\hbar})$ will be positive for large τ values, that is, w_0 is increasing since $\mid \psi_0(r_1) \mid^2$ increases and $\mid \psi_1(r_1) \mid^2$ decreases as τ increases. For small τ values, since $\mid \psi_1(r_1) \mid^2$ is larger than $\mid \psi_0(r_1) \mid^2$, Δw_0 will be negative, that is, w_0 is decreasing. Thus w_0 will have a minimum for an intermediate τ value.

In Figure 6.10, we exhibit $w_1 = \frac{E_2 - E_1}{\hbar}$ for the transition between the second and the first excited states.

By plotting $|\psi_2|^2$ for the second excited state in Figure 6, it is shown that the value of $|\psi_2|^2$ gets smaller as τ increases. Since both $|\psi_1|^2$ and $|\psi_2|^2$ become very small for very large τ values, hence $\Delta w_1 = \Delta(\frac{E_2 - E_1}{\hbar}) \approx 0$ at the location of delta function, that is, w_1 goes to a constant value as τ becomes very large as shown in Figure 6.10.

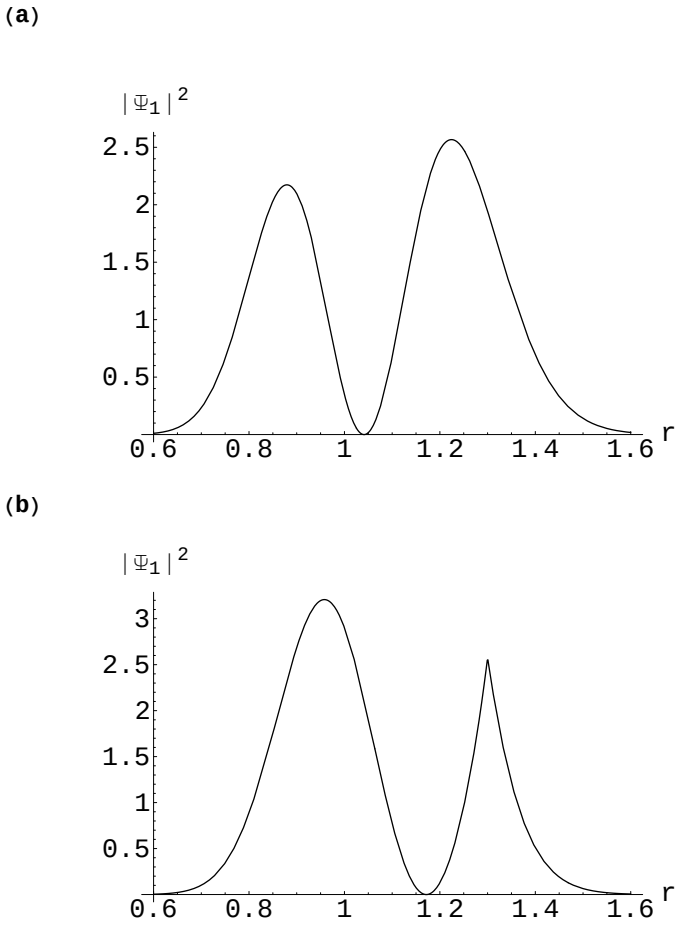


Figure 6.9. The normalized square of the first excited state wave function $|\Psi_1|^2$ vs. r where $\gamma = 25.04$ and r is in units of r_0 for (a) $\sigma_1 = 0$ and (b) the Dirac delta function located at $r_1 = 1.3r_0$ for $\sigma_1 r_0 = 15$.

Since $|\psi_1(r_1)|^2 > |\psi_2(r_1)|^2$ for very small τ values, $\Delta w_1 > 0$, that is, w_1 is increasing for small τ values. Figure 6.10 shows that w_1 also increases as a function of τ for intermediate τ values.

In Figure 6.12, we plot average bond distance $< r >$ as a function of strength of delta function and see that $< r >$ is a decreasing function of strength of delta function. The reason for this decreasing of $< r >$ may result from deformation of the Morse potential due to delta function. This deformation leads to decreasing of $< r >$. In

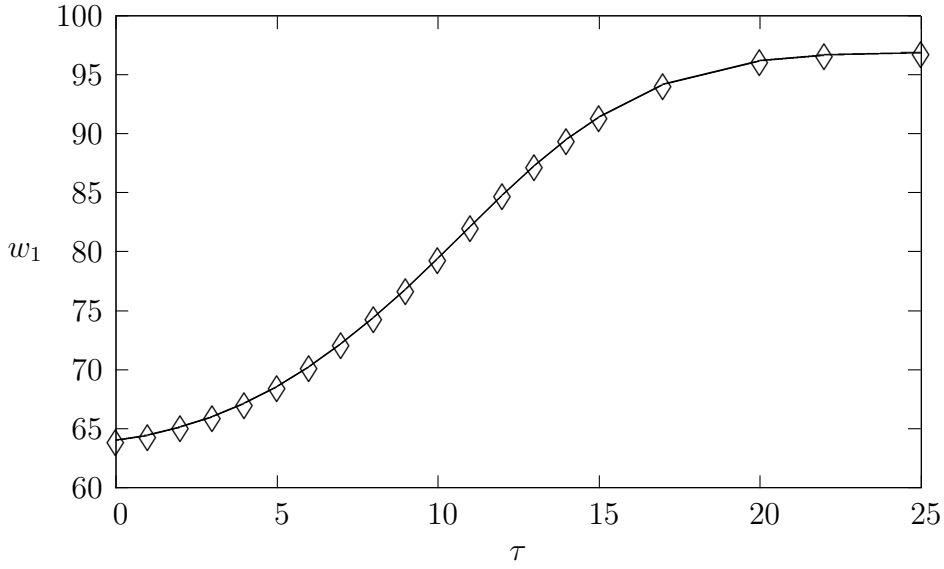


Figure 6.10. The change of the frequency for the transition between the second excited and the first excited states, $w_1 = \frac{E_2 - E_1}{\hbar}$ (in units of $\frac{\hbar}{2mr_0{}^2}$) vs. $\tau = \sigma r_0$ for one Dirac delta function located at $r_1 = 1.3r_0$ for $\gamma = 25.04$.

Figure 6.13, we investigate average bond distance $< r >$ as a function of r_1. For small and large values of r_1, average bond distance for delta decorated Morse potential goes to its value for free Morse potential case. Average bond distance takes intermediate values with respect to the location of delta function between the boundaries since the effect of delta function changes with its location.

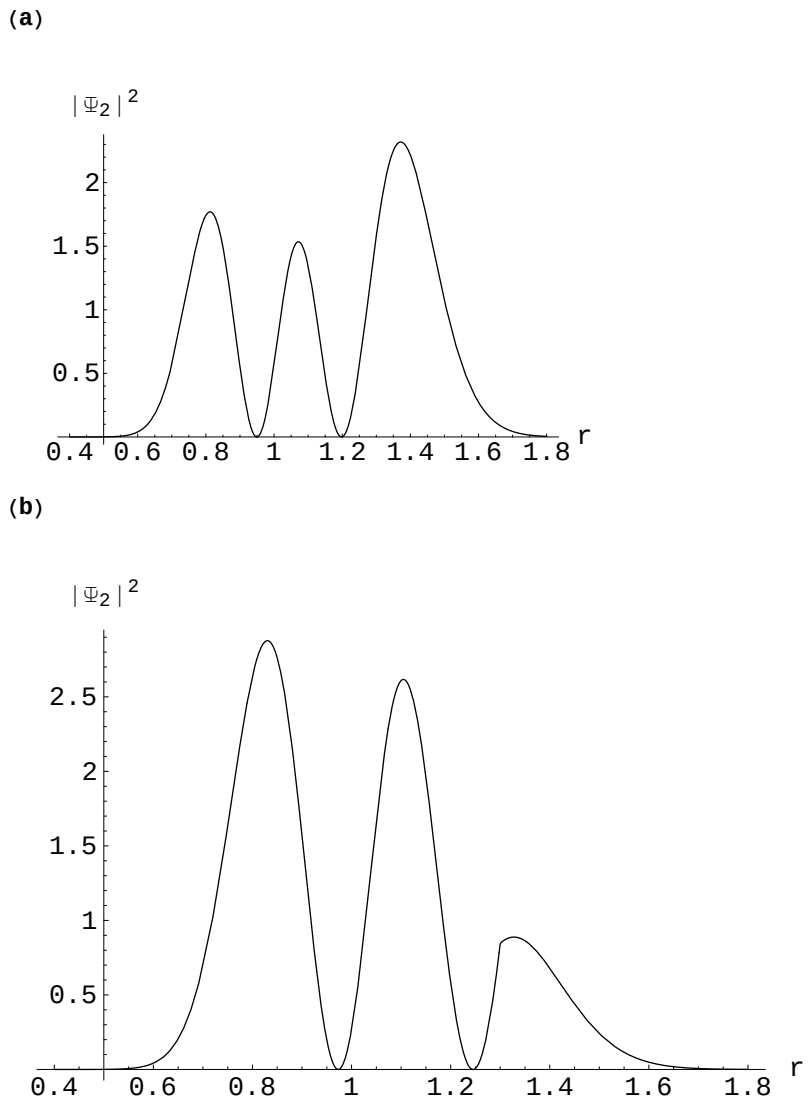


Figure 6.11. The normalized square of the second excited state wave function $|\Psi_2|^2$ vs. r where $\gamma = 25.04$ and r is in units of r_0 for (a) $\sigma_1 = 0$ and (b) the Dirac delta function located at $r_1 = 1.3r_0$ for $\sigma_1 r_0 = 15$.

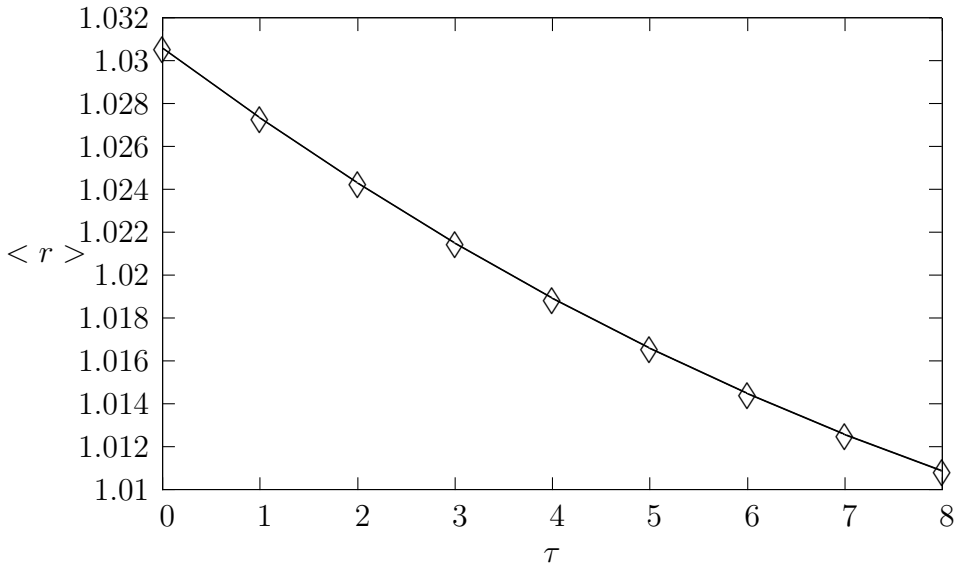


Figure 6.12. Expectation value of r is in units of r_0, $< r >= \int_0^\infty \Psi_0^* r \Psi_0 dr$ vs. $\tau = \sigma r_0$ for one Dirac delta function located at $r_1 = r_0$ for $\gamma = 25.04$.

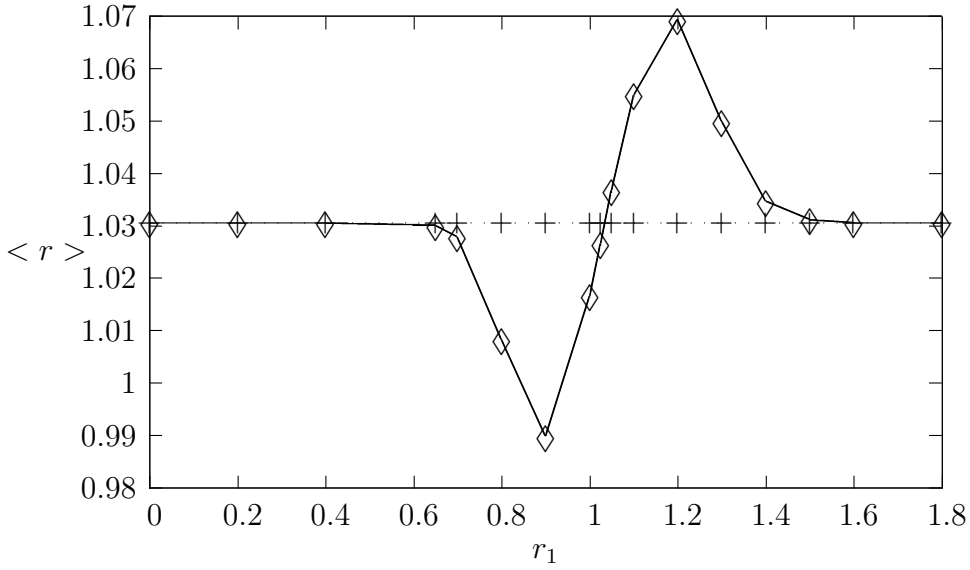


Figure 6.13. Expectation value of r is in units of r_0, $< r >= \int_0^\infty \Psi_0^* r \Psi_0 dr$ vs. r_1 for $\tau = 5$ and $\gamma = 25.04$. ($\Diamond$ and $+$ represent one delta and no delta function cases, respectively.)

6.1. Sudden Perturbations

For another application of our method, we calculate the P_{fi}, which is the transition probability, if the interatomic interactions of the diatomic molecular system initially is described by the Morse potential and is perturbed suddenly by a very local, spherical disturbance. We also performed numerical calculations for P_{fi} by using our numerical result which we already obtained for H_2 molecule.

For the sudden perturbation of the Morse potential with the Dirac delta shell interaction, we have

$$P_{fi} = \mid \int \Phi^*_{M\delta} \Phi_M dV \mid^2 = \mid \int \Psi^*_{M\delta} \Psi_M dr \mid^2 \tag{6.45}$$

where Φ_M is an eigenstate of the Hamiltonian with the Morse potential and $\Phi_{M\delta}$ is the eigenstate of the perturbed Hamiltonian and $\Phi_J = \frac{\Psi_J(r)}{r} Y_{00}(\theta, \varphi)$ for J=M, Mδ. For a H_2 molecule initially in the Morse potential, we study the change in vibrational structure of H_2 molecule when a sudden, shell-like perturbation applied to this system. By modeling this type of perturbation with a Dirac delta shell interaction and using "sudden approximation" [70, 71], we obtain the transition probabilities P_{fi} for $i, f = 0, 1, 2$ (ground, the first and the second excited states, respectively) and present them in Table 6.1. Here, we use the Morse parameters of H_2 molecule given in references [64, 69] and $\sigma_1 r_0 = 15$, $r_1 = 1.3 r_0$ for the numerical calculations. The results in Table 6.1. show that for these parameters, it is probable (with a probability 0.384) to have transition to the first excited state by applying this shell interaction if the system is initially in the ground state. Similarly, if the system is initially in the first excited state, it will stay in that state after the perturbation with a probability 0.508.

Table 6.1. Transition probabilities between the initial eigenstate ($i \equiv \Phi_M$) and the final eigenstate ($f \equiv \Phi_{M\delta}$) for the low-lying states ($i, f = 0, 1, 2$).

$i \backslash f$	0	1	2
0	0.605	0.384	0.004
1	0.270	0.508	0.185
2	0.077	0.074	0.774

6.2. Encapsulation of H_2 in C_{60} Fullerene Cage

After the discovery of fullerene forms of carbon, encapsulations of atoms and molecules inside spherical C_{60} cage have been also studied experimentally [43], [72]-[75]. Encapsulation of H_2 in C_{60} was achieved by Murata et al. [43] and the frequency measurement was performed by Mamone et al. [76]. The stabilization energy, ΔE = E(C_{60}+ molecule) - E(C_{60}) - E(molecule) and the vibrational frequency shift $\Delta\ \nu = \nu$(molecule in C_{60} cage) - ν(free molecule) have been calculated by using Hartree-Fock(HF), Møller-Plesset Perturbations (MP2), Density Functional Theory (DFT) methods [77, 78]. For the stabilization energy ΔE, these calculations gave very different results in the range from -7.81 kcal/mol to +1.22 kcal/mol [77, 78]. It is interesting that different methods (HF, MP2, DFT) give qualitatively different results for the encapsulation energy of H_2 in C_{60} for the observed geometries. Negative ΔE indicates that encapsulation of molecule in C_{60}, i.e. (C_{60} + molecule) complex, is favored energetically to the separate, free C_{60} and the molecule. In the case of HF calculation [78], the hydrogen molecule bond distance is optimized while C_{60} cage was kept frozen and for the other cases of DFT and MP2 calculations [77], C_{60} and H_2 interactions were calculated without optimizing the whole complex. For ΔE, HF calculation gave positive value (+1.22 kcal/mol) [78], but MP2 and DFT calculations with different basis sets give negative stabilization energies: MP2 results are(-0.49 to -6.94 kcal/mol) [77, 79] and DFT results (-5.81 to -7.81 kcal/mol) [77, 79] except B3LYP/cc-pVDZ method calculation (+2.24 kcal/mol) [77]. Slanina et al. claimed that "B3LYP functional does not produce reliable values for non-bonding fullerene encapsulations". Thus, we expect that the encapsulated H_2 in C_{60} is a stable complex with negative

stabilization energy by considering results of other MP2 and DFT calculations.

The vibrational frequency calculations for H_2 showed upward shifts of +90 cm^{-1} for HF calculation [78] and +23 and +25 cm^{-1} for DFT calculations [77]. The experimental value of the vibrational frequency of free (gas phase) hydrogen molecule is 4161 cm^{-1} [80]. The only experimental study for the vibration frequency of H_2 in C_{60} lead to the result of 4071 cm^{-1} [76] with a downward shift of -90 cm^{-1} from the frequency of the free H_2. Thus, HF, DFT calculations do not reproduce experimental frequency shift (see Table 1).

It is quite reasonable to take C_{60} cage as a spherically symmetric object. By using HF calculations, the center of mass of the encapsulated H_2 was found to be at the center of C_{60} cage [81]. Thus, symmetric stretching vibrational motion of H_2 molecule is assumed to be along the diameter of the cage. These full quantum mechanical (HF, DFT, MP2) calculations require large amount of computational time. The Morse potential reproduce the vibration frequency of H_2 accurately. By considering C_{60} as a spherical cage, we represent the interaction between H_2 and C_{60} by a Dirac delta interaction potential and apply our method. Thus, we get a reasonable potential model for H_2 molecule in C_{60} cage (see Figure 6.14 [82]).



Figure 6.14. Encapsulation of hydrogen molecule in C_{60} fullerene cage [82].

We fit the experimental vibrational frequency shift to obtain σ, which is the

strength of the Dirac delta potential for encapsulated H_2 in C_{60} cage by modeling the interactions between H_2 and C_{60} with the Dirac delta function at the van der Waals contact distance (see Figure 6.15).

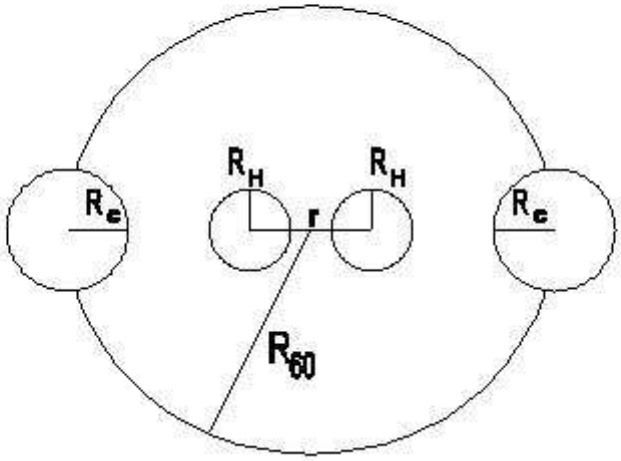


Figure 6.15. Van der Waals contact model for H_2 in C_{60} fullerene cage. R_H, R_C and R_{60} represent the radius of hydrogen, carbon and C_{60} cage, respectively.

We take the Morse parameters for hydrogen which are given in references [64, 69]. By using van der Waals contact model, we consider C and H atoms as van der Waals spheres. When these H and C spheres come to contact with each other, we model their contact interactions by introducing the Dirac potential. We use the notation "$H_2.C_{60}$" for H_2 encapsulated in C_{60} cage. The contact distance r_1= Diameter of C_{60} - 2(van der Waals radius of C + van der Waals radius of H) $\approx$ 7.0 Å -2(1.7 Å + 1.2 Å) = 1.2 Å.

Full Hamiltonian for "$H_2.C_{60}$" system,

$$H_{full} = H_{C_{60}} + H_{H_2} + H_{int} \tag{6.46}$$

where $H_{C_{60}}$, H_{H_2} and H_{int} are Hamiltonians for C_{60}, H_2 and the interaction between H_2 and C atoms. Hamiltonian for C_{60} becomes the potential energy of C_{60} since we assume rigid C_{60} cage and the center of mass of C_{60} is at rest. Hamiltonian for H_2 in equation (6.46) is given by

$$H_{H_2} = \sum_{i=1}^{2} (\frac{-\hbar^2}{2m_H}) \nabla^2_{r_i} + V_{H_2}(\overrightarrow{r_2} - \overrightarrow{r_1}) \tag{6.47}$$

where V_{H_2} is the potential energy of H_2. By separating central and relative motion for H_2 with $\overrightarrow{R} = \frac{m_H \overrightarrow{r_1} + m_H \overrightarrow{r_2}}{m_H + m_H}$, $\overrightarrow{r} = \overrightarrow{r_2} - \overrightarrow{r_1}$ and $M = 2m_H$, $m = \frac{m_H}{2}$, equation (6.47) becomes:

$$H_{H_2} = \frac{-\hbar^2}{2M} \nabla^2_R + \frac{-\hbar^2}{2m} \nabla^2_r + V_{H_2}(\overrightarrow{r}). \tag{6.48}$$

For spherically symmetric case, by assuming that symmetric stretching vibrational motion of H_2 molecule to be along the diameter of the cage and the center of mass of H_2 in C_{60} to be at the center of cage and at rest, Hamiltonian for H_2 reduces to the following equation:

$$H_{H_2} = \frac{-\hbar^2}{2m} \nabla^2_r + V_{H_2}(r) \tag{6.49}$$

where $m = \frac{m_H}{2}$ is the reduced mass. Thus, full hamiltonian for "$H_2.C_{60}$" becomes:

$$H_{full} = H_{C_{60}} + \frac{-\hbar^2}{2m} \nabla^2_r + V_{H_2}(r) + H_{int} \tag{6.50}$$

and

$$H_{full}\Psi_{full} = (H_{C_{60}} + H_{H_2} + H_{int})\Psi(C_{60})\Psi(H_2) = (E(C_{60}) + E^{\delta}(H_2))\Psi_{full} \quad (6.51)$$

where Ψ_{full} is the wave function of "$H_2.C_{60}$" and $E(C_{60})$, $E^{\delta}(H_2)$ are the energies for C_{60} and hydrogen molecule together with the Dirac delta potential, respectively.

Hence, for rigid, spherical C_{60} cage, the interaction potential can be written as a function of the interatomic distance between H atoms, that is, V_{int}=$A\delta(r - r_1)$ where r is the interatomic distance between H atoms and $r_1 = 1.2$ Å as the location of the contact interaction. By rewriting the interaction strength A in terms of our parameter σ, we get $V_{int} = -\frac{\hbar^2}{2m}\sigma\delta(r - r_1)$. The energy of $H_2.C_{60}$ can be approximated as the energy of C_{60} plus the energy of H_2 in an effective potential which is sum of the Morse potential and the Dirac delta interaction. Thus, for the ground state energies, $E_0(H_2.C_{60})\approx\ E_0(C_{60})+E_0^{M\delta}(H_2)$ where $E_0^{M\delta}(H_2)$ is the energy of H_2 for the Morse potential together with the Dirac delta interaction. Then,

$$\Delta E = E_0(H_2.C_{60}) - E_0(C_{60}) - E_0^{M}(H_2), \quad (6.52)$$

$$\Delta E \approx E_0(C_{60}) + E_0^{M\delta}(H_2) - E_0(C_{60}) - E_0^{M}(H_2) \quad (6.53)$$

and, we get,

$$\Delta E \approx E_0^{M\delta}(H_2) - E_0^{M}(H_2) \quad (6.54)$$

where E_0's are the ground state energies of the related systems and $E_0^M(H_2)$ is the ground state energy of free H_2 in the Morse potential. In our case, the vibrational frequency for free H_2 is 4165 cm^{-1} by using the Morse potential with the given parameters. The experimental frequency shift $\Delta\nu$= ν(H_2 in C_{60})- ν(H_2)=-90 cm^{-1} to obtain σ where, $\nu = \frac{E_1 - E_0}{h}$ where E_0 and E_1 are the ground and the first excited state energies of the related system (H_2 in C_{60} or free H_2), respectively. At r_1 = 1.2 Å, by fitting frequency shift -90 cm^{-1}, we obtain σ=38.77(1/Å). For these r_1 and σ=38.77(1/Å) values, we get the stabilization energy, ΔE= -4.27 kcal/mol. We present our results in Table 1. Thus our potential form with r_1 = 1.2Å, σ=38.77(1/Å) can describe the interaction between the C_{60} cage and the encapsulated H_2.

Table 6.2. Vibrational frequency ν and stabilization energy ΔE are in units of cm^{-1} and kcal/mol, respectively. For DFT calculations, basis set superposition error corrections are included.

	$\nu(H_2)$	$\nu(H_2.C_{60})$	$\Delta\nu$	ΔE
Experiment	4161[a]	4071[b]	-90	$NA^{\ddagger}$
This Work	4165	4075	-90[§]	-4.27
$HF^{(i)}$	4591.8	4681.3	89.5	1.22
DFT $^{(ii)}$	4466	4491	25	2.24
DFT $^{(iii)}$	4513	4536	23	-5.81

a: Auffray et al. [80], b: Mamone et al. [76], ‡: NA: Not available, §: The frequency shift is fitted to obtain σ, (i): Cioslowski [78], (ii): B3LYP method Lee et al. [77], (iii): M05-2X Hybrid DFT method Lee et al. [77].

7. THE ONE DIMENSIONAL MORSE POTENTIAL WITH POINT INTERACTIONS

The one dimensional Morse potential is given by

$$V_M(x) = D(e^{-2\alpha\frac{x-x_0}{x_0}} - 2e^{-\alpha\frac{x-x_0}{x_0}}). \tag{7.1}$$

Here, x_0 is the equilibrium interatomic distance, D is the well depth and α is a dimensionless parameter which modifies the shape of the potential.

Damski et al. showed that slow driving of a focused laser beam through a cloud of trapped cold fermions creates a collective excitation in the system [45]. The effective potential for the atomic motion in 1D model, $V(x) = \frac{x^2}{2} + U_o(x_o)exp(-\frac{(x-x_o)^2}{2\sigma^2})$ where $U_o(x_o) < 0$ (for an appropriately chosen laser detuning). The amplitude $U_o(x_o)$ is proportional to the laser intensity, $x_o = x_o(t)$ is a time-dependent position of the centre of the beam, while σ is directly related to the cross section of the (Gaussian) laser beam. Thus Gaussian shape potentials are used to describe laser fields. It is well-known that the Dirac delta function $\delta(x - x_o)$ can be expressed in terms of a limit $(\sigma \to 0)$ of $f(x) = \frac{1}{\sqrt{2\pi\sigma^2}}exp(-\frac{(x-x_o)^2}{2\sigma^2})$. The collective excitation due to the laser beam is very local (Gaussian) so that it can be represented by the Dirac delta potential. A focused laser beam through hydrogen molecule may lead to a very local deformation on the potential energy curve for hydrogen. Thus, such a deformed system can be investigated by using our approach.

We decorate the Morse potential with a finite number (P) of the Dirac delta functions. The potential is given as

$$V(x) = D(e^{-2\alpha\frac{x-x_0}{x_0}} - 2e^{-\alpha\frac{x-x_0}{x_0}}) - \frac{\hbar^2}{2m}\sum_{i=1}^{P}\sigma_i\delta(x - x_i). \tag{7.2}$$

Here, x_i's are the positions of P Dirac delta functions and the σ_i's are strengths. We

treat (-$\frac{\hbar^2}{2m}\sigma_i$) as the strengths of the Dirac delta functions for calculational convenience. In one dimension, we search for the solutions of the time-independent Schrödinger equation

$$-\frac{\hbar^2}{2m}\frac{d^2}{dx^2}\Psi + V\Psi = E\,\Psi \ . \tag{7.3}$$

For bound states, we take

$$E = -\frac{\hbar^2 k^2}{2m}. \tag{7.4}$$

By using equation (7.3), we obtain:

$$\frac{d^2\Psi(x)}{dx^2} + \left(\frac{-2m}{\hbar^2}D(e^{-2\alpha\frac{x-x_0}{x_0}} - 2e^{-\alpha\frac{x-x_0}{x_0}}) + \sum_{i=1}^{P}\sigma_i\delta(x-x_i) - k^2\right)\Psi(x) = 0. \tag{7.5}$$

We denote $(-\infty, x_1)$ as the 1^{st}, (x_i, x_{i+1}) as the $(i+1)^{th}$, and (x_P, ∞) as the $(P+1)^{th}$ intervals for $i = 1, ..., P-1$. For $x \neq x_i$, equation (7.5) reduces to

$$\frac{d^2\Psi(x)}{dx^2} + \left[\left(\frac{-2m}{\hbar^2}D(e^{-2\alpha\frac{x-x_0}{x_0}} - 2e^{-\alpha\frac{x-x_0}{x_0}})\right) - k^2\right]\Psi(x) = 0. \tag{7.6}$$

By defining

$$q = \frac{x-x_0}{x_0}, \tag{7.7}$$

$$-\beta^2 = \frac{2mE}{\hbar^2}{x_0}^2 = -k^2{x_0}^2 \tag{7.8}$$

and

$$\gamma^2 = \frac{2mD}{\hbar^2}{x_0}^2, \tag{7.9}$$

equation (7.6) takes the following form:

$$\frac{d^2\Psi(q)}{dq^2} + (-\beta^2 + 2\gamma^2 e^{-\alpha q} - \gamma^2 e^{-2\alpha q})\Psi(q) = 0. \tag{7.10}$$

By using a new variable

$$y = \frac{2\gamma}{\alpha}e^{-\alpha q}, \tag{7.11}$$

equation (7.10) becomes

$$y^2\frac{d^2\Psi(y)}{dy^2} + y\frac{d\Psi(y)}{dy} + (-\frac{\beta^2}{\alpha^2} + \frac{\gamma}{\alpha}y - \frac{1}{4}y^2)\Psi(y) = 0. \tag{7.12}$$

By introducing

$$\Psi(y) = y^{\frac{\beta}{\alpha}}e^{\frac{-y}{2}}f(y), \tag{7.13}$$

this differential equation reduces to confluent hypergeometric differential equation with the parameters

$$c = \frac{2\beta}{\alpha} + 1 \tag{7.14}$$

and

$$a = \frac{\beta}{\alpha} - \frac{\gamma}{\alpha} + \frac{1}{2} : \tag{7.15}$$

$$\frac{d^2 f\,(y)}{dy^2} + (c - y)\frac{df\,(y)}{dy} - af\,(y) = 0\ . \tag{7.16}$$

This equation has two linearly independent solutions ${}_1F_1(a, c; y)$ and $y^{1-c}\ {}_1F_1(a - c + 1,\ 2 - c; y)$ where ${}_1F_1(\alpha, \beta; y)$ is the confluent hypergeometric function. The general solution of equation (7.16) is

$$f\,(y) = c_1\ {}_1F_1(a, c; y) + c_2\ y^{1-c}\ {}_1F_1(a - c + 1, 2 - c; y). \tag{7.17}$$

For the Morse potential, we note that $\gamma^2 > \beta^2$ for bound states.

From now on, for a short-hand notation, we will use notations

$$F(y) \equiv\ {}_1F_1(\frac{\beta}{\alpha} - \frac{\gamma}{\alpha} + \frac{1}{2}, \frac{2\beta}{\alpha} + 1; y) \tag{7.18}$$

and

$$G(y) \equiv y^{-\frac{2\beta}{\alpha}}\ {}_1F_1(-\frac{\beta}{\alpha} - \frac{\gamma}{\alpha} + \frac{1}{2}, -\frac{2\beta}{\alpha} + 1; y). \tag{7.19}$$

Since $x = -\infty$ and $x = \infty$ correspond to $y = \infty$ and $y = 0$, we have $\psi(\infty) = 0$ and $\psi(0) = 0$ as the boundary conditions. Let us define

$$\Psi_A = y^{\frac{\beta}{\alpha}} e^{\frac{-y}{2}} F \tag{7.20}$$

and

$$\Psi_B = y^{\frac{\beta}{\alpha}} e^{\frac{-y}{2}} [F - \lambda G] \tag{7.21}$$

where

$$\lambda = \frac{F(y \to \infty)}{G(y \to \infty)}. \tag{7.22}$$

For $\beta > 0$, by using the same steps which are given in chapter 5, we obtain the eigenvalue equation for one Dirac delta function:

$$\sigma x_0 = \frac{\lambda \alpha y_1 (F(y_1)G(y_1)' - F(y_1)'G(y_1))}{F(y_1)(F(y_1) - \lambda G(y_1))} \tag{7.23}$$

where $y_1 = \frac{2\gamma}{\alpha} e^{-\alpha \frac{x_1 - x_0}{x_0}}$ for the Dirac delta function located at x_1 and $'$ denotes derivative with respect to x. Since F and G are functions of β, we solve this equation for the eigenvalues. Note that equation (7.23) reduces to the well known energy eigenvalue equation for the one dimensional Morse potential as $\sigma \to 0$,

$$\lambda = \frac{F(y \to \infty)}{G(y \to \infty)} \to 0 \qquad \text{or} \qquad F(y \to \infty) \to 0 \quad . \tag{7.24}$$

By using asymptotic expansions of $F(y)$ and $G(y)$, it can be shown that for $y \to \infty$, $\lambda \to 0$ and the wavefunction is finite *only if* $\frac{\beta}{\alpha} - \frac{\gamma}{\alpha} + \frac{1}{2} = -n$ for $n = 0, 1, 2, ...$ This result leads to the energies

$$E(n) = -D + \hbar\omega_0 \{(n + \frac{1}{2}) - \frac{\hbar\omega_0}{4D}(n + \frac{1}{2})^2\} \tag{7.25}$$

where $\hbar\omega_0 = \frac{\hbar^2}{2mx_0^2} 2\alpha\gamma$ and $n = 0, 1, 2, ...$

For $D \to 0$ ($\gamma \to 0$), we recover the results for the potential that is described only with the Dirac delta functions. For $\gamma \to 0$, $\alpha \to 0$ and $\frac{\gamma}{\alpha} \equiv$finite, we have finite y values and the following asymptotics of F(y), G(y), W and λ:

$$F(y) =_1 F_1(\frac{\beta}{\alpha} - \frac{\gamma}{\alpha} + \frac{1}{2}, \frac{2\beta}{\alpha} + 1; y) \sim e^{\frac{y}{2}}, \tag{7.26}$$

$$G(y) = y^{-\frac{2\beta}{\alpha}}\ {}_1F_1(-\frac{\beta}{\alpha} - \frac{\gamma}{\alpha} + \frac{1}{2}, -\frac{2\beta}{\alpha} + 1; y) \sim y^{-\frac{2\beta}{\alpha}} e^{\frac{y}{2}}, \tag{7.27}$$

$$W_i \sim (-\frac{2\beta}{\alpha}) e^{y_i} y_i^{-\frac{2\beta}{\alpha}-1}, \tag{7.28}$$

and

$$\frac{1}{\lambda} = \frac{G(y \to \infty)}{F(y \to \infty)} \sim y^{-\frac{2\beta}{\alpha}} \to 0. \tag{7.29}$$

We insert these quantities into equation (7.23), and write y_1 in terms of exponential. Then, for $\gamma \to 0$, $\alpha \to 0$, $\frac{\gamma}{\alpha} \equiv$ finite limits and $\beta = kx_0$, we get

$$k = \frac{\sigma}{2}. \tag{7.30}$$

By writing k in terms of E ($E = -\frac{\hbar^2 k^2}{2m}$), this equation leads to well known eigenvalue equation:

$$E = -\frac{\hbar^2 \sigma^2}{8m} \tag{7.31}$$

for the one Dirac delta potential.

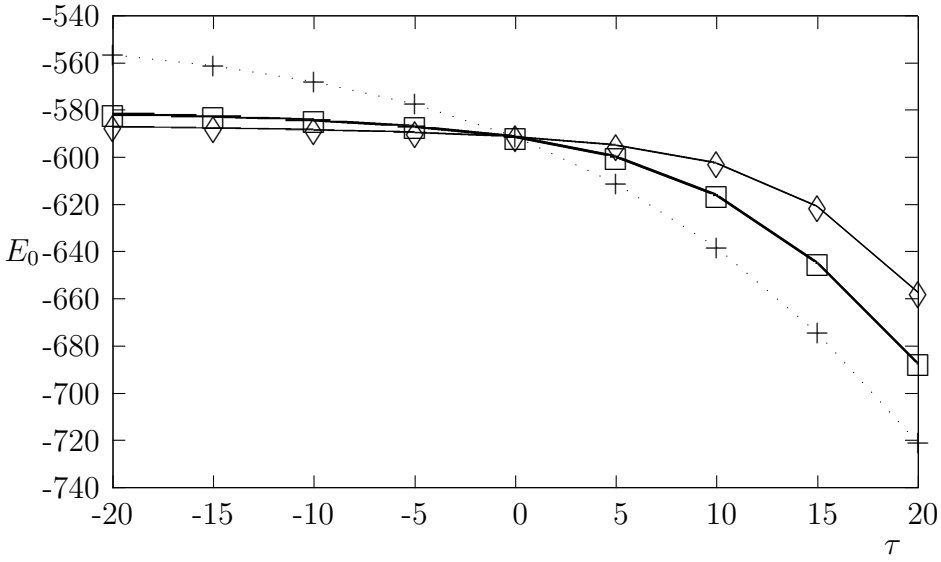


Figure 7.1. The ground state energy E_0 (in units of $\frac{\hbar^2}{2m{x_0}^2}$) vs. $\tau = \sigma x_0$ for $\gamma = 25.04$. ($\Diamond$, +, $\Box$ represent $x_1 = 0.8x_0, x_0, 1.2x_0$ cases respectively.)

For molecular physics applications, we take the Morse parameters for H_2 molecule from references [64, 69], $D = 4.748$eV, $x_0 = 0.741$Å and $\hbar w_0 = 0.548$eV. These values lead to $\gamma = 25.04$ and $\alpha = 1.445$.

For different x_1 values ($x_1 = 0.8x_0, x_0, 1.2x_0$), we calculated numerically the ground state energy, E_0, in units of $\frac{\hbar^2}{2mx_0^2}$. We define a dimensionless quantity $\tau = \sigma x_0$. Figure (7.1) shows how E_0 changes as a function of a dimensionless parameter of $\tau = \sigma x_0$.

We note that attractive Dirac delta case is more effective than repulsive Dirac delta case. This effect can also be seen in Figure 7.1 for one Dirac delta case. We can explain this effect by considering the change of the wave function. The wave function has a kink and its derivative has a finite jump at the location of delta function, $x = x_i$. Hence, the wave function forms an outward kink and increases the value of $|\Psi|^2$ for attractive Dirac delta potential and forms an inward kink and decreases the value of $|\Psi|^2$ for repulsive Dirac delta potential. Thus, attractive Dirac delta functions result in bigger changes in the ground state energy since the energy change due to the Dirac delta functions is proportional to $|\Psi|^2$ from the first order perturbation theory calculations.

We also investigated the change of the ground state energy with location of delta function for different strength values and found that our results are similar to the results of three-dimensional case.

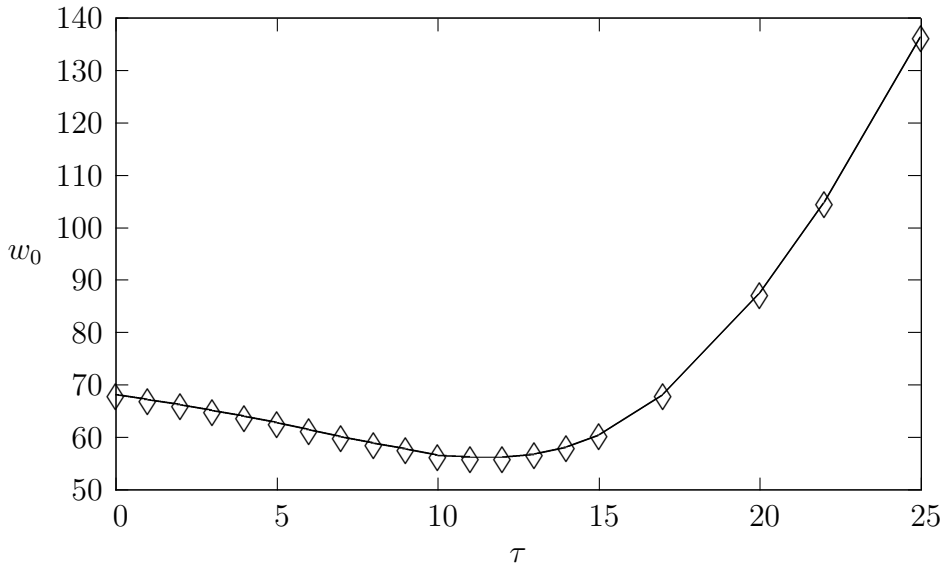


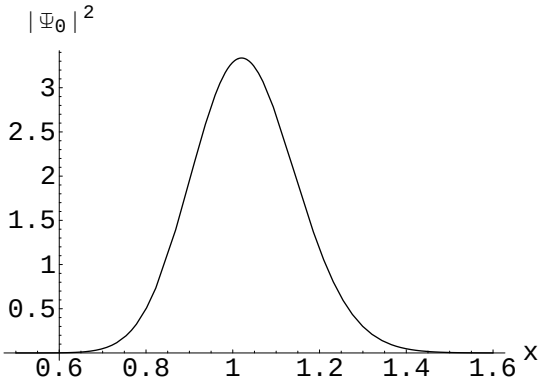
Figure 7.2. The change of the frequency for the transition between the first excited and the ground states, $w_0 = \frac{E_1 - E_0}{\hbar}$ (in units of $\frac{\hbar}{2mx_0{}^2}$) vs. $\tau = \sigma x_0$ for one Dirac delta function located at $x_1 = 0.8x_0$ for $\gamma = 25.04$.

Figure 7.2 exhibits the frequency $w_0 = \frac{E_1 - E_0}{\hbar}$ for the transition between the first excited and the ground states as a function of τ. This frequency decreases first for small τ values and then makes a minimum and increases for large τ values. This behavior of w_0 can be explained by examining the change of the normalized $|\psi|^2$ since $\frac{\partial E_i}{\partial \sigma} = -\frac{\hbar^2}{2m} |\psi_i(x_1)|^2$ and for small σ_i, $\Delta E_i = (-\frac{\hbar^2}{2m}) |\psi_i(x_1)|^2 \Delta\sigma_i$.

For the ground state, Figure 7 shows $|\psi_0|^2$ versus x for $\sigma_1 = 0 (\tau = 0)$ and $\tau = \sigma_1 x_0 = 15$, respectively. $|\psi_0|^2$ at the location $x_1 = 0.8x_0$ of delta function increases as τ increases. Thus, the change in E_0 gets larger as τ increases.

Figure 7 shows $|\psi_1|^2$ versus x for the first excited state. The wave functions change such that they also satisfy orthonormality relations. If $|\psi_0|^2$ gets very large values at $x = x_1$ for very large τ values, then $|\psi_1|^2$ will have very small values. Hence, $\Delta w_0 = \Delta(\frac{E_1 - E_0}{\hbar})$ will be positive for large τ values, that is, w_0 is increasing since $|\psi_0(x_1)|^2$ increases and $|\psi_1(x_1)|^2$ decreases as τ increases. For small τ values, since

(a)



(b)

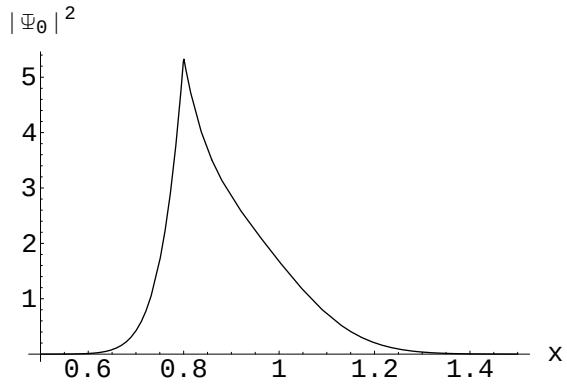


Figure 7.3. The normalized square of the ground state wave function $|\Psi_0|^2$ vs. x where $\gamma = 25.04$ and x is in units of x_0 for (a) $\sigma_1 = 0$ and (b) the Dirac delta function located at $x_1 = 0.8x_0$ for $\sigma_1 x_0 = 15$.

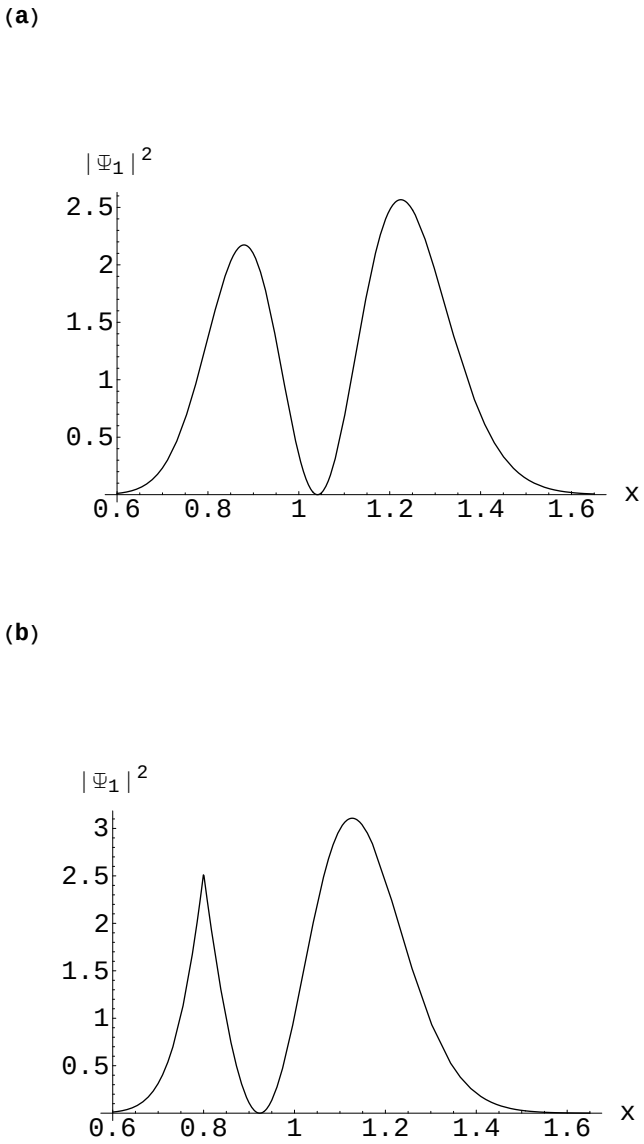


Figure 7.4. The normalized square of the first excited state wave function $|\Psi_1|^2$ vs. x where $\gamma = 25.04$ and x is in units of x_0 for (a) $\sigma_1 = 0$ and (b) the Dirac delta function located at $x_1 = 0.8x_0$ for $\sigma_1 x_0 = 15$.

$|\psi_1(x_1)|^2$ is larger than $|\psi_0(x_1)|^2$, Δw_0 will be negative, that is, w_0 is decreasing. Thus, w_0 will have a minimum for an intermediate τ value.

In Figure 7.5, we exhibit $w_1 = \frac{E_2 - E_1}{\hbar}$ for the transition between the second and

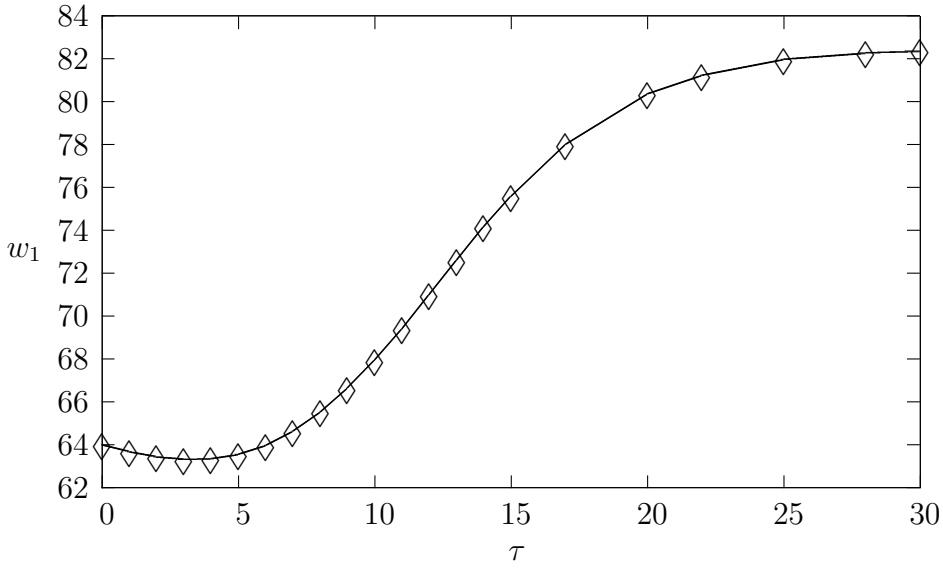


Figure 7.5. The change of the frequency for the transition between the second excited and the first excited states, $w_1 = \frac{E_2 - E_1}{\hbar}$ (in units of $\frac{\hbar}{2mx_0{}^2}$) vs. $\tau = \sigma x_0$ for one Dirac delta function located at $x_1 = 0.8x_0$ for $\gamma = 25.04$.

the first excited states.

By plotting $|\psi_2|^2$ for the second excited state in Figure 7, it is shown that the value of $|\psi_2|^2$ gets smaller as τ increases. Since both $|\psi_1|^2$ and $|\psi_2|^2$ become very small for very large τ values, hence $\Delta w_1 = \Delta(\frac{E_2 - E_1}{\hbar}) \approx 0$ at the location of delta function, that is, w_1 goes to a constant value as τ becomes very large as shown in Figure 7.5. For small τ values, since $|\psi_2(x_1)|^2$ increasing larger than $|\psi_1(x_1)|^2$, Δw_1 will be negative, that is, w_1 is decreasing. Thus w_1 will have a minimum for an intermediate τ value.

In Figure 7.7, we investigate the change of the oscillator strength corresponding to the transition between the first excited and the ground states, $f_{10}{=}\frac{2m}{\hbar^2}\ (E_1 - E_0)\left|\int_{-\infty}^{\infty}\Psi_1^* x \Psi_0 dx\right|^2$, as a function of the strength of delta function, $\tau = \sigma x_0$ for delta function located at $x = 0.8x_0$. For small values of strength ($\tau = \sigma x_0 < 5$), the oscillator strength changes very slightly since the effect of delta function is very small for these small strength values. On the other hand, for larger strength values, the oscillator strength f_{10} decreases since $\left|\int_{-\infty}^{\infty}\Psi_1^* x \Psi_0 dx\right|^2$ decreases for larger $\tau = \sigma x_0$. At the location of delta function, absolute square of wave function increases but except around this location, absolute square of wave function gets smaller. For this reason,

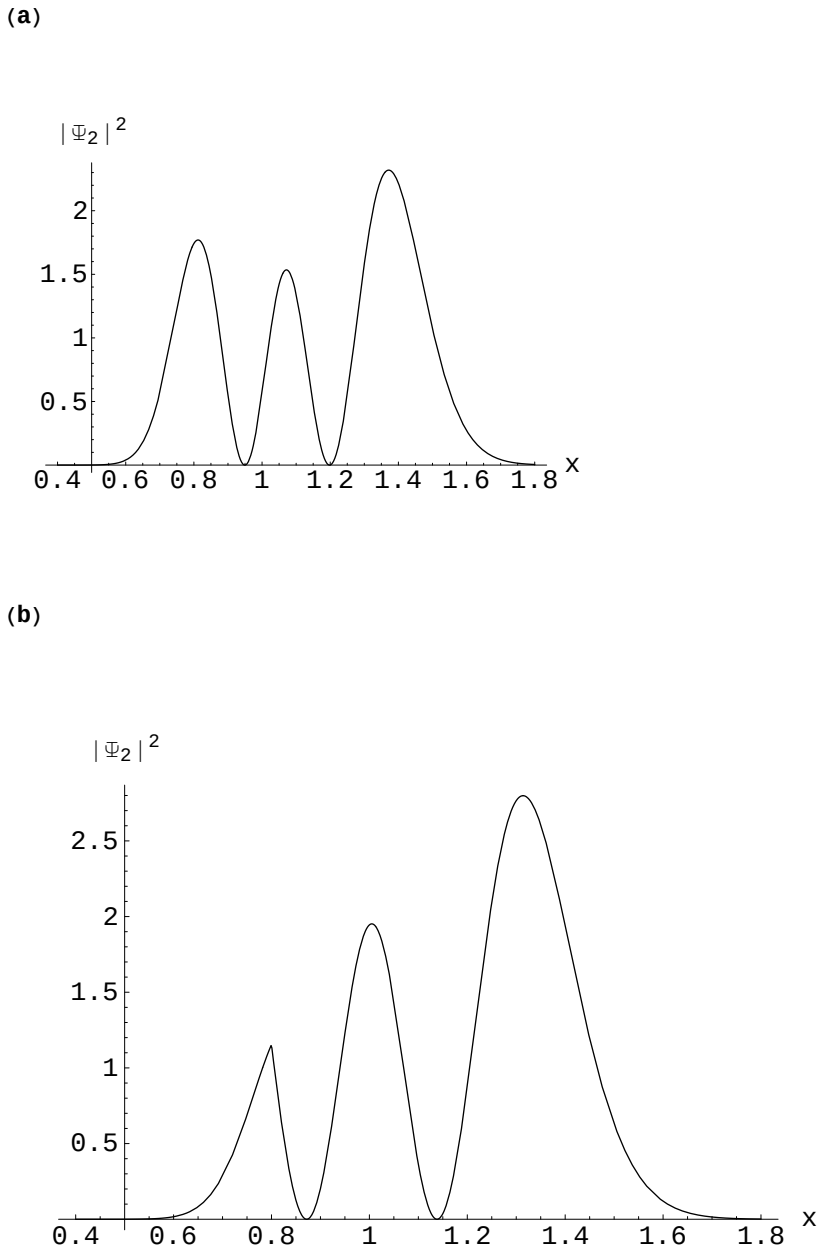


Figure 7.6. The normalized square of the second excited state wave function $|\Psi_2|^2$ vs. x where $\gamma = 25.04$ and x is in units of x_0 for (a) $\sigma_1 = 0$ and (b) the Dirac delta function located at $x_1 = 0.8x_0$ for $\sigma_1 x_0 = 15$.

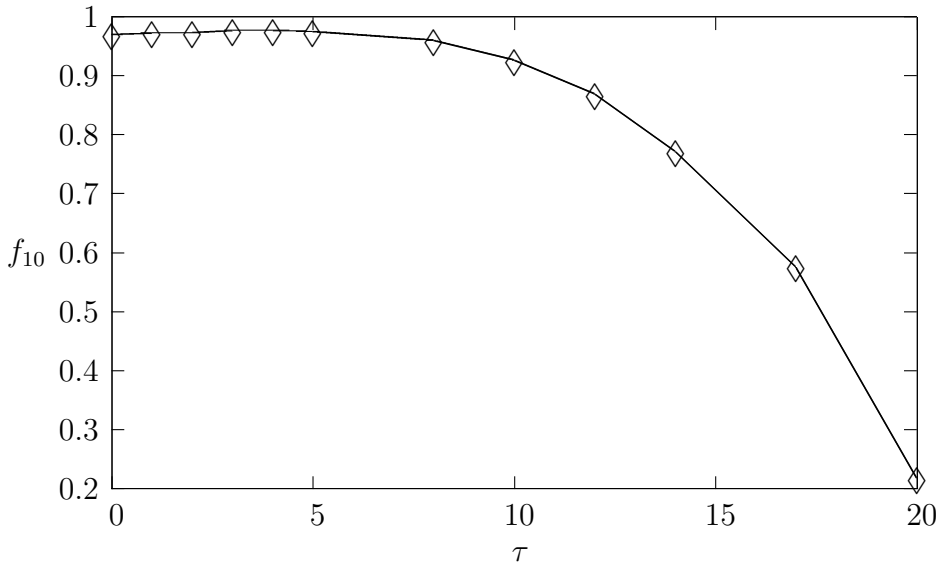


Figure 7.7. The change of the oscillator strength for the transition between the first excited and the ground states, $f_{10}=\frac{2m}{\hbar^2}\ (E_1 - E_0)\left|\int_{-\infty}^{\infty} \Psi_1^* x \Psi_0 dx\right|^2$ vs. $\tau = \sigma x_0$ for one Dirac delta function located at $x_1 = 0.8x_0$ for $\gamma = 25.04$.

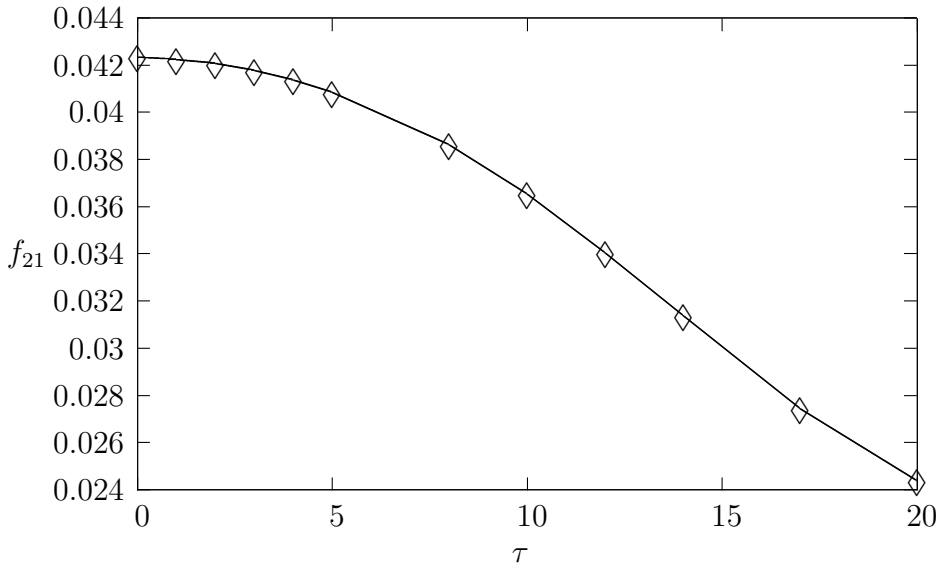


Figure 7.8. The change of the oscillator strength for the transition between the second and the first excited states, $f_{21}=\frac{2m}{\hbar^2}\ (E_2 - E_1)\left|\int_{-\infty}^{\infty} \Psi_2^* x \Psi_1 dx\right|^2$ vs. $\tau = \sigma x_0$ for one Dirac delta function located at $x_1 = 0.8x_0$ for $\gamma = 25.04$.

the change of $\left|\int_{-\infty}^{\infty} \Psi_1^* x \Psi_0 dx\right|^2$ is decreasing with τ. Hence, the probability of the transition between the ground and the first excited states decreases for larger strength of delta function. In Figure 7.8, we also analyze the change of the oscillator strength corresponding to the transition between the second and the first excited states, $f_{21}=\frac{2m}{\hbar^2}(E_2 - E_1)\left|\int_{-\infty}^{\infty} \Psi_2^* x \Psi_1 dx\right|^2$, as a function of the strength of delta function, $\tau = \sigma x_0$, and find that f_{21} decreases since $\left|\int_{-\infty}^{\infty} \Psi_2^* x \Psi_1 dx\right|^2$ decreases with larger $\tau = \sigma x_0$.

8. CONCLUSIONS

In this thesis, we have studied bound states of the Schrödinger equation including a finite number of the Dirac delta functions. We have presented a formalism to calculate bound state energies of the Schrödinger equation for the solvable potentials decorated with a finite number (P) of the Dirac delta functions for one and three dimensions.

We have obtained the conditions on the number of bound states for some potentials.

We have applied our formalism to the Woods-Saxon potential. The potential is given as

$$V(r) = -\frac{V_0}{1+e^{\frac{r-R}{a}}} - \frac{\hbar^2}{2m}\sum_{i=1}^{P}\sigma_i\delta(r-r_i).$$

We have obtained transfer matrices and the eigenvalue equation by using x_{22} element of the total transfer matrix $\mathbb{X}$. We have presented the wave functions in terms of hypergeometric functions. For P=1, we have obtained a transcendental equation for the bound state energies. We have solved this equation and obtained the change of the ground state energy with increasing dimensionless (σa) values at different locations. We have plotted the change of the ground state energy with increasing r_1 values for the attractive and repulsive delta functions and found that the ground state energy has an extremum for $r_1 = 13a$. The ground state energy does not change for very small and very large r_1 values due to the boundary conditions. We have also solved the eigenvalue equation for $P = 2$ and investigated the ground state energy for different positions of the Dirac delta functions. We have found that for the same $|\sigma|$ value, the change in the ground state energy is larger for attractive delta functions than the repulsive ones. We have also investigated eigenvalue solutions by considering some limit cases of the Woods-Saxon potential parameters and found consistent results with some other works.

We applied the formalism to calculate bound state energies of the Schrödinger

equation with the Dirac delta decorated Morse potential for any finite number (P) of the Dirac delta functions for s-wave ($l = 0$) states. The potential is given as

$$V(r) = D(e^{-2\alpha\frac{r-r_0}{r_0}} - 2e^{-\alpha\frac{r-r_0}{r_0}}) - \frac{\hbar^2}{2m}\sum_{i=1}^{P}\sigma_i\delta(r-r_i).$$

We obtained transfer matrices and eigenvalue equation by using x_{22} element of the total transfer matrix $\mathbb{X}$. We presented the wave functions in terms of confluent hypergeometric functions. For P=1, we obtained a transcendental equation for the bound state energies. We solved this equation and obtained the change of the ground state energy with increasing dimensionless (σr_0) values at different locations. We found that for the same $|\sigma|$ value, the change in the ground state energy is larger for attractive delta functions than the repulsive ones. We plotted the change of the ground state energy with increasing r_1 values for both attractive and repulsive Dirac delta functions and found that the ground state energy has an extremum around $r_1 = r_0$. The ground state energy does not change for very small and very large r_1 values due to the boundary conditions. We found the frequencies corresponding to the transitions between bound states as a function of the strength of the Dirac delta function. We analyzed the frequency corresponding to the transition between the first excited and the ground states. We saw that the Dirac delta function leads to bigger change in the first excited state energy than the ground state energy for small τ values. On the other hand, delta function leads to a change in the ground state energy more than the first excited state energy for large τ values so that the frequency $w_0 = \frac{E_1-E_0}{\hbar}$ increases with τ. We also investigated the frequency corresponding to the transition between the first and the second excited states. The frequency $w_1 = \frac{E_2-E_1}{\hbar}$ increases with τ and goes to a limit since the first and the second excited state energies do not change considerably for large τ values. We plotted the normalized square of the bound state (the ground, the first and the second excited states) wave function for both no delta and one delta cases. The square of the wave function has a deformation at the location of the Dirac delta function. The Dirac delta function has stronger effect on the ground state compared to the first and the second excited states. We also investigated the change of the average value of the interatomic bond distance as a function of strength and location of delta

function. We saw that average value of interatomic bond distance is a decreasing function of strength of delta function. Average value of interatomic bond distance goes to its value for just Morse potential case for large and small values of location of delta function because delta function begins to lose its effect.

We also calculated transition probabilities between the initial eigenstates for the Morse potential and the final eigenstates for the potential perturbed by the Dirac delta interaction. Numerical calculations for the vibrational states of H_2 molecule have shown that it is probable to have transition (with a probability 0.384) to the first excited eigenstate of the perturbed Hamiltonian by applying the Dirac delta shell interaction.

We applied our method to H_2 molecule in C_{60} cage by considering van der Waals sphere model for the contact interaction of H and C atoms. We found the strength of the Dirac delta function and then stabilization energy by using experimental vibrational frequency shift of hydrogen molecule in C_{60} cage. We compared our results with some experimental and theoretical results. Our results are in good accordance with literature. The solutions of the Schrödinger equation for Morse potential together with one Dirac delta function in three-dimension can be used to describe encapsulation of a H_2 molecule in a hollow, spherical C_{60} cage. This system is also studied experimentally.

We investigated the bound state solutions of the Schrödinger equation for the one dimensional Morse potential. The potential is given as

$$V(x) = D(e^{-2\alpha\frac{x-x_0}{x_0}} - 2e^{-\alpha\frac{x-x_0}{x_0}}) - \frac{\hbar^2}{2m}\sum_{i=1}^{P}\sigma_i\delta(x-x_i).$$

We obtained similar bound state results to the three-dimensional case.

We also investigated some limit cases of the Morse potential decorated with one Dirac delta function for the one and three-dimensional Morse parameters. When the Morse potential parameters go to zero, we have found the eigenvalue equation which

is the same as the free particle. When the strength of the Dirac delta function goes to zero, we have obtained the eigenvalue equation of the Morse potential.

We investigated the change of the oscillator strength for the transition between the first excited and the ground states and then for the transition between the second and the first excited states.

In addition to this, our method can also be used to describe such a system which has a collective excitation due to slow driving of a focused laser beam through a cloud of trapped cold fermions. The effective potential for the atomic motion in 1D model, $V(x) = \frac{x^2}{2} + U_o(x_o)exp(-\frac{(x-x_o)^2}{2\sigma^2})$ where $U_o(x_o) < 0$ and σ is directly related to the cross section of the (Gaussian) laser beam. Thus Gaussian shape potentials are used to describe laser fields. The Dirac delta function $\delta(x - x_o)$ can be expressed in terms of a limit $(\sigma \to 0)$ of $f(x) = \frac{1}{\sqrt{2\pi\sigma^2}}exp(-\frac{(x-x_o)^2}{2\sigma^2})$. Hence, the collective excitation due to the laser beam is very local (Gaussian) so that it can be represented by the Dirac delta potential. A focused laser beam through hydrogen molecule may lead to a very local deformation on the potential energy curve for hydrogen. Thus, such a deformed system can be investigated by using our approach.

APPENDIX A: SOME PROPERTIES OF THE DIRAC DELTA FUNCTION

The Dirac delta function is defined by

$$\delta(x) = \begin{cases} 0 & for\ x \neq 0, \\ \infty & for\ x = 0. \end{cases} \tag{A.1}$$

and

$$\int_{-\infty}^{\infty} \delta(x)dx = 1. \tag{A.2}$$

The Dirac delta function can also be defined for higher dimensions. For example, in three dimension ;

$$\delta(\overrightarrow{r}) = \begin{cases} 0 & for\ |\overrightarrow{r}| \neq 0, \\ \infty & for\ |\overrightarrow{r}| = 0. \end{cases}, \tag{A.3}$$

where $|\overrightarrow{r}| = \sqrt{x^2 + y^2 + z^2}$.

The integral representation of the Dirac delta function is given by

$$
\begin{aligned}
(i) \quad & \delta(x) = \frac{1}{2\pi}\int_{-\infty}^{\infty} e^{ikx} dk \ , \\
(ii) \quad & \delta(\overrightarrow{\rho}) = \frac{1}{(2\pi)^2}\int_{surface} e^{i\,\overrightarrow{k}\,.\,\overrightarrow{\rho}}\, d^2k \ , \\
(iii) \quad & \delta(\overrightarrow{r}) = \frac{1}{(2\pi)^3}\int_{volume} e^{i\,\overrightarrow{k}\,.\,\overrightarrow{r}}\, d^3k \ ,
\end{aligned}
\tag{A.4}
$$

for one, two and three dimensions, respectively where $\rho^2 = x^2+y^2$ and $r^2 = x^2+y^2+z^2$.

By using equation (A.4), we can show equation (A.2) is satisfied. To see this note that from equation (A.4) into equation (A.2), we get

$$
\frac{1}{2\pi}\int_{-\infty}^{\infty}\int_{-\infty}^{\infty} e^{ikx} dk dx = \lim_{k\to\infty}\frac{1}{2\pi i}\int_{-\infty}^{\infty}\frac{e^{ikx}-e^{-ikx}}{x} dx \tag{A.5}
$$

and

$$
\lim_{k\to\infty}\frac{1}{\pi}\int_{-\infty}^{\infty}\frac{\sin(kx)}{x} dx = 1 \tag{A.6}
$$

since $\int_{-\infty}^{\infty}\frac{\sin(kx)}{x}dx = \pi$ for $k > 0$.

The Dirac delta function can be represented by some functions such as

$$
\begin{aligned}
(i) \quad & \delta(x) = \lim_{\epsilon\to 0}\frac{1}{2\epsilon} e^{-|x|/\epsilon} \ , \\
(ii) \quad & \delta(x) = \lim_{\epsilon\to 0}\frac{1}{\pi}\frac{\epsilon}{x^2+\epsilon^2} \ , \\
(iii) \quad & \delta(x) = \lim_{\epsilon\to 0}\frac{1}{\epsilon\sqrt{\pi}} e^{-|x|^2/\epsilon^2} \ , \\
(iv) \quad & \delta(x) = \lim_{\epsilon\to 0}\frac{1}{\pi}\frac{\sin(x/\epsilon)}{x} \ ,
\end{aligned}
\tag{A.7}
$$

$$(v) \quad \delta(x) = \lim_{\epsilon \to 0} \epsilon \mid x \mid^{\epsilon - 1} ,$$

$$(vi) \quad \delta(x) = \lim_{\epsilon \to 0} \frac{\epsilon}{\pi} \frac{\sin^2(x/\epsilon)}{x^2} .$$

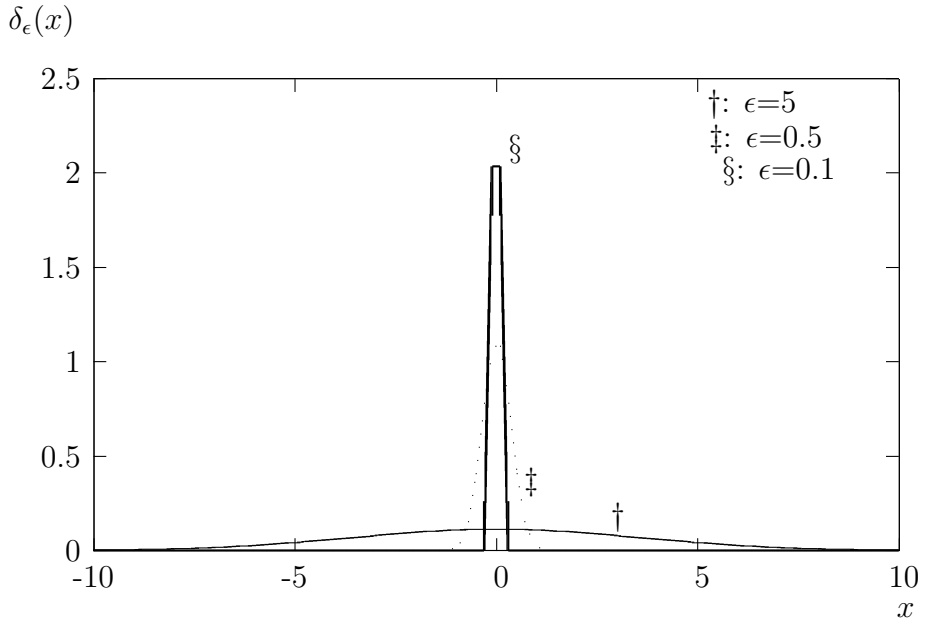


Figure A.1. $\delta_\epsilon(x)=\frac{1}{\epsilon\sqrt{\pi}}e^{-\frac{x^2}{\epsilon^2}}$ vs. x for $\epsilon = 5, 0.5, 0.1$ values.

In Figure A.1, function $\frac{1}{\epsilon\sqrt{\pi}}e^{-\frac{x^2}{\epsilon^2}}$ behaves like a delta function when ϵ gets smaller.

Some important properties of the Dirac delta function,

$$\begin{aligned}
&(i) \quad \int_{-\infty}^{\infty} \delta(x-a) f(x) dx = f(a) , \\
&(ii) \quad \delta[f(x)] = \sum_i \frac{\delta(x - x_i)}{\frac{\partial f(x)}{\partial x_i} \mid_{x=x_i}} , \\
&(iii) \quad x\frac{d\delta(x)}{dx} = -\delta(x) , \\
&(iv) \quad \delta(ax) = \frac{1}{|a|}\delta(x) , \\
&(v) \quad \frac{dU}{dx} = \delta(x) ,
\end{aligned} \tag{A.8}$$

where x_i's are the roots of the equation $f(x) = 0$ and U is the heaviside unit step function defined as

$$U = \begin{cases} 1 & if\ x > 0, \\ 0 & if\ x < 0. \end{cases} \tag{A.9}$$

REFERENCES

1. Kittel, C., *Introduction to Solid State Physics*, John Wiley & Sons, New-York, 1996.

2. Griffiths, D. J., *Introduction to Quantum Mechanics*, Prentice Hall Inc., New Jersey, 1995.

3. Mèndez, B., F. Domìnguez-Adame and E. Maćia, "A transfer matrix method for the determination of one-dimensional band structures", *J. Phys A: Math. Gen.*, vol. 26, pp. 171-177, 1993.

4. Maksymowicz, A. Z. and M. Wołoszyn, "Density of states in structurally disordered 1D chains of atoms", *Journal of Non-Crystalline Solids*, vol. 352, pp. 4200-4205, 2006.

5. Arrighini, G. P., C. Guidotti and N. Durante, "One- and two-photon ionization of model atoms: The spherical δ-shell potential", *Phys. Rev. A*, vol. 35, pp. 1528-1534, 1987.

6. Mur, V. D., V. S. Popov, "Coulomb problem with short-range interaction: Exactly solvable model", *Theor. Math. Phys.*, vol. 65, pp. 1132-1140, 1984.

7. Blinder, S. M., "Modified delta-function potential for hyperfine interactions", *Phys. Rev. A.*, vol. 18, pp. 853-861, 1977.

8. Uncu, H., H. Erkol, E. Demiralp and H. Beker, "Solutions of the Schrödinger equation for Dirac Delta Decorated Linear Potential", *CESJ*, vol. 1, pp. 1-19, 2005.

9. Barker, J. R., *The physics and fabrication of microstructures and microdevices. Proceedings in Physics Kelly, M.S.Weisbuch, C. (eds.)*, Springer, Berlin, 1986.

10. Uncu, H. and E. Demiralp, "Bound state solutions of the Schrödinger equation for a $\mathcal{PT}$-symmetric potential with Dirac delta functions.", *Phys. Lett. A*, vol. 359, pp. 190-198, 2006.

11. Demiralp, E., "Properties of a Bose-Einstein Condensate in a Harmonic Trap Decorated with Dirac Delta Functions", *Talk Given at Albert Einstein Century International Conference*, Paris, 2005.

12. Uncu, H., D. Tarhan, E. Demiralp, et al., "Bose-Einstein condensate in a harmonic trap decorated with Dirac delta functions", *Phys. Rev. A.*, vol. 76, pp. 013618, 2007.

13. Altunkaynak, B. İ., "Spectral and Scattering Properties of Point Interactions", M.S. Thesis, Boğaziçi University, 2005.

14. Altunkaynak, B. İ., F. Erman and O. T. Turgut, "Finitely Many Dirac-Delta Interactions on Riemannian Manifolds", *J. Math. Phys.*, vol. 47, pp. 082110-1-082110-23, 2006.

15. Woods, R. D. and D. S. Saxon, "Diffuse Surface Optical Model for Nucleon-Nuclei Scattering ", *Phys. Rev.*, vol. 95, pp. 577-578, 1954.

16. Williams, W. S. C., *Nuclear and Particle Physics*, Clarendon Press, Oxford, 1996.

17. Walz, M., et al., "Absolute Magnitude of (P, Alpha) AND (Alpha, P) Cross-Sections - New Results Concerning a Long-Standing Problem", *J. Phys. G: Nucl. Phys.*, vol. 14, pp. L91-L96, 1988.

18. Garcia, F., et al., "Woods-Saxon potential parametrization at large deformations for plutonium odd isotopes", *Eurapean Physical Journal A*, vol. 6 (1), pp. 49-58, 1999.

19. Bespalova, V., E. A. Romanovsky and T. I. Spasskaya, "Nucleon-nucleus real potential of Woods-Saxon shape between -60 and +60 MeV for the $40 \leq A \leq 208$ nuclei", *Journal of Physics G- Nuclear and Particle Physics*, vol. 29 (6), pp. 1193-

121, 2003.

20. Dasgupta, M., D. J. Hinde, J. O. Newton and K. Hagino, "The Nuclear Potential in Heavy-Ion Fusion", *Progress of Theoretical Physics Supplement*, vol. 154, pp. 209-216, 2004.

21. Sadeghi, J. and M. R. Pahlavani, "The Hierarchy of Hamiltonians for Spherical Woods-Saxon Potential", *African J. Mathematical Phys.*, vol 1, pp. 195-199, 2004.

22. Fakhri, H. and J. Sadeghi, "Supersymmetry Approaches to the Bound States of the Generalized Woods-Saxon Potential", *Modern Physics Letters A*, vol. 19 (8), pp. 615-625, 2004.

23. Goldberg, V., et al., "Low-lying levels in F-15 and the shell model potential for drip-line nuclei ", *Physical Review C.*, vol. 69 (3), pp. 031302, 2004.

24. Syntfelt, A., et al., "First Structure Information on the Exotic ^{149}La from the β^- Decay of ^{149}Ba", *European Physical Journal A*, vol. 20 (3), pp. 359-363, 2004.

25. Khounfais, K., T. Boudjedaa and L. Chetouani, "Scattering Matrix for Feshbach-Villars Equation for Spin 0 and 1/2: Woods-Saxon Potential", *Chechoslowak Journal of Physics*, vol. 54 (7), pp. 697-710, 2004.

26. Newton J. O., et al., "Systematic Failure of the Woods-Saxon Nuclear Potential to Describe both Fusion and Elastic Scattering: Possible Need for a New Dynamical Approach to Fusion", *Physical Review C.*, vol. 70 (2), pp. 024605, 2004.

27. Guo, J. Y. and Q. Sheng, "Solution of the Dirac Equation for the Woods-Saxon Potential with Spin and Pseudospin Symmetry", *Physics Letters A*, vol. 338 (2), pp. 90-96, 2005.

28. Diaz-Torres, A. and W. Scheid, "Two Center Shell Model with Woods-Saxon Potentials: Adiabatic and Diabatic States in Fusion", *Nuclear Physics A*, vol. 757 (3-4), pp. 373-389, 2005.

29. Mierzynski, P. and K. Pomorski, "Shell Structure of Cesium Layer Covering the C-60 Fullerene Core", *Eur. Phys. J. D.*, vol. 21, pp. 311-314, 2002.

30. Greenhow, R. C. and J. A. D. Matthew, "Relationships Between the Positions and Breadths of Single Channel Resonances", *J. Phys. B.*, vol. 24, pp.4677-4683, 1991.

31. Hwang, J. L. and Y. Yang, "Radii, Surface Diffuseness, and Binding Energies of Atomic Nuclei", *Chinese J. Phys.*, Vol 2, No. 1, pp. 32-41, 1964.

32. Morse, P. M., "Diatomic Molecules According to the Wave Mechanics. II. Vibrational Levels ", *Phys. Rev.*, vol. 34, pp. 57-64, 1929.

33. Mahlanen, R., J. P. Jalkanen and T. A. Pakkanen , "Potential energy surfaces of CF4, CCl4 and CBr4 dimers", *Chem. Phys.*, vol. 313, pp. 271-277, 2005.

34. Tanimura, Y., "Fifth-Order Two-Dimensional Vibrational Spectroscopy of a Morse Potential System in Condensed Phases", *Chem. Phys.*, vol. 233, pp. 217-229, 1998.

35. Lim, T. C., "A functionally Flexible Interatomic Energy Function Based on Classical Potentials", *Chem. Phys.*, vol. 320, pp. 54-58, 2005.

36. Dominiak, P. M., et al., "Continua of Interactions between Pairs of Atoms in Molecular Crystals", *Chem. Eur. J.*, vol. 12, pp. 1941-1949, 2006.

37. Yeganeh, S. and M. A. Ratner, "Effects of Anharmonicity on Nonadiabatic Electron Transfer: A Model", *J. Chem. Phys.*, vol. 124, pp. 044108, 2006.

38. Vela, A. G., "An Empirical Potential Energy Surface for the He-Br2 (B3Πu) van der Waals Complex", *J. Phys. Chem. A*, vol.109, pp. 5545-52, 2005.

39. Sim, E., "Parametrization of an anharmonic Kirkwood-Keating Potential", *J. Chem. Phys.*, vol. 122, pp. 174702, 2005.

40. Chen, E. S. and E. C. M. Chen, "Semiempirical Characterization of Homonuclear

Diatomic Ions: 5. The General Classification of Herschbach Ionic Morse Potential Energy Curves", *J. Phys. Chem. A*, vol.106, pp. 6665-69, 2002.

41. Zhou, Y., M. Karplus, K. D. Ball and R. S. Berry, "The Distance Fluctuation Criterion for Melting: Comparasion of Square Well and Morse Potential models for Clusters and Homopolymers", *J. Chem. Phys.*, vol. 116, pp. 2323, 2002.

42. Kolos, W. and L . Wolniewicz, "Theoretical investigation of the lowest double-minimum state E, $F^1\Sigma_g^+$ of the hydrogen molecule", *J. Chem. Phys.*, vol. 50, pp. 3228-3240, 1969.

43. Komatsu, K., M. Murata and Y. Murata, "Encapsulation of molecular hydrogen in fullerene C60 by organic synthesis", *Science*, vol. 307, pp. 238, 2005.

44. Uncu, H., E. Demiralp, et al., "Bose-Einstein condensate in a harmonic trap with an eccentric dimple potential", *Laser Phys.*, vol. 18, pp. 331-334, 2008.

45. Damski, B., K. Sacha and J. Zakrzewski, "Collective Excitation of Trapped Degenerate Fermi Gases", *J. Phys. B: At. Mol. Opt. Phys.*, vol. 35, pp. L153-L159, 2002.

46. Vanilse, S., F. A. B. Countinho and J. F. Perez, "Operator Domains and Self-Adjoint Oprators", *Am. J. Phys.*, vol. 72, pp. 203-213, 2004.

47. Countinho, F. A. B., Y. Nogami and J. F. Perez, "Generalized Point Interactions in one Dimensional quantum mechanics", *J. Phys. A: Math. Gen.*, vol. 30, pp. 3937-3945, 1997.

48. Bonneau, G., J. Faraut and G. Valent, "Self-adjoint extentions of operators and teaching of quantum mechanics", *Am. J. Phys.*, vol. 69, pp. 322-331, 2001.

49. Albeverio, S., L. Dąbrowski and P. Kurasov, "Symmetries of Schrödinger Operators with Point Interactions", *Lett. Math. Phys.*, vol. 45, pp. 33-47, 1998.

50. Thirring, W., *Quantum Mathematical Physics*, Springer, New-York, 2002.

51. Demiralp, E. and H. Beker, "Properties of bound states of the Schrödinger Equation with attractive Dirac delta potentials", *J. Phys. A: Math. Gen.*, vol. 36, pp. 7449-7459, 2003.

52. Demiralp, E., " Bound states of n-dimensional harmonic oscillator decorated with Dirac delta functions", *J. Phys. A: Math. Gen.*, vol.22, pp. 4783-4793, 2005.

53. Erkol, H. and E. Demiralp, "The WoodsSaxon potential with point interactions", *Phys. Lett. A*, vol. 365, pp. 55-63, 2007.

54. Uncu, H., "Bound State Solutions of the Schrödinger Equation for Potentials with Dirac Delta Functions", P.h.D. Thesis, Boğaziçi University, 2007.

55. Beker, H., *Fen ve Mühendislikte Matematik Metotlar*, Boğaziçi Üniversitesi Yayınevi, İstanbul, 2006.

56. Erkol, H., "Approximate Ground State Energies of One Dimensional Potential Wells by the S- Matrix Formalism", M.S. Thesis, Boğaziçi University, 2003.

57. Jost, R. and A. Pais, "On the scattering of a particle by a static potential", *Phys. Rev.*, vol. 82, pp. 840-851, 1951.

58. Bargmann, V., "On the number of bound states in a central field of force", *Proc. Acad. Sci.* USA, vol. 38, pp. 961-966, 1952.

59. Cohn, J., "On the number of negative eigen-values of a singular boundary value problem", *J. London Math. Soc.*, vol. 40, pp. 523-525, 1965.

60. Calegero, F., "Sufficient conditions for an attractive potential to possess bound states", *J. Math. Phys.*, vol. 6, pp. 161-164, 1965.

61. Calegero, F., "Necessary conditions for the existence of bound states", *Nuovo Ci-*

mento, vol. 36, pp. 199-201, 1965.

62. Calegero, F., "Upper and lower limits for the number of bound states in a given central potential", *Commun. Math. Phys.*, vol. 1, pp. 80-88, 1965.

63. Brau, F., "Necessary and sufficient conditions for the existance of bound states in a central potential", *J. Phys. A: Math. Gen.*, vol. 36, pp. 9907-9913, 2003.

64. Persson, M., et al., "A First Principles Potential Energy Surface for Eley-Rideal Reaction Dynamics of H Atoms on Cu(111)", *J. Chem. Phys.*, vol. 110, pp. 22402249, 1999.

65. Flügge, S., *Practical Quantum Mechanics*, Springer-Verlag, New York Heidelberg Berlin, 1974.

66. Antoine, J. P., F. Gesztesy and J. Shabani, "Exactly solvable models of sphere interactions in quantum mechanics", *J. Phys. A: Math. Gen.*, vol. 20 pp. 3687-3712, 1987.

67. Porter, L. E., "Light λ^0 Hypernuclei and the Lambda-Nucleon Potential", *American Journal of Physics*, Vol. 39, pp. 97-102, 1971.

68. Albeverio, S., F. Gesztesy, R. Høegh-Krohn, H. Holden, and P. Exner, *Solvable Models in Quantum Mechanics*, Rhode Island: AMS, 2005.

69. Kolos, W. and L. Wolniewicz, "Potential-Energy curves for the $X\Sigma_g^1$, $b^3\Sigma_u^+$, and $C^1\Pi_u$ states of the hydrogen molecule", *J. Chem. Phys.*, vol. 43, pp. 2429-2450, 1965.

70. Landau, L. D. and L. M. Lifshitz, *Quantum Mechanics* (New York: Pergamon Press), 1977.

71. Messiah, A., *Quantum Mechanics* (New York: Dover), 1999.

72. Kawasaki, S., T. Haraa and A. Iwataa, "He intercalated C-60 solid under high pressure", *Chem Phys. Lett.*, vol. 447, pp. 316-319, 2007.

73. Ohtsuki, T., et al., "Insertion of Be Atoms in C_{60} Fullerene Cages: Be@C60 ", *Phys. Rev. B.*, vol. 77, pp. 3522-3524, 1996.

74. Saha, S. K., et al., "Encapsulation of radioactive isotopes into C_{60} fullerene cage by recoil implantation technique", *Nuclear Instruments and Methods in Physics Research Section B*, vol. 243, pp. 277-281, 2005.

75. Slalina, Z. and S. Nagase, "A computational characterization of $N_2@C_{60}$", *Mol. Phys.*, vol. 104, pp. 3167-3171, 2006.

76. Mamone, S., et al., "Rotor in a cage: Infrared spectroscopy of an endohedral hydrogen-fullerene complex", *J. Chem. Phys.*, vol. 130, pp. 081103-081103-4, 2009.

77. Lee, T. B. and M. L. Mckee, "Endohedral Hydrogen Exchange Reactions in C-60 (nH(2)@C-60, n=1-5): Comparison of Recent Methods in a High-Pressure Cooker", *J. Am. Chem. Soc.*, vol. 130, pp. 17610-17619, 2008.

78. Cioslowski, J., "Endohedral Chemistry: electronic structures of molecules trapped inside the $C60$ cage", *J. Am. Chem. Soc.*, vol. 113, pp. 4139-4141, 1991.

79. Slanina, Z., P. Pulay and S. Nagase, "H-2, Ne, and N-2 energies of encapsulation into C-60 evaluated with the MPWB1K functional", *J. Chem. Theory Comput.* vol. 2, pp. 782-785, 2006.

80. Auffray, J. P. and J. W. Cooley, "Oscillator frequency and vibrational quanta in the hydrogen molecule", *Phys. Rev.*, vol. 124, pp. 1, 1961.

81. Cross, R. J., "Does H_2 Rotate Freely Inside Fullerenes?", *J. Phys. Chem. A*, vol. 105, pp. 6943-6944, 2001.

82. Columbia University, Department of Chemistry, *Symposium on H2@C60*, 2008.